An investigation of the role of microglia in axonal damage, in the context of demyelination

A thesis presented to the College of Medical,
Veterinary and Life Sciences,
Institute of Infection, Immunity and Inflammation
University of Glasgow

for the degree of Master of Science

Gemma Heather Thomson

2012

Abstract

Axonal loss is the main determinant of permanent neurological disability in the demyelinating disease, multiple sclerosis. However, there remains uncertainty regarding the nature of the cellular factors that elicit axonal injury. Using a non-immune mediated model of demyelination, the *Plp1*-overexpressing mouse (line #72), it has been shown that early axonal changes occur most frequently in regions of active demyelination where microglia/macrophages are phagocytosing myelin debris (Edgar et al.2010). With this in mind, it seems reasonable to hypothesise that myelin-laden microglia/macrophages are axono-toxic. However, the literature is contradictory, with both pro- (Williams et al., 1994;Mosley and Cuzner, 1996;van der Laan et al., 1996) and anti-inflammatory (Boven et al., 2006;Liu et al., 2006) properties having been ascribed to this population. The aims of this study were therefore to determine, using an *in vitro* myelinating culture system as a model of CNS white matter, whether myelin-laden microglia/macrophages acquire a (i) pro-inflammatory/axono-toxic or (ii) anti-inflammatory/axono-protective phenotype.

Myelinating cultures were prepared from embryonic mice expressing cyan fluorescent protein under the *Thy1* promoter, rendering a subset of neurons fluorescent. Myelin-enriched tissue fractions, to mimic myelin debris, were prepared from wild type or *Plp1*-overexpressing adult mouse spinal cord and labelled with a rhodamine antibody labelling kit. Myelin fractions were added directly to myelinating cultures at 20, 24 or 27 days *in vitro* (DIV), for 7, 3 or 1 day(s), respectively. Rhodamine-labelled myelin was phagocytosed by CD45 positive microglia/macrophages within 24 hours of its addition to the cell cultures. The phagocytosis of myelin had no effect on CD45 positive cell density, size or morphology, even after incubation for up to 7 days. Densities of CFP-positive neurites were quantified and the proportion of CFP-positive neurites manifesting signs of injury were calculated. There was no evidence that myelin-laden microglia/macrophages could elicit axonal injury *in vitro,* with no changes in neuritic density or integrity observed in myelin treated cultures compared to controls. To determine if myelin-laden cells exert an anti-

inflammatory, axono-protective effect in an inflammatory environment, cultures were treated with 100 ng/ml lipopolysaccharide (LPS). Pro-inflammatory cytokines, such as IL-1α, IL-1β, IL-6 and TNF-α were up-regulated in the medium from the LPS-stimulated cultures. However, these levels were not altered when cultures were pre-treated with myelin debris, to generate myelin-laden microglia. In these LPS-stimulated cultures, neuritic densities and neuritic integrity remained unaltered, either in the presence or absence of myelin-laden microglia/macrophages, compared to controls. Therefore the putative axono-protective effect of these cells could not be determined.

Dedication

This thesis is dedicated with love to my wonderful family and partner Alistair, with many thanks for all their support, encouragement and patience.

Table of Contents

List of Tables

List of Figures

Accompanying materials

Accompanying this thesis is a compact disk containing the time-lapse videos expressed as stills in Figures 6 and 21. The videos were generated from images taken every five minutes on the bright field (phase) and Cherry (rhodamine) channels over a 15 hour period and overlaid using ImageJ software (as described in Chapter 2.7)

Acknowledgement

I would firstly like to say a very big thank you to my supervisors Dr Julia Edgar, Professor Thomas Anderson and my assessor Professor Jacques Panderis for all their support and guidance during this project.

Many thanks also to the Multiple Sclerosis Society for funding this project and the University of Glasgow Graduate School for allowing me to submit this body of work to undertake this degree.

Thanks also to Professor Klaus-Armin Nave for originally donating the *Plp1*-transgenic mice (line #72) and Professor Wesley Thomson for donating the *Thy*-1 CFP expressing line of mice. My appreciation also goes to all the staff of Biological services for providing excellent care for all the animals used in this investigation.

I would like to acknowledge the help of Dr Julia Edgar and Allan Hall for some of the morphological measurements and axonal counts.

I would also like to take the time to give thanks to Dr Mark McLaughlin, Dr Fredrik Gruenenfelder, Dr Paul Montague, Jennifer Barrie, Mailis McCulloch, Kalliopi Ioannidou and Marie Ward for all their help, support and friendship.

Finally, I would like to thank my beloved Alistair and my family for all their love and support during my study, it was very much appreciated.

Declaration

I, Gemma Heather Thomson, do hereby declare that the work carried out in this thesis is original, was carried out by myself or with due acknowledgement, and has not been presented for award or degree at any other university.

Abbreviations

ANOVA	analysis of variation statistical test
AOI	area of interest
APC	antigen presenting cells
APES	3-aminopropyltriethoxy-silane
APP	amyloid precursor protein
BCA	Bichinoic acid
BSA	Bovine serum albumin
CCL8	chemokine (c-c motif) ligand 8
CD11B	cluster of differentiation molecule 11B
CD45	cluster of differentiation 45 surface antigen
CD68	cluster of differentiation 68 glycoprotein
CFP	cyan fluorescent protein
CNP	2',3'-Cyclic-nucleotide 3'- phosphodiesterase
CNS	central nervous system
CSF	cerebral spinal fluid
DAPI	4',6-diamidino-2-phenylindole
DIV	days *in vitro*
dH_2O	distilled water
DM20	26.5 kDa protein isoform encoded by *Plp1* gene
DMEM	Dulbecco's modified eagle medium
DNA	deoxyribonucleic acid
DRG	dorsal root ganglion neuron
DTT	dithiothreitol
EAE	experimental autoimmune encephalomyelitis
ECL	enhanced chemiluminescent substrate

E11.5	embryonic day 11.5
E13	embryonic day 13
FcR	Fc receptor
FITC	fluorescein isothiocyanate
GFAP	glial fibrillary acidic protein
HBSS	Hanks balanced salt solution
ID4B	lysosomal membrane protein antibody
IL	interleukin
LPS	lipopolysaccharide
MBP	myelin basic protein
MHC	Major histocompatibility complex
MS	Multiple sclerosis
mRNA	messenger ribonucleic acid
NFL-68	neurofiliment light chain-68 kDa
NGS	normal goat serum
NHS	*N*-hydroxy-succinimidyl-Rhodamine
NO	nitric oxide
OPC	oligodendrocyte precursor cell
P60	postnatal day 60
P120	postnatal day 120
PBS	phosphate buffered saline
PCR	polymerase chain reaction
PLL	poly-L-lysine
PLP	proteolipid protein
Plp1	proteolipid protein (non-human gene)
P-L-P	Periodate-lysine-paraformaldehyde

PMD	Pelizaeus-Merzbacher disease
PNS	peripheral nervous system
PVDF	polyvinylidene fluoride transfer membrane
SDS	sodium dodecyl sulphate
SDS-PAGE	sodium dodecyl sulphate polyacrylamide gel electrophoresis
TAE	tris acetate ethylene-di-amine-tetra-acetate buffer
TBS	tris buffered saline
TGF-β	transforming growth factor beta
TLR4	Toll-like receptor 4
TNF-α	Tumour necrosis factor alpha
UV	ultraviolet
WT	wild type
YFP	yellow fluorescent protein
5xSDS/DTT	5 x concentration sodiumdodecylsulphate/dithiothreitol

Presentation of work

The work in this thesis was presented at:

Glasgow Neuroscience Meeting, Glasgow Caledonian University, Glasgow, January 2011. Poster. An investigation of the role of microglia/macrophages in axonal damage, in the context of demyelination

MS Frontiers, London, June 2011. Poster and invited short oral presentation. An investigation of the role of microglia/macrophages in axonal damage, in the context of demyelination

Publication

Gruenenfelder,F.I.; Thomson,G.; Penderis,J.; Edgar,J.M. "Axon-glial interaction in the CNS: what we have learned from mouse models of Pelizaeus-Merzbacher disease". Journal of Anatomy 219 (2011) 33-43

1 Introduction

1.1 Overview of the mammalian central nervous system

The mammalian nervous system comprises the peripheral nervous system (PNS) and the central nervous system (CNS). The CNS consists of the brain and spinal cord, which are themselves comprised of grey matter and white matter. Grey matter contains neurons and glia; white matter contains glial cells and myelinated and non-myelinated axons that extend from neuronal cell bodies in the grey matter. Both grey and white matter contain a rich network of blood vessels.

1.1.1 Neurons

Neurons are highly specialised cells that constitute around 10 percent of total CNS cells. They comprise a cell body (perikaryon) containing a nucleus and surrounding cytoplasm, axon and several dendritic processes which extend from the cell body and branch multiple times. Most neurons have only a single long axonal projection, but some have multiple axonal projections. Neurons are electrically excitable cells, capable of transmitting information by means of electrical impulses. The dendritic processes are responsible for receiving stimuli from adjacent neurons or receptor organs. The information then passes from the neuronal cell body along the axon to the synaptic terminal. The information is then transmitted to dendrites of another neuronal cell or, in the PNS, to an effector organ (reviewed in (Edgar and Griffiths, 2009)).

1.1.2 Axons

Axons are the main transmission lines of the nervous system. Axons may extend over very long distances. For example, in man, some axons extend for a meter or more from the cell body. The axonal diameter is much smaller than that of the neuronal cell body. Axons range in diameter from between <0.3 and >10

micrometers in humans (Graf and Schramm, 1984). However, for each axon, the diameter remains relatively constant throughout its length (Friede and Samorajski, 1970).

The axonal cytoskeleton comprises actin filaments and a network of neurofilaments and microtubules, which are arranged parallel to the length of the axon. Neurofilaments provide structure to the axon and are the main determinant of axonal diameter (Cleveland et al., 1991;Hoffman et al., 1984). Microtubules provide the main 'tracks' for transportation upon which motor proteins, such as kinesin and dynein, carry organelles such as mitochondria, lysosomes and vesicles and also cytoskeletal polymers, in anterograde and retrograde directions.

Axonal transport occurs throughout the life of the axon and is essential for axonal growth and maintenance. The rates at which cargoes are transported along the axon are defined as fast or slow (Brown, 2003). For example, fast transport traffics membranous organelles containing proteins, lipids and polysaccharides required for general axonal integrity, and mitochondria which are targeted to sites of metabolic demand (Morris and Hollenbeck, 1993). The transport of cytoskeletal proteins such as actin and tubulin, occurs at a much slower rate and the delivery of these proteins is required for cytoskeletal maintenance and long range remodelling during axonal outgrowth (Brown, 2003).

Since axonal integrity relies on the axonal transport of vital molecules and organelles, interruption to this transport system, by acute axonal injury or as a consequence of a genetic abnormality, may eventually result in axonal degeneration (reviewed in (Edgar and Nave, 2009)).

1.1.3 CNS glial cells

1.1.3.1 Oligodendrocytes

The majority of CNS axons are ensheathed in a lipid-rich myelin membrane that is produced by oligodendrocytes. The relationship between the oligodendrocyte and the axon is a complex and reciprocally dependant one. The axon has a crucial influence on both the differentiation and survival of the oligodendrocyte during development, while the oligodendrocyte maintains long term integrity of the myelinated axon (Nave, 2010;Edgar and Nave, 2009) and shapes the axon during its development (Nave, 2010;Edgar and Nave, 2009). However, the maintenance of the myelin sheath also depends on the health of the axon. For example axonal degeneration or transaction leads to myelin breakdown (reviewed in Edgar and Griffiths 2009).

A single oligodendrocyte is capable of myelinating several axonal segments simultaneously. As oligodendroglia mature, they form elaborate sheet-like projections that are extensions of their plasma membrane. Transport of myelin proteins or their mRNAs, for example myelin basic protein (MBP), proteolipid protein (PLP) and its isofom DM20, and 2',3'-cyclic-nucleotide 3'-phosphodiesterase (CNP) are transported from the oligodendrocyte cell body to the myelin membrane during myelination. Although not fully understood, the sequence of events that culminate in myelination ensues when the oligodendrocyte process comes into contact with the axonal membrane. The process then begins to spirally wrap around the axon several times, expelling cytoplasm to form dense layers of compact myelin. The cytoplasm filled channel that remains around the periphery of the oligodendrocyte process forms the inner and outer non-compact tongues and the paranodal loops.

The myelin sheath is not continuous along the length of the axon. It is interrupted at regular intervals by small amyelinated regions, approximately one micrometre long, called nodes of Ranvier that facilitate saltatory conduction of electrical impulses.The main purpose of myelin is to increase the speed at which

impulses propagate along the nerve fibres from the neuronal cell body to the axon terminus.

1.1.3.2 Astrocytes

The other CNS macroglial cell is the astrocyte. Astrocytes perform many functions including maintaining normal levels of extracellular ion concentration during neuronal activity and providing biochemical support to epithelial cells that form the blood brain barrier. They have also been shown to have a role in repair and in scar formation within the CNS following traumatic injury (Renault-Mihara et al., 2008;Nash et al., 2011).

1.1.3.3 Microglia

Microglia, unlike oligodendrocytes and astrocytes, derive from mesenchymal tissue rather than from neuroepithelium, and account for around 10-15 percent of all CNS glial cells (Rock et al., 2004). However the true origin of microglia remains controversial (Prinz et al., 2011). It was previously assumed that embryonic and postnatal myeloid progenitors, derived from the bone marrow, contributed the majority of microglia of the brain. However more recent studies (Ginhoux et al., 2010) investigating the origin of microglia in mice, found that embryonic macrophages from the yolk sac were responsible for almost the entire population of adult microglia in the brain, with peripheral myeloid cells contributing minimally (Ginhoux et al., 2010;Prinz et al., 2011). Such recent studies also suggest that resident microglia are functionally distinct from other bone marrow or blood derived monocytes that may enter the CNS as a result of systemic inflammation or injury (Prinz et al., 2011).

Microglia perform many essential functions including scavenging, antigen presentation and phagocytosis, the last of which is the main focus of this thesis. Microglia cells become activated upon CNS insult, encouraging circulating monocyte recruitment and causing localised inflammation. Microglia can be identified using a variety of antibodies. For example, antibodies to cluster of differention factor 45 (CD45) or CD11b (Mac 1) recognise molecules that reside

on the cells' surface. Antibodies to CD68 recognise a specific antigen in the lysosomal membrane of phagocytes that is upregulated during phagocytotic activity (Bauer et al., 1994). Although it is possible to differentiate between macrophages and monocytes using antibodies against surface antigens such as DC11b and CD45, in the CNS, endogenous microglia and recruited macrophages are indistinguishable.

1.2 The immune system

1.2.1 The innate immune system of the CNS

Microglia are the resident macrophages of the CNS and are part of the innate immune system. As mentioned previously, one of their main roles is to scavenge and breakdown debris by phagocytosis. Phagocytosis is one of the first mechanisms of defence against invading micro-organisms and is also important in the removal of damaged tissue or senescent cells (Magnus et al., 2001). For example, in areas of active demyelination, microglia (probably in combination with infiltrating macrophages) must remove large volumes of myelin debris. During this process microglia become 'activated', undergoing morphological changes and an upregulation in expression levels of major histocompatibility complex (MHC) class II (Beyer et al., 2000). For example, in enriched microglial cultures exposed to membranes of either neuronal or glial origin, there is a notable increase in expression of MHC class II (Beyer et al., 2000). Morphometric analyses of the same cultures showed that the cells also acquire morphological changes towards an amoeboid appearance, compared to non-treated controls. Interestingly, similar morphological changes were observed in microglia exposed only to latex beads (Beyer et al., 2000), indicating that phagocytosis *per se*, is sufficient to induce such changes. However, although there was an obvious change in appearance in response to the phagocytosis of beads, there was no enhanced MHC class II expression, which was in contrast to their membrane exposed counterparts (Beyer et al., 2000). This suggests that there are different degrees of activation of phagocytic microglia/macrophage (Beyer et al., 2000).

Although morphological and biochemical changes associated with phagocytic activity have been documented (Perry, 1994;Ransohoff and Perry, 2009;Polazzi and Monti, 2010), the issue surrounding the effect that this has on the cells' phenotype is a matter of debate with both pro- (van der Laan et al., 1996;Mosley and Cuzner, 1996;Williams et al., 1994) and anti-inflammatory (Boven et al., 2006) phenotypes having been described (see Section 1.4).

1.2.2 The adaptive immune system

The adaptive immune system comprises, among other cells, B- and T-lymphocytes. B- and T-cells as well as natural killer (NK) cells are derived from the same multipotent hematopoietic stem cells, and are morphologically indistinguishable from one another until after they are activated (Janeway C.A. et al., 2005). There are a number of subgroups of T-cells including cytotoxic T-cells (CD8 +ve cells), which are responsible for inducing cell death of infected, damaged or dysfunctional cells and T-helper cells (CD4 +ve cells), which can be further subdivided into Th1, Th2 , Th17 and T-regulatory cells. B-cells are the major cells involved in the production of antibodies that circulate in blood plasma. The main difference between B-cells and T-cells is how they recognise antigen. T-cells recognise an antigen in its processed form, for example, as a peptide expressed by an MHC molecule (explained below), while a B-cell is capable of recognising an antigen in its native form.

After a single encounter with a specific pathogen, the cells of the adaptive immune system, in particular memory T-cells, have the ability to recognise the same pathogen in order to mount increasingly strong attacks each time the pathogen is encountered. The system is very adaptive in order to generate the diversity in the native immune repertoire. This is due to a method of somatic hypermutation (a process of accelerated somatic mutations) that allows a small number of genes to generate a number of different antigen receptors, which are then uniquely expressed on each individual lymphocyte. Due to these small irreversible changes in each cell's DNA, all the progeny of that cell will inherit

the genes encoding that same specific receptor repertoire, providing the key to long-lived immunity.

1.2.3 Interaction between cells of the adaptive and innate immune systems

Interaction between these two systems is controlled by a complex cytokine/chemokine network and expression of cellular surface antigens. MHC molecules are found in all nucleic cells and are involved in regulating immune responses. Protein molecules, either the host's own or invading entities, are degraded within a cell and then epitopes of these proteins are displayed on the cell surface by MHC molecules and presented to resident immune cells. By themselves, naive T-cells are unable to recognise foreign antigens unless they have been processed by an antigen presenting cell (APC) and expressed via the MHC molecules on the APC's surface. There are two types of MHC molecules, class I and class II. Most cells in the body are capable of presenting foreign peptides to cytotoxic T-cells through MHC class I molecules and therefore act as APCs. MHC class II molecules are present on certain immune cells themselves, for example dendritic cells and microglia/macrophages, which are also known as professional APCs. These professional APCs are very efficient at internalising invading entities, either by phagocytosis or by receptor-mediated endocytosis and then displaying the foreign peptides through MHC class II. Once the APCs have internalised the invading entity, they migrate to lymph nodes where they present the foreign peptides to neighbouring T-cells which can recognise them as being foreign. Subsequently, the presenting cell and all others displaying a similar protein can be destroyed.

1.3 Axonal injury in myelin disorders

Axonal injury is an integral part of a number of myelin disorders, with axonal loss contributing to the irreversible disease progression and clinical disability (Bjartmar et al., 1999). Such myelin disorders include multiple sclerosis (MS) (see 1.3.1) in which there exists a strong correlation between inflammatory demyelination and axonal transection (Trapp et al., 1998a), and the leukodystrophies such as Pelizaeus-Merzbacher disease (PMD) and their mouse models (see 1.3.2), in which a secondary inflammatory response at sites of

active demyelination is associated with acute axonal injury (Edgar et al., 2010;Garbern et al., 2002b)

1.3.1 Multiple sclerosis

MS is a prevalent neurological disease that affects over 100, 000 people in the UK alone (Multiple Sclerosis Society.org, 2012). It is thought to be an autoimmue mediated disorder, in which the body's own immune cells inappropriately recognise proteins on the myelin surface as foreign. It is a very variable and complex disease associated with the breakdown of the myelin sheath (demyelination). Although MS is classically considered an inflammatory demyelinating disease it is now recognised that axonal loss is the main cause of permanent neurological disability (Ferguson et al., 1997;Trapp et al., 1998b;De Stefano et al., 1998).

MS follows various courses; relapse/remitting, primary progressive and secondary progressive. The factors that contribute to axonal damage in MS and other demyelinating diseases are still uncertain. However, there is evidence to suggest that activated immune system cells, including T and B lymphocytes, macrophages and microglia, can harm axons (Edgar et al., 2010;Rasmussen et al., 2007;Hendriks et al., 2005) (Sobottka et al., 2009;Howe et al., 2007).

1.3.2 Pelizaeus-Merzbacher disease and the Plp1 overexpressing mouse model

Pelizaeus-Merzbacher disease (PMD) is classically considered a dysmyelinating disorder, in which myelin formation is perturbed. Many mutations in the *PLP1* gene have been identified in man and give rise to a broad spectrum of disease severity. The many mutations include point mutations and splice mutations, however, duplication of the *PLP1* gene is the most common cause of PMD, as reviewed by (Yool et al., 2000). PMD is not classically considered an inflammatory disorder, however low grade inflammation has been observed in *Plp1* over expressing models mouse models (Ip et al., 2006;Edgar et al., 2010).

Axonal degeneration in PMD has been reported (Shy et al., 2003;Garbern et al., 2002a).

The proteolipid protein (*Plp1*) gene over expressing mouse (line #72; (Readhead et al., 1994)) is a model of PMD, due to gene duplication. The homozygous #72 model has an approximate 2-fold increase in steady state levels of *Plp1* mRNA. The *Plp1* gene encodes proteolipid protein (PLP) and its isoform, DM20. PLP/DM20 is one of the key proteins expressed by the oligodendrocyte and is located in the compact myelin sheath, where it is involved in stabilizing membrane junctions (Klugmann et al., 1997b). PLP/DM20 is also important for glial/axonal interactions and axonal survival (Klugmann et al., 1997a;Edgar et al., 2002;Griffiths et al., 1998).

The homozygous *Plp1*-transgenic mouse forms CNS myelin initially, albeit in reduced amounts, but the biochemically abnormal myelin subsequently breaks down. Previous studies showed that the pattern of demyelination occurred in a rostral to caudal gradient within the optic nerve, producing two distinct regions at postnatal day (P)120; a chronic non-inflammatory demyelinated region and an active inflammatory, demyelinating region. The region undergoing active inflammatory demyelination contained a 10-fold increase in the number of CD45 positive cells (Edgar et al., 2010). CD45 is a pan-leukocytic marker that marks leukocytes including B and T- lymphocytes, macrophages and resident microglia. Unlike immune mediated models of demyelination, the breakdown of myelin in the #72 mouse occurs in the absence of large numbers of T-cells, which are infrequent, or B-cells, which are absent (Edgar et al., 2010). Therefore, the CD45 positive cells at the site undergoing active demyelination are likely to be resident microglia or invading macrophages.

In MS lesions, acute axonal damage (probably representing sites of axonal transport impairment) is associated with active inflammatory demyelination. Previous work using immunohistochemical assessment of amyloid precursor protein (APP), a marker for axonal transport impairment, showed an accumulation of APP at inflammatory demyelinating regions in MS brain

(Ferguson et al., 1997). Interestingly, in the *Plp1*-transgenic mouse, focal sites of axonal transport impairment correlate with active, inflammatory demyelination. In the *Plp1*-transgenic mouse, functional axonal transport was assessed using fluorescently labelled cholera toxin B subunit (CtB). On analysis, it was observed that there was accumulation of the FITC CtB within focal axonal swellings at sites of active, inflammatory demyelination (Edgar et al., 2010). This raises the possibility that the phagocytosis of myelin debris, at sites of active demyelination by the microglia/macrophages (CD45 positive cells) causes them to secrete pro-inflammatory factors that have a direct influence on adjacent 'naked' axons. This is in line with studies that demonstrate the myelin-laden macrophages produce pro-inflammatory cytokines (Williams et al., 1994;Mosley and Cuzner, 1996;van der Laan et al., 1996). This observation forms the basis of this MSc project.

1.4 Neuroprotective versus neurotoxic microglia

1.4.1 Different microglia/macrophage phenotypes

It is now known that in association with disease or injury, microglia/macrophage can adopt either a pro- or anti-inflammatory phenotype depending upon cues received from their microenvironment (Lawson et al., 1990;Boven et al., 2006). Therefore the question of whether microglia/macrophages play a detrimental or protective role may differ between neurological disorders and between different cellular injuries (Popovich and Longbrake, 2008;Schwartz et al., 2006;Neumann et al., 2008).

Two broad subsets of macrophages have been defined. These are M1, activated pro-inflammatory or M2, alternatively activated. The latter express anti-inflammatory molecules including transforming growth factor beta (TGF-β), IL-1 receptor antagonist (IL-1ra) and CCL8, the last being a specific marker for human alternatively activated macrophages (Boven et al., 2006). There are many micro-environmental cues that drive microglia/macrophages towards one particular state or another. For example Interferon-gamma (IFN-gamma) or

tumor necrosis factor (TNF)-α drives the M1 phenotype and IL-10 or IL-4 drive the M2 phenotype (Boven et al., 2006). The effects that myelin debris exerts as a micro-environmental cue is still controversial. Studies have shown that phagocytosis of myelin drives macrophages towards an M1 phenotype and secretion of pro-inflammatory cytokines including TNF-α and free radicals, for example nitric oxide (NO) (van der Laan et al., 1996;Mosley and Cuzner, 1996) which can be detrimental to other cells of the CNS. For example, secretion of TNF-α and NO have previously been shown to cause injury to axons by perturbing axonal transport *in vitro* (Stagi et al., 2005;Stagi et al., 2006;De Vos et al., 2000), and injuring oligodendrocytes, particularly precursor cells (Pang et al., 2010) *in vitro*. However, a recent study by Boven and colleagues showed that myeloid cells which had ingested myelin actually adapted an anti-inflammatory phenotype and expressed a number of anti-inflammatory surface molecules while in the absence of pro-inflammatory cytokines (Boven et al., 2006) .

1.4.2 Cytotoxic phenotype of microglia/macrophages in dys- or demyelinating disorders

Previous studies have provided evidence that in dys- or demyelinating disorders microglia/macrophages can adapt a cytotoxic phenotype with secretion of proinflammatory mediators capable of inflicting injury to axons and oligodendroglia (for example (Nikic et al., 2011;Howell et al., 2010). In the context of MS, it has been demonstrated that CSF derived from MS patients in a chronic disease stage, induces axonal damage in primary embryonic rat neuron cultures following increased exposure (Alcázar et al., 2000;Hendriks et al., 2005). This indicates that soluble mediators, which were present in the CSF, such as TNF-α, IL-1 and IL-6, secreted during the course of the disease by the microglia/infiltrating macrophages, are capable of inducing direct axonal damage *in vitro*.

In animal models, the cytotoxic effects of microglia was observed, for example, in an *in vivo* study using Long Evans shaker rats (*les*), in which oligodendroglial progenitor cells (OPCs) were the target of microglial-mediated injury. The *les*

rat is a myelin mutant in which the primary genetic defect in the oligodendrocyte is associated with progressive microglial activation. In this model, microglial activation peaked at postnatal day 30 (P30) when "expression of MHC II, mRNAs of inflammatory cytokines, and nitric oxide synthase accompanies phagocytosis of myelin debris" (Zhang et al., 2003). Zhang's study showed that injection of neonatal *les* rat brain derived OPCs into the spinal cord of these mutants at peak microglial activation was detrimental to the grafted cells. Conversely however, if the OPCs were grafted at P14 when there was only partial activation of the microglia or if the rats were pretreated with minocycline, there was substantial myelination of the dorsal columns after transplantation, suggesting that partial activation of the microglia facilitated myelination (Zhang et al., 2003). 'Activation' of microglia was characterised initially by "increased cell proliferation, enlarged cell volume and upregulated expression of antigen such as complement 3 receptor" (Zhang et al., 2001).

In a *Plp1* transgenic mouse model of Pelizaeus Merzbacher disease (line #66) a primary genetic defect in the oligodendrocyte, causes dysmyelination. However, it has been demonstrated that subsequent activation of microglia/macrophages exacerbate the disease process (Ip et al., 2006). Late onset demyelination and axonal injury in the white matter tract of this model is accompanied by an elevation in both CD11b positive "macrophage-like" cells and CD8 positive T-lymphocytes (Ip et al., 2006). Crossbreeding the *Plp1*-transgenic mouse with a mouse deficient in the mature T- and B-lymphocyte recombinant activating gene-1 (RAG-1) led to a reduction in the numbers of CD11b positive cells and an alleviation of pathological changes, demonstrating that the immune cells (including microglia/macrophages) play a pathogenetically relevant role in manifestation of the disease (Ip et al., 2006).

At sites of myelin degeneration in MS brain, microglia/macrophages phagocytose myelin debris and take on a 'foamy' appearance (Boven et al., 2006). Williams and colleagues demonstrated that following myelin phagocytosis, human derived microglial in culture, adopt a pro-inflammatory phenotype (Williams et al., 1994). At the peak of myelin phagocytosis (within 12-24 hours after incubation with purified myelin), a peak in recorded oxidative bursts and secretion of pro-

inflammatory cytokines including IL-1, TNF-α and IL-6, was recorded (Williams et al., 1994). Similarly, enriched rat-derived macrophage cultures incubated with opsonised rat myelin, up-regulated production of pro-inflammatory soluble factors including TNF-α and nitric oxide, after myelin phagocytosis (van der Laan et al., 1996;Mosley and Cuzner, 1996). These soluble factors have been shown to be toxic to oligodentrocyte precursor cells (Pang et al., 2010) and elicit axonal injury *in vitro,* in particular by damaging axonal mitochondria (Haider et al., 2011) and obstructing axonal transport (Stagi et al., 2005;Stagi et al., 2006;De Vos et al., 2000), suggesting that myelin-laden microglia/macrophages are cytotoxic.

Together, these data suggest that in the context of a dys- or demyelinating environment, endogenous microglia and/or recruited macrophages can exert injury to neighbouring cells.

1.4.3 Neuroprotective phenotype of microglia/macrophages in dys- and demyelinating disorders

Conversely, myelin-laden macrophages have been shown to secrete anti-inflammatory factors and possibly to facilitate repair of the injured CNS (Boven et al., 2006;Polazzi and Monti, 2010). It has been suggested that the prevention of infinite expansion of MS lesions is due to a ‘counter-regulatory mechanism' that controls inflammation within the CNS and also promotes tissue repair (Boven et al., 2006). These authors showed that foamy macrophages within demyelinating MS lesions from post-mortem tissue express various anti-inflammatory markers and phenotypically resemble M2 macrophages (Boven et al., 2006). In line with these observations, it has been demonstrated that the uptake of human myelin by purified human-derived macrophages in culture causes them to express anti-inflammatory molecules including IL-10 and TGF-β in response to a pro-inflammatory stimulus, for example lipopolysaccharide LPS (Boven et al., 2006;Polazzi and Monti, 2010).

Furthermore, there is increasing evidence that suggests that microglia/macrophages actually protect or promote the development and survival of neurons and oligodendrocytes. Such studies have shown that conditioned media from mouse peritoneal macropahges stimulated with myelin, contained factors that were neurotrophic for adult dorsal root ganglion neurons (DRG) *in vitro* (Hikawa and Takenaka, 1996), resulting in both enhanced neuronal survival and neurite regeneration. This neurotrophic media was specific for myelin, as media taken from macrophages treated with the endotoxin, LPS or latex beads failed to produce the same effect (Hikawa and Takenaka, 1996). Furthermore, secretion of microglia/macrophage derived molecules such as TNF α (Arnett et al., 2001) and induction of MHC-II by TNF-α are important modulatory events in remyelination (Arnett et al., 2003) and NO protects against apoptotic death of oligodendrocytes (Arnett et al., 2002). Accordingly, depletion of macrophages caused delayed CNS remyelination in a rat model of chemically induced demyelination (Kotter et al., 2005).

Together, these data demonstrate the multiplicity of microglial/macrophage phenotypes in the context of myelin abnormalities.

1.5 Thy1-fluorescent mice as tools to examine axonal injury

The use of transgenic mice in scientific research is ever increasing and several strains are available that express fluorescent proteins in specific cell or tissue types. The main focus of this study is to observe what influence phagocytic microglia/macrophages have on the integrity of adjacent axons. To answer this specific question, myelinating cultures were generated using transgenic mice expressing cyan fluorescent protein (CFP) under the *Thy1* promoter, in a subset of neurons (Feng et al., 2000). Unlike traditional techniques to observe axonal pathology including Haematoxylin and Eosin (H and E) staining, amyloid precursor protein (APP) histochemistry and electron microscopy, which carry a number of limitations and time constraints, expression of this particular fluorescent protein facilitates longitudinal imaging of single axons within culture and provides a sensitive marker of axonal injury. In conditions such as MS or in

instances of traumatic brain injury, axonal swellings have been shown to accumulate APP and axonal organelles (Ferguson et al., 1997;Edgar et al., 2001;Edgar et al., 2007) suggesting a 'traffic jam' effect or breakdown of axonal transport. Other studies using transgenic mice expressing an analogue of CFP showed that these fluorescent swellings correlated with most, although not all of the APP accumulated swellings (Bridge et al., 2007) showing that such fluorescent markers are suitable markers of axonal injury.

1.6 Aim

The broad aim of this thesis is to use an *in vitro* model of myelination to determine if and how microglia/macrophages that have phagocytosed myelin debris influence axonal integrity.

2 Materials and Methods

2.1 Animals

All animal studies were approved by the Ethical Committee of the University of Glasgow and licensed by the UK Home Office

2.1.1 Breeding

2.1.1.1 Mice used for myelinating cell culture

C57BL/6N (Charles River) wild type females were mated with C57BL/6N hemizygous *Thy1*-CFP males (Feng et al., 2000). The resultant embryos were wild type or hemizygous at the *Thy1*-CFP locus.

2.1.1.2 Mice used for myelin fraction preparation

Plp1-transgenic mice (line #72) carry a transgene cassette harbouring three copies of the murine *Plp1* gene (Readhead et al., 1994). Wild type males and females or homozygous *Plp1* transgenic males and females, on the C57BL/6N background, were mated to produce wild type or homozygous *Plp1* transgenic offspring, respectively. Adult females, aged between P60 and P120 ± 5 days were used for myelin extraction.

2.1.1.3 Genotyping

To identify mice carrying the *Plp1* transgene, a small length (approximately 3 mm) of tail was collected under anaesthesia. This procedure was carried out by members of Biological Services.

To identify mice carrying the *Thy1*-CFP transgene (see 2.2.2 below) a small ear notch was taken and examined under the fluorescent microscope (Olympus IX70 microscope) using the green wavelength filter.

2.1.1.4 Preparation of genomic DNA

To obtain genomic DNA for genotyping, the tail samples were lysed in 100 µl of 50 mM sodium hydroxide (Fisher, Leicestershire) at 95 ºC for 90 minutes (based on BioTechniques protocol, published in 2000). The samples were vortexed thoroughly to assist cell lysis then neutralised using 10 µl of 1 M Tris (Fisher, Leicestershire) pH 5.0.

2.1.1.5 PCR to determine the *Plp1* transgene status

One µl of each of the lysed tissue samples, 1 µl of water and 1 µl of purified positive and negative control genomic DNAs were each added to 24 µl of prepared PCR master mix (12.5 µl REDTaq ReadyMix PCR reaction mix with MgCl2 (Sigma-Aldrich, Dorset), 0.5 µl forward primer PLP (sequence 5′-CAGGTGTTGAGTCTGATCTACACAAG-3′, 0.5 µl reverse primer αT7 (sequence 5′-GCATAATACGACTCACTATAGGGATC-3′) (Readhead et al., 1994), 10.5 µl MilliQ water (Millipore, Livingston). PCR was performed on a Biometra UNO-thermoblock PCR thermocycler. The PCR reactions consisted of an initial denaturing step of 94 ºC for 3 minutes, annealing step 58 ºC for 1 minute and an elongation step 72 ºC for 2 minutes. This was followed by 35 core cycles of 93 ºC for 40 seconds, 58 ºC for 1 minute, 72 ºC for 30 seconds and a final cycle of 40 seconds at 93 ºC, 1 minute at 58 ºC and 3 minutes at 72 ºC. After the final cycle the reaction mix was cooled to 4 ºC. PCR products were then separated using gel electrophorisis. A 2.5 % agarose (Gibco, Invitrogen, Paisley) gel, containing 1.25 x 10^{-4} mg/ml ethidium bromide, was prepared. The gel was prepared and immersed in 1 X Tris acetate ethylene-diamine-tetra-acetate buffer (TAE see

Appendix 7.1.1). Ten µl of each PCR reaction product, as well as positive and negative controls were run in the gel. Samples were electrophoresed at a constant voltage of 70 for approximately 20 minutes.

Gels were viewed on a Herolab UVT-28M transilluminator to reveal PCR product bands and images were captured with a COHU CCD camera system attached to a Sony Digital Image printer. The presence of the *Plp1* transgene cassette yielded a 250 bp fragment. Fragment size was determined by side-by-side comparison with a 1 kb DNA ladder (Invitrogen, Paisley) which was run in parallel.

2.2 Myelinating cell culture

2.2.1 Preparation of Poly-L-Lysine coated coverslips

Using sterile technique, sterilised 13 mm glass coverslips (Fisher Scientific, Leicestershire) were carefully immersed in 0.01 % Poly-L-Lysine (PLL) (Sigma-Aldrich, Dorset) at room temperature for at least one hour, to coat them. For the 35 mm glass bottom Petri dishes, containing a single 14 mm coverslip, (MatTek corporation, Ashland, USA) used for time-lapse imaging, 500 µl of 0.01 % PLL was added directly onto the glass bottom at room temperature and incubated for 1 hour. After this time the PLL was aspirated off and the coverslips/glass bottom dishes were washed twice in deionised water. Using sterile forceps, coverslips were individually placed into 35 mm Nunclon (NUNC) (Thermo Scientific, Surrey) Petri dishes (3 coverslips per Petri dish) and allowed to dry. Petri dishes were used immediately or repackaged and stored at 4 ºC until required. Glass bottom dishes were left to air dry after washing and used immediately or repackaged and stored at 4 ºC until required.

2.2.2 Myelinating cell culture

Myelinating cultures (Thomson et al., 2008) were generated from spinal cords of embryonic day 13 (E13) mice expressing CFP under the Thy1 promoter. Spinal cords were dissected and stripped of their meninges. The cords were then chopped into small pieces with a sterile scalpel and incubated at 37 ºC for 20 minutes in 2-4 ml of Hanks Balanced Salt Solution (HBSS) without Mg^{2+} and Ca^{2+} (Gibco, Invitrogen, Paisley), containing trypsin (final concentration 0.12 %) and type I collagenase (final concentration 0.047 %). The reaction was stopped using soybean trypsin inhibitor and DNAase (SD solution, see appendix 7.2.1). Cells were than dissociated gently four times through a 21 gauge needle and twice through a 23 gauge needle to produce a homogenous single cell suspension. The cells were then centrifuged in 5 ml plating medium (DMEM 50 %, HBSS 25 % and horse serum25%, see Appendix 7.2.2) on a WIFUG lab centrifuge at 800 rpm for 5 minutes. The supernatant was removed and the remaining pellet resuspended in ~0.33 ml plating medium per spinal cord. Twenty µl of the cell suspension was then mixed with 20 µl of trypan blue and the trypan blue negative cells counted on a haemocytometer. Cells were then plated on poly-L-lysine coated coverslips (see 2.2.1) at a density of 150,000 cells/cover slip in 100 µl of medium. Each 35 mm diameter Nunclon dish (Thermo Scientific, Surrey) contained 3 coverslips. Two hours after the cells were plated; another 150 µl of plating medium was applied to each NUNC dish and uniformly spread using a fine tip artist brush which had been UV light sterilised. One hour after the addition of the extra plating medium, 500 µl of differentiation medium (DMEM plus glucose and hormones, see Appendix 7.2.3) was added. Cells were cultured in differentiation medium until 12 days *in vitro* (DIV) and then in differentiation media minus insulin until 28 (± 1) DIV.

2.3 Tissue Preparation

2.3.1 Tissue collection and fixation

For immunohistochemical analysis of intact E13 mouse spinal cords, three cords from littermates of embryos used for the myelinating cultures were stripped of

their meninges and immediately immersed in periodate-lysine-paraformaldehyde fixative (P-L-P fixative see Appendix 7.3.1). After two hours at room temperature, they were transferred to a solution of 20 % sucrose in PBS and incubated overnight for cryoprotection.

2.3.2 Preparation of APES (3(aminopropyl)triethoxysilane) coated slides

For APES (3(aminopropyl)triethoxysilane) (Sigma-Aldrich) coating, glass microscope slides were soaked overnight in 5 % Decon 90 (Decon Lab Ltd), rinsed in running distilled water for at least two hours and then oven dried at 70 °C The slides were then dipped for 1 minute in methylated spirit, then for 2 minutes in 0.25 % APES/methylated spirit, rinsed in distilled water, oven dried again at 70 °C, then wrapped in foil and stored at room temperature.

2.3.3 Cryopreservation and sectioning

The P-L-P fixed and sucrose saturated E13 spinal cords were cut transversely to produce rostral and caudal blocks which were then suspended in Tissue-Tec O.C.T compound (Miles Laboratories Inc.) in tin foil moulds. The tissue was fast frozen in isopentane (Fisher, Leicestershire) cooled in liquid nitrogen. The frozen blocks were wrapped in NescoFilm (Bando Chemical Ind. Ltd.) and stored at -20 ºC until required. 10 µm thick sections were cut from both regions of the cord using an OFT cryostat (Bright Instrument Company, Huntingdon, Cambridgeshire) and mounted onto APES-coated microscope slides, air dried for 1 hour and stored at -20 ºC until required.

2.3.4 Immunohistochemistry

The frozen E13 spinal cord cryostat tissue sections were allowed time to come to room temperature before being washed in PBS for 10 minutes to remove surrounding Tissue-Tec. The sections were then immersed in -20 ºC methanol for 10 minutes to permeabilise for intracellular or membrane antibody labelling. Once permeabilised, the sections were washed in PBS for a further 3 x 10 minutes. Sections were then immersed in 10 % normal goat serum (NGS) (Sigma-Alderich, Dorset) for one hour to block non-specific binding sites before being incubated in primary antibody diluted in 10 % NGS overnight at 4 ºC. The next day, the sections were washed again in PBS for 3 x 10 minutes and incubated in secondary antibody conjugated with fluorescein isothiocyanate (FITC) (Southern Biotech, Burmingham), diluted in 10 % NGS for one hour at room temperature. After incubation with the secondary antibody, the sections were washed in PBS as before. 0.83 µg/ml -1 4,6-diamidino-2-phenylindole (DAPI), a nuclear marker, was applied to the sections for 60 seconds. This was followed by another brief wash in PBS prior to mounting the sections in antifade mounting medium (Citifluor, London). Sections were then examined by epifluorescence using an Olympus IX70 microscope and images were captured using a CCD camera system (Photonic Science Colour Coolview) and ImagePro 6.0 software (Media Cybernatics, Wokingham, Berkshire). FITC absorbs light with a wavelength of 495 nm and emits light at a wavelength of 525 nm, which is visualised as a green light using a blue filter.

The primary antibodies used for immunohistochemistry were commercially available and their source and dilutions are illustrated in Table 1. Anti-CD45, a pan-leukocytic marker was used to recognise leukocytes including microglia/macrophages. Anti-CD11B and anti-CD68 were used as macrophage specific markers. Secondary antibodies used were all raised in goat and their source and dilutions are illustrated in Table 2.

Table 1. Immunohistochemistry primary antibodies

Primary antibody	Isotype	Dilution	Source
CD45	Rat IgG	1:300	AbD Serotec, Kidlington
CD11B conjugated FITC	Rat IgG	1:20	BioLegend UK Ltd., Cambridge
CD68	Rat IgG	1:200	Abcam, Cambridge

Table 2. Immunohistochemistry secondary antibodies

Secondary antibody	Dilution	Source
Rat Alexa Fluor 488	1:1000	Invitrogen, Paisley

2.4 Myelin isolation

Sterile myelin was isolated from spinal cords of adult (postnatal day 60-120 (P60-P120)) wild type and homozygous *Plp1*-transgenic mice by the technique based on the method of (Norton and Poduslo, 1973). Cords were rapidly removed from the spinal enclosure by introducing sterile saline under pressure to the lumbar spinal column using an 18 gauge hypodermic needle. Cords were ejected through the cervical column, which had been severed just below the base of the skull. The cords were placed in cryotubes, snap frozen and stored in liquid nitrogen or processed immediately. The cords were first homogenised in a 0.85 M sucrose with 10 mM HEPES using a polytron homogeniser at full speed for 12 strokes. Seven and a half ml of the homogenised tissue was transferred to Beckman SW41 rotor. Three ml of a 0.25 M sucrose solution in 10 mM HEPES was slowly added on top until two obvious phases could be seen. The samples were then spun at 70 000 x g for 90 minutes at 4˚C. Subsequently, the upper sucrose phase was removed and the interface containing the membrane fraction was gently aspirated off and transferred to a fresh Beckman tube. This membrane fraction was subjected to osmotic shock using 6ml of chilled MilliQ water. The myelin/water mix was vortexed then spun at 23 000 x g for 30 minutes in a J21

rotor. This step was repeated three times removing all water in-between. The final spin was done at 17 000 x g. The myelin pellet that was left was resuspended again in 0.85M sucrose and the entire process repeated, but with only one osmotic shock treatment at the end. The myelin pellet was then resuspended in sterile phosphate buffered saline (PBS see Appendix 7.1.2). Protein and phosphatase inhibitors were not used during the myelin preparation.

2.4.1 Protein assay

The protein assay was performed using Peirce protein assay system (Perbio, Northumberland) based on the Lowry Method using bicinchoninic acid (BCA) as a reagent. Two mg/ml bovine serum albumin (BSA) (Perbio, Northumberland) was diluted to 0.05, 0.1, 0.2, 0.4 and 0.6mg/ml with MilliQ water. One ml of BCA reagent was added to each of the five standards and to water (all 50 μl volumes) and to 5 μl of the myelin samples, which were each assayed in triplicate. The samples were then incubated at 37 °C for 30 minutes. Measurement of the absorbance of 562 nm wavelength light was then performed using a spectrophotometer (Cecil 1100). A standard curve was generated from the known standards and the sample concentrations were calculated using the standard curve. Myelin stock concentrations were prepared to 2 mg/ml for subsequent labelling with NHS-rhodamine antibody labelling kit (Pierce, Cramlington, Northumberland). Prior to labelling with the NHS-rhodamine antibody, 10 μl of the prepared myelin sample was incubated at 37 °C for 1 week in DMEM (Gibco, Invitrogen, Paisley) to check for sterility.

2.4.2 SDS PAGE (sodium dodecyl(lauryl)sulphate polyacrylamide gel electrophoresis) and western blotting

2.4.2.1 Sample preparation

To check that the myelin emulsion generated from the isolated *Plp1*-transgenic or wild type spinal cord was enriched for myelin proteins, western blots were carried out on selected preparations using antibodies against various myelin proteins. Twenty µl of the myelin tissue fraction emulsion was prepared to 1 mg/ml in PBS including 4 µl of 5 x loading buffer (Sodium dodecyl sulfate/Dithiothreitol denaturing buffer (SDS/DTT, see Appendix 7.1.6) and heated to 65 ºC for ten minutes to linearise the proteins by denaturing secondary and non-disulfide-linked tertiary structures and apply a uniform negative charge each protein, prior to running on an acrylamide gel.

Ten µg of myelin emulsion obtained from the wild type or *Plp1*- transgenic mice was run on a 4-12 % gradient NuPAGE bis-tris acrylamide gel (Invitrogen, Paisley, UK) at 200 Volts for between 40 and 50 minutes. Following a brief wash in cathode buffer (see Appendix 7.1.3) the proteins in the gel were then transferred using a semi-dry blotting system to a PVDF membrane (Millipore; Watford, UK). The gel was placed on top of 1 sheet of blotting paper soaked in anode 1 (Appendix 7.1.3.1) buffer, followed by 2 sheets soaked in anode 2 buffer (Appendix 7.1.3.2) and a single PVDF membrane. The PVDF membrane had been 'wet' in methanol for 10 seconds, then washed in MilliQ water and finally in anode 2 buffer for 5 minutes prior to use. A further 3 sheets of blotting paper soaked in cathode buffer (Appendix 7.1.3.3) were placed on top of the gel. Each layer was gently pressed using a small roller before the next was applied to remove any air bubbles.

The transfer was carried out at a constant current of 225mA for one hour for two gels. To check that the transfer was successful, the blots were briefly stained with Ponceau S (see Appendix 7.1.4). PVDF membranes were then washed in tris buffered saline (TBS) tween, blocked in 5% milk in 1 X TBS/tween (pH 7.4),

incubated overnight with primary antibody in blocking solution at 4°C, with gentle agitation, washed and incubated in HRP-conjugated goat anti-mouse or goat anti-rabbit secondary antibodies (New England Biolabs; Dundee) in blocking solution for 1 hour at room temperature. The secondary antibody was detected using enhanced chemiluminescence (ECL) (SuperSignal West Pico, Pierce Biotechnology Inc. Perbio Science UK Ltd.) The PVDF membrane was wrapped in saranwrap and exposed to x-ray film (AGFA) over a range of exposures from 30 seconds to 20 minutes to obtain an optimal exposure.

The primary antibodies used for the western blots were either gifted or commercially available and their source and dilutions are illustrated in Table 3. Secondary antibodies (either anti-mouse or anti-rabbit, also shown in Table 3.), all raised in goat, were conjugated with horse radish peroxidise (New England Biolabs; Hertfordshire, UK) and diluted 1:10 000.

Table 3. Western blot antibodies

Primary antibody	Dilution	Source	Secondary antibody
Neurofilament light chain (NFL-68)	1:10 000	Affiniti Research Products Ltd., Derbyshire	Anti-mouse HRP
Glial fibrillary acidic protein (GFAP)	1:200 000	Sigma-Aldrich, Dorset	Anti-rabbit HRP
CNP	1:5000	Cambridge Bioscience, Cambridge	Anti-mouse HRP
PLP/DM20 (226)	1:50 000	gift from M.P Groome	Anti-rabbit HRP

2.4.3 Rhodamine labelling of the isolated myelin

In order to visualise the phagocytosed myelin, purified myelin was labelled with NHS-Rhodamine fluorescent tag using a Rhodamine antibody labelling kit following manufacturer's protocol (Pierce, Cramlington, Northumberland). Forty

µl of Borate Buffer (0.67M) was added to 0.5ml of myelin at a concentration of 2mg/ml protein. 0.5ml of the protein/Borate Buffer mixture was then added directly to a vial of NHS-Rhodamine reagent and gently mixed by pipetting up and down several times until all the dye was dissolved. The sample was then briefly centrifuged (1000 x g for 30-45 seconds) and incubated at room temperature for 1 hour, protected from light. While the myelin was incubating the purification resin was prepared. Four hundred µl of reuspended purification resin was added to two separate spin columns in separate microcentrifugation collection tubes. The columns were then centrifuged for 30-45 seconds at 1000 x g to remove the storage solution from the resin. The spin columns that contained the resin were then transferred to fresh microcentrifugation tubes. After incubation, 250µl of the labelled myelin was added to each column and then the columns were centrifuged again at 1000 x g for a further 30-45 seconds. The samples, containing the fluorescently labelled myelin from both microcentrifugation tubes were then combined and the spin columns were discarded. The labelled myelin was then stored at -80ºC until required.

2.4.4 Myelin addition to cell culture

Myelinating cultures were established for 20, 24 or 27 (all ±1 day) days *in vitro* (DIV). Before the myelin was added, the entire medium was removed from each well and replaced with fresh differentiation medium minus insulin. Sterile (rhodamine-labelled) myelin in PBS, extracted from either wild type or *Plp1*-tg mouse spinal cord was then added directly to the cell culture wells at different concentrations and for different durations. From previous studies in which myelin was added to cell culture systems, a starting concentration was determined. Previous studies used 0.05 mg/ml of myelin (Boven et al., 2006), therefore concentrations above and below this were tested. The concentrations of myelin tested were 0.025 mg/ml, 0.05 mg/ml, 0.075 mg/ml and 0.1 mg/ml for either 7, 3 or 1 days *in vitro*. To ensure that the myelin was present at saturating amounts for all time tested, the final concentrations myelin tested in subsequent experiments were 0.075 mg/ml and 0.1 mg/ml.

To allow for a uniform solution and facilitate an even distribution, the myelin was vortexed thoroughly immediately before adding to the culture medium. An equivalent volume of PBS was applied to separate cultures as a control for the myelin delivery medium. Three x 10^6 one μm diameter Flurobite fluorescently labelled latex beads (Polyscience, Park scientific, Northampton, UK) were also used as a control for phagosytosis *per se*. At the end of the selected time points culture medium was removed from the wells and stored for cytokine analysis. The cells were fixed and analysed using immunocytochemistry (see section 2.5 below)

2.4.5 Lipopolysaccharide stimulation of microglia/macrophages in vitro

Lipopolysaccharide (LPS), E-coli mutant O111:B4 (VWR) was added directly to the myelinating cultures (100 ng/ml) for 48 hours (Domercq et al., 2007). To determine if the known pro-inflammatory effects of LPS were enhanced or ameliorated in the presence of myelin-laden microglia/macrophages, *Plp1* transgenic myelin (0.1 mg/ml) was added to the cultures (as described previously) 3 days prior to the treatment with LPS. All medium was removed then LPS was added for 48 hours. Equivalent volumes of PBS were added to separate coverslips as a control. After the entire 5 days incubation, all medium was removed for cytokine analysis and the cells fixed and analysed using immunocytochemistry.

2.5 Immunocytochemistry

Medium was aspirated from myelinating cultures and the cells were then immediately washed twice in PBS (37oC) to remove any media , then fixed using 4% paraformaldehyde (37 °C) for 10 minutes. The cells were then permeabilised using methanol, at -20 °C for 5 minutes. Non-specific binding sites were blocked using 10 % normal goat serum (Sigma-Aldrich, Dorset) in PBS and then the cultures were incubated at 4°C overnight in primary antibody in blocking solution. The next day, the coverslips were washed 3 times in PBS and the

secondary antibody, diluted in blocking solution, was applied for one hour at room temperature. After incubation with the secondary antibody, the cells were washed again in PBS as before and 0.83 µg/ml -1 4,6-diamidino-2-phenylindole (DAPI), a nuclear marker, was applied for 60 seconds. This was followed by another brief wash in PBS prior to mounting in antifade mounting medium (Citifluor, London).

The primary antibodies used for immunocytochemistry were commercially available and their source and dilutions are illustrated in Table 4. Secondary antibodies used were all raised in goat and their source and dilutions are illustrated in Table 5.

Table 4. Immunocytochemistry primary antibodies

Primary antibody	Isotype	Dilution	Source
CD45	Rat IgG1	1:600	AbD Serotec, Kidlington
MBP	Rat IgG	1:500	AbD Serotec, Kidlington
GFP	Rabbit IgG	1:1000	Abcam, Cambridge
CD68	Rat IgG2a	1:200	AbD Serotec, Kidlington
CD11B conjugated FITC	Rat IgG2b	1:20	BioLegend UK Ltd., Cambridge
SMI31	Mouse IgG1	1:1500	Affiniti Research Products Ltd., Derbyshire
ID4B	Rat IgG	1:2	Gifted from Developmental Studies Hybridoma Bank, University of Iowa

Table 5. Immunocytochemistry secondary antibodies

Secondary antibody	Dilution	Source
Anti-Rabbit Alexa Fluor 488	1:1000	Invitrogen
Anti-Rat Alexa Fluor 488	1:1000	Invitrogen
Anti-Rat Alexa Fluor 594	1:1000	Invitrogen

2.6 Quantification and statistical analysis

Quantification of rhodamine-labelled myelin treated cultures was carried out, blinded, on 10 randomly selected images of the green (CD45), red (rhodamine) and DAPI channels. Images were captured using a x20 objective over two 13 mm coverslips per experiment using a CCD camera system (Photonic Science Colour Coolview) and ImagePro 6.0 software (Media Cybernatics, Wokingham, Berkshire). Images were selected on the DAPI channel to avoid bias and captured from the middle and 4 corners of each coverslip.

2.6.1 Quantification of CD45 positive cell density and percentage of rhodamine-positive cells in myelin-treated cell cultures

To calculate CD45 positive cell density, manual counts of CD45 positive cells that contained a DAPI-labelled nucleus, within an area of interest (AOI, 124384 sq microns), were performed on digital images using ImagePro 6.0 software (Media Cybernatics, Wokingham, Berkshire), All cell within the AOI and those touching or crossing the north and west borders were counted. Those cells that touched or crossed the south and east borders of the AOI were excluded. Densitites were presented as cells/mm^2. Manual counts were also made of the number of CD45 positive cells that contained rhodamine-labelled myelin debris. The number of CD45 positive cells containing rhodamine was expressed as a percentage of all CD45 positive cells.

2.6.2 Quantification of the mean area per CD45 positive cell and the mean area occupied by rhodamine-labelled myelin per CD45 positive cell

To calculate the mean area per CD45 positive cell, automatic segmentation was carried out on digital images of the total CD45 positive staining within a known AOI (124384 sq microns) using ImagePro 6.0 software Media Cybernatics, Wokingham, Berkshire). The segmented image was then compared to the original image and then (if required) adjusted to provide the best representation of the original image. The system then automatically quantified the area occupied (using a count/size application) by all bright objects within the AOI to give the total area occupied by the staining. Prior to application the count/size limits were set (calculate area, no borders, holes not filled) and the system calibration set to x 20 magnification. The total area was then given in square microns and divided by the CD45 cell density to generate an average area per CD45 positive cell. The same process was carried out on the red channel (rhodamine) to quantify area occupied by myelin. The area given from the automatic count was then divided by the density of CD45 positive cells that contained the rhodamine-labelled myelin to generate the average area of rhodamine-labelled myelin per CD45 positive cell.

2.6.3 Quantification of neuritic changes

Coverslips from each experimental paradigm were assigned a numerical identity for the purposes of blinding the assessor. For each independent experiment, five images were taken, at random on both the red (MBP) and green (GFP) channels, of each of two coverslips per treatment. An AOI of 124384 mm^2 was placed on each digital image. Manual counts of all CFP positive neurites that crossed a horizontal line through the centre of the AOI were performed and the total number of neurites recorded. Neurites were then grouped as myelinated or non-myelinated and categorised by signs of neuritic changes. Neurites were examined and characterised as either (i) normal, (ii) beaded (small focal

swellings <20 μm^2 along otherwise intact neurites), (iii) degenerate/transected (fragmented or severed) or (iv) focally swollen but intact (swellings greater than 20 µm2).

2.7 Time lapse imaging

To observe myelin uptake and degradation, time lapse imaging was carried out on myelinating cultures (see 2.2.2) plated on 35 mm glass bottom Petri dishes (MatTek corporation, Ashland, USA) and cultured for 20-22 days *in vitro* (DIV). Immediately prior to imaging, 0.05 mg/ml of rhodamine-labelled myelin tissue fraction was vortexed and added directly to the culture Petri dish. The culture was then set in a Nikon TE 2000 time lapse microscope inside a temperature/CO2 controlled chamber. Using Metamorph 7.5.2 imaging software set for multi-stage positions and multiple wavelengths, positions of interest were then selected on the bright field (phase) Cherry (rhodamine) and CFP channels and the co-ordinates recorded. Focus for each position was then set using a PSF perfect focus control. Images were taken of each position on each channel every five minutes over a 15 hour period. AVI videos of the stills collected were then generated using ImageJ software.

2.8 Proteome array analysis of culture medium

2.8.1 Sample preparation and application

Medium collected from myelinating cells cultures, which had been incubated in the presence of either wild type or *Plp1*-tg myelin (0.1 mg/ml), 3 $x10^6$ Flurobite latex beads or PBS, for either 1, 3 or 7 days, was tested for 40 different cytokines/chemokines (see Appendix 2) using a mouse cytokine array panel A kit (R&D systems, Abingdon). Sample preparation and procedure were carried out according to manufacturers' protocol. All kit solutions were brought to room temperature prior to use and culture medium samples were thawed and kept on ice. The cell culture medium was first centrifuged using a Sigma desktop centrifuge at 12470 x g for 1 minute to remove any cellular or myelin debris.

Next, four cytokine nitrocellulose membrane panels were placed in a 4-well Multi-dish in 2 ml of blocking buffer (Array Buffer 6 supplied in kit) and placed on a rocking platform to incubate for one hour at room temperature. Whilst the membranes were blocking, up to 1 ml of each of the samples was added to 0.5 ml of Array Buffer 4 (supplied in kit). If the volume of sample was less than 1 ml, the final volume of the mix was adjusted to 1.5 ml using Array Buffer 5 (supplied in kit). Fifteen µl of a reconstituted (in 100 µl of deionised water) Cytokine Array Panel A Detection Antibody cocktail (supplied in kit) was then added to each sample and then incubated at room temperature for one hour. After incubation, the Array Buffer 6 was aspirated from the 4-well Multi-dish and the sample/antibody mixture was then added to each of the four membranes and incubated at 4 ºC over night on a rocking platform. The next day, the membranes were carefully removed from the 4-well Multi-dish and placed into individual containers containing 20 ml of 1 x Wash Buffer (25 x Wash Buffer supplied in kit diluted in deionised water) for 3 x 10 minutes. After being washed to remove excess sample/antibody mix, the membranes were carefully transferred back into the 4-well Multi-dish containing 1.5 ml of Streptavidin-HRP (supplied in kit) diluted in Array Buffer 5 (1:2000) in each well. The membranes were then incubated at room temperature for 30 minutes and then washed as before 3 x 10 minutes in 20 ml 1 x Wash buffer. Membranes were exposed to chemiluminescent detection reagents ECL (Super signal West Pico chemiluminescent substrate, Pierce) and wrapped in Saranwrap and exposed to x-ray film (AGFA) for various exposure times between 30 seconds to 10 minutes.

3 Characterisation of myelin-laden microglia/macrophages *in vitro*

3.1 Introduction

Microglia, which are derived from primitive myeloid progenitors (Ginhoux et al., 2010), are the resident macrophages of the CNS. They enter the CNS from the periphery during embryogenesis, and in the mouse, can be observed in the spinal cord as early as embryonic day 11.5 (E11.5) (Rigato et al., 2011). Microglia continuously survey the CNS environment (Nimmerjahn et al., 2005;Wake et al., 2009) and help maintain homeostasis (Aloisi, 2001;Neumann et al., 2009). Their phagocytic activity represents one of the first mechanisms of defence against invading microorganisms and is also important in the removal of damaged tissue, for example, during demyelination (Neumann et al., 2009;Walter and Neumann, 2009) and in response to apoptosis (Peri and Nusslein-Volhard, 2008;Nakamura et al., 1999).

Microglia are exceptionally sensitive to the micro-environment in which they reside, and respond to tissue injury by altering their phenotype from an 'inactive' (though motile) down regulated one to an 'activated' one (Perry et al., 2010). 'Activation' of microglia/macrophages *in vivo* is associated with increased proliferation (Ip et al., 2008), production of inflammatory cytokines and chemokines (Palin et al., 2008;Zhang et al., 2001) and morphological changes (Walter and Neumann, 2009). Changes in morphology and in cytokine/chemokine profiles also occur in response to activating stimuli *in vitro* (Beyer et al., 2000).

In the optic nerve of the *Plp1* overexpressing mouse, sites of acute axonal transport impairment correlate with active demyelination and elevated densities of CD45 positive microglia/macrophages (Edgar et al., 2010); many of which contain myelin debris. These observations led to the suggestion that the phagocytosis of large amounts of myelin debris may drive microglia/macrophages towards an 'activated' axono-toxic phenotype. This, in

line with *in vitro* studies that show that the phagocytosis of a myelin-enriched tissue fraction (mimicking myelin debris) by isolated microglia or macrophages *in vitro* triggers the production of pro-inflammatory cytokines and nitric oxide (Williams et al., 1994;Mosley and Cuzner, 1996), both of which have been shown to impair axonal transport *in vitro* (Stagi et al., 2006;Stagi et al., 2005).

However, the effects of the phagocytosis of myelin on the status of microglia/macrophage are controversial and more recent studies suggest that ingestion of myelin by this population, triggers an anti-inflammatory response (Boven et al., 2006;Liu et al., 2006).

In this thesis, an *in vitro* model of myelination (Thomson et al., 2008) was used to test the hypothesis that myelin-laden microglia are axono-toxic. Myelin-laden microglia/macrophages were generated through the addition of an exogenous, myelin-enriched tissue fraction to the cultures. Before beginning these experiments, it was important to determine optimal conditions for generating myelin-laden microglia/macrophages and to characterise the microglial population in the myelinating culture system.

The aims of this chapter were to:

1. Confirm that microglia are present in the E13 mouse spinal cord from which the myelinating cultures are generated.

2. Confirm that the intrinsic microglial/macrophage population in the myelinating culture system is capable of phagocytosing exogenous myelin debris

3. Determine the optimal parameters for generating myelin-laden microglia/macrophages

4. Assess putative phenotypic changes in myelin-laden microglia/macrophages.

3.2 Materials and methods

3.2.1 Myelinating cultures

Myelinating cultures were established from spinal cords of E13 *Thy1*-CFP mouse embryos, as described in Chapter 2.2.

3.2.2 Immunohistochemistry of E13 spinal cord

Embryonic mouse spinal cords, prepared as for the myelinating cultures (i.e. having been stripped of their meninges) were immersion fixed, frozen and sectioned on a cryostat (Chapter 2.3). Sections were immunostained with antibodies against CD45 (a pan-leukocyte marker) or CD68 (a macrophage-specific marker). Tissue sections from the spleen of a P90 *Plp1*-transgenic mouse were used as positive controls for immunohistochemistry (Chapter 2.3.4).

3.2.3 Preparation of a myelin-enriched tissue fraction

A myelin enriched tissue fraction from adult wild type or *Plp1*-transgenic mice was prepared according to the protocol of (Norton and Poduslo, 1973) with minor modifications (See Chapter 2.4).

3.2.4 SDS PAGE and western blot of myelin-enriched tissue fraction

To confirm myelin enrichment, the myelin fraction was analysed by western blot (Chapter 2.4.2). Equal amounts of a myelin-enriched tissue fraction and a total spinal cord homogenate were subjected to SDS-PAGE then transferred to a PVDF membrane (Chapter 2.4.2). Membranes were probed with antibodies against the myelin proteins CNP and PLP/DM20, and against astroglial and neuronal proteins, GFAP and NF68, respectively (Chapter 2.4.2, Table 3). The remaining myelin fraction was diluted to 2 mg of protein ml^{-1} and tested for sterility (Chapter 2.4.1), then labelled with an NHS-rhodamine antibody labelling kit (Chapter 2.4.3).

3.2.5 Quantification of myelin up-take by microglia/macrophages and analysis of 'activation' parameters

Cultures were treated with various concentrations (0.025 – 0.1 mg protein ml^{-1}) of rhodamine-labelled myelin-enriched tissue fraction in PBS, with 3 x 10^6 Flurobrite fluorescently labelled latex beads in PBS, or with PBS alone, at DIV 21 (± 1 day), 25 (± 1 day) or 27 (± 1 day), then fixed on day 28 (± 1 day). Cultures were immunostained with an antibody to CD45 and labelled with DAPI (Chapter 2.5). Myelin up-take, CD45 positive cell size and density were quantified from minimum of three independent experiments (Chapter 2.6).

3.2.6 Time lapse imaging of rhodamine-labelled myelin treated cultures

A rhodamine-labelled myelin-enriched tissue fraction (0.05 mg of protein ml^{-1}) was added to 20 DIV cultures. Time-lapse imaging was carried out immediately afterwards, over a 15 hour period. Images were taken on bright field (phase contrast), 'cherry' (rhodamine) and CFP/YFP (neurites) channels with 5 minute intervals between frames (Chapter 2.7). For each area imaged, a composite movie was generated from the bright field and cherry channels.

3.2.7 Lipopolysaccharide treatment of myelinating cultures

LPS was added to the myelinating cultures at 23 DIV, for 48 hours, following incubation of the cultures with myelin (0.1 mg protein ml^{-1}) or PBS on DIV 20 (Chapter 2.4.4). Culture medium was collected and stored at -80oC (see Chapter 5.2.2) and cells were immunostained with an antibody against CD45 (Chapter 2.5). Images of microglia/macrophages were captured using both phase-contrast and fluorescence microscopy.

3.2.8 Statistical analysis

Statistical analysis was carried out using GraphPad Prism 5 software. The percentage of CD45 positive cells taking up myelin over 3 time points was

analysed using one way ANOVA. Comparisons between wild type and *Plp1*-transgenic myelin treated cultures at specific time points and specific concentrations of myelin were made using an unpaired Student's t-test.

Changes in CD45 positive cell density and cell size after 7 days incubation with the myelin-enriched tissue fraction was also analysed using one way ANOVA. Comparisons between the myelin- or bead-treated cultures and the PBS treated controls were made using one-way ANOVA followed by Dunnett's multiple comparison test. Significance was set at $p < 0.05$.

3.3 Results

3.3.1 CD45 positive cells in the E13 mouse spinal cord parenchyma

To determine the origin of the CD45 positive cells in the myelinating cultures, a section of embryonic day 13 spinal cord was immunostained with antibodies against CD45 and CD68. Both CD45 (Figure 1A) and CD68 (Figure 1B) positive cells, with the morphology of microglia, were observed in the parenchyma of the E13 spinal cord. Therefore it was concluded that at least some of the CD45 (Figure 2A), CD11B (Figure 2B) or CD68 (Figure 2C), positive cells in the cultures (see later) were resident microglia. However, CD45 and CD68 positive cells were also evident in blood vessels and around the outer surface of the cord and are probably monocytes.

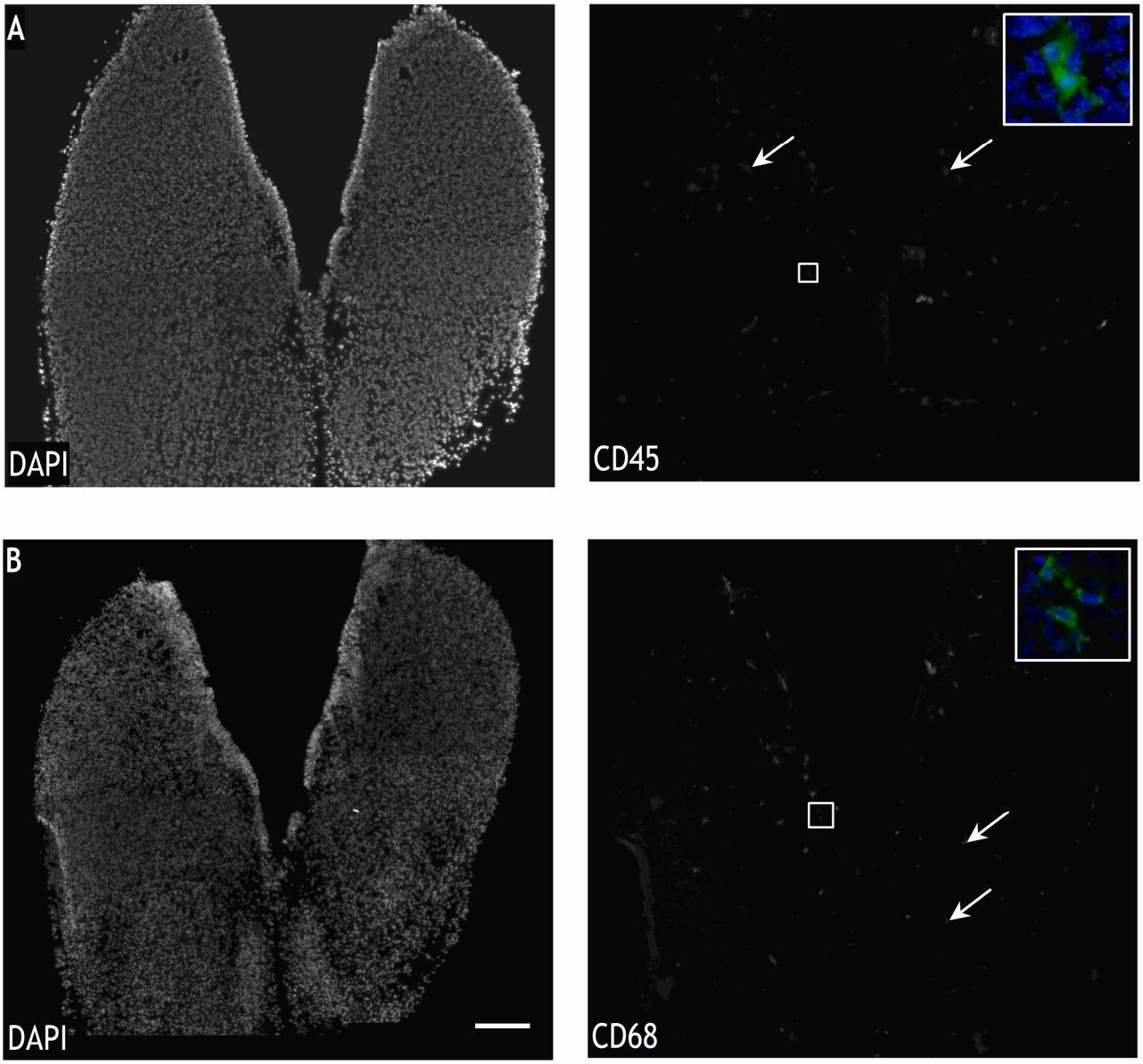

Figure 1: Microglia/macrophages in the parenchyma of E13 mouse spinal cord. Micrographs of mouse spinal cord stained with (A) DAPI (left) and antibody to CD45 (right), a pan leukocyte marker, indicating CD45 positive cells within the parenchyma (arrows). Insert: high magnification image of a CD45 positive cell with a DAPI stained nucleus. (B) Same spinal cord stained with DAPI (left) and with an antibody to CD68 (right), a phagocyte specific marker, indicating the presence of CD68 positive cells within the cord parenchyma (arrows). Insert: high magnification image of a CD68 positive cell with a DAPI stained nucleus. Scale bar 50 μm

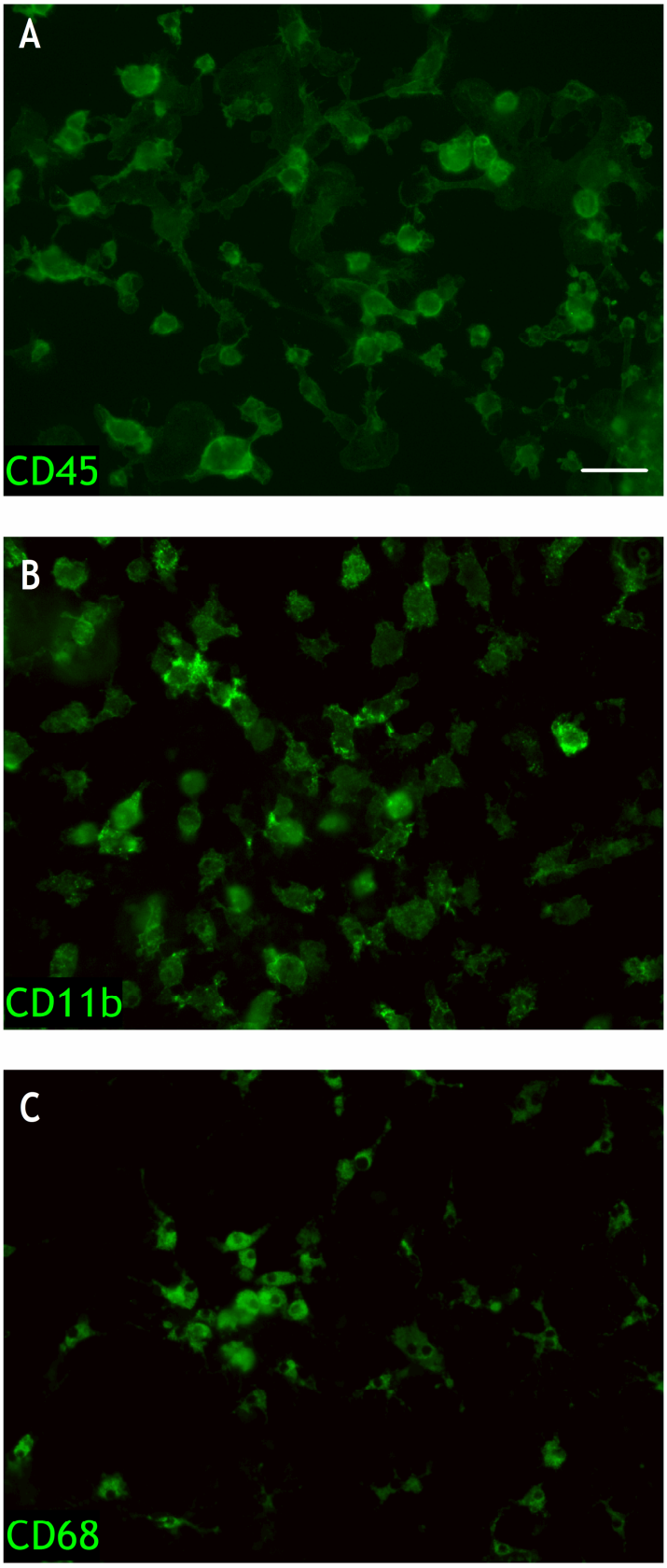

Figure 2: Microglia/macrophage are present in the myelinating cultures at 20 DIV. Micrographs of myelinating cultures stained with (A) CD45, (B) CD11b and (C) CD68 showing the presence of microglia/macrophages within the myelinating cultures. Scale bar 50 μm

3.3.2 Western blot analysis confirms that a myelin-enriched tissue fraction was obtained

To confirm that the tissue fraction obtained from adult mouse spinal cord was enriched for myelin, a sample of wild type 'myelin' emulsion was run alongside a wild type spinal cord total homogenate and analysed using western blot with antibodies against CNP, PLP/DM20, GFAP and NFL-68. Western blots demonstrated higher steady state levels of CNP and PLP/DM20 in the myelin fraction compared to the total spinal cord homogenate (Figure 3, lower two blots). In contrast, GFAP and NFL-68 were enriched in the total spinal cord homogenate (Figure 3, upper two blots), as indicted by the absence of a signal in the myelin containing lane. Therefore, it was concluded that the fraction obtained following the myelin enrichment protocol described in Chapter 2 (subsequently referred to as myelin) was enriched in myelin-specific proteins.

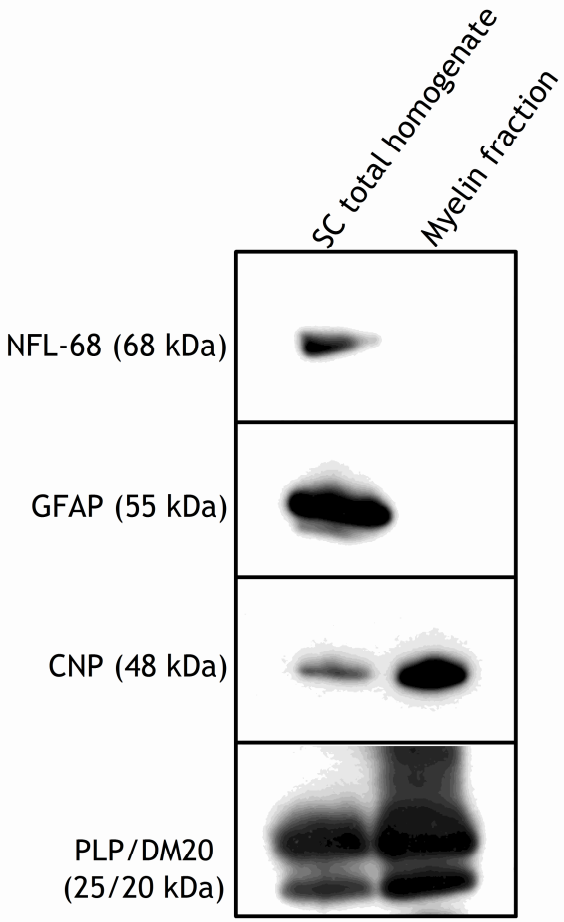

Figure 3: Western blotting of a total and a myelin-enriched tissue fraction. Western blots of 5µg of wild type total spinal cord homogenate and a myelin-enriched tissue fraction generated from adult (P60) wild type spinal cord, showing enrichment of myelin specific proteins in the myelin-enriched tissue fraction. Blots were probed with mouse anti-NFL-68 (68 kDa), rabbit anti-GFAP (55 kDa), mouse anti-CNP (48 kDa) and rabbit 226 antibody (which recognises PLP and DM20, 25 kDa and 20 kDa respectively). Specific myelin proteins were present in both the spinal cord total homogenate and the isolated myelin tissue fraction. However astroglial and neuronal proteins were only detected in the total spinal cord homogenate. Images obtained from exposures of X-ray film for between 1 and 5 minutes.

3.3.3 Myelin is phagocytosed by microglia/macrophages in vitro

To determine if the intrinsic microglial population in the myelinating cultures is capable of phagocytosing myelin debris, cultures were treated with various concentrations of rhodamine-labelled myelin for increasing incubation times. Rhodamine-labelled myelin was visible within CD45 positive cells within 24 hours of treating the cultures, demonstrating that microglia/macrophages phagocytose myelin debris *in vitro* (Figure 4). The rhodamine staining was never observed in the cell nucleus and the pattern appeared punctuate, suggesting that the labelled myelin was contained within endosomes/lysosomes. This was confirmed by co-labelling with an antibody, ID4B, against a lysosomal membrane protein, lysosomal associated membrane protein 1 (LAMP1) (Figure 5).

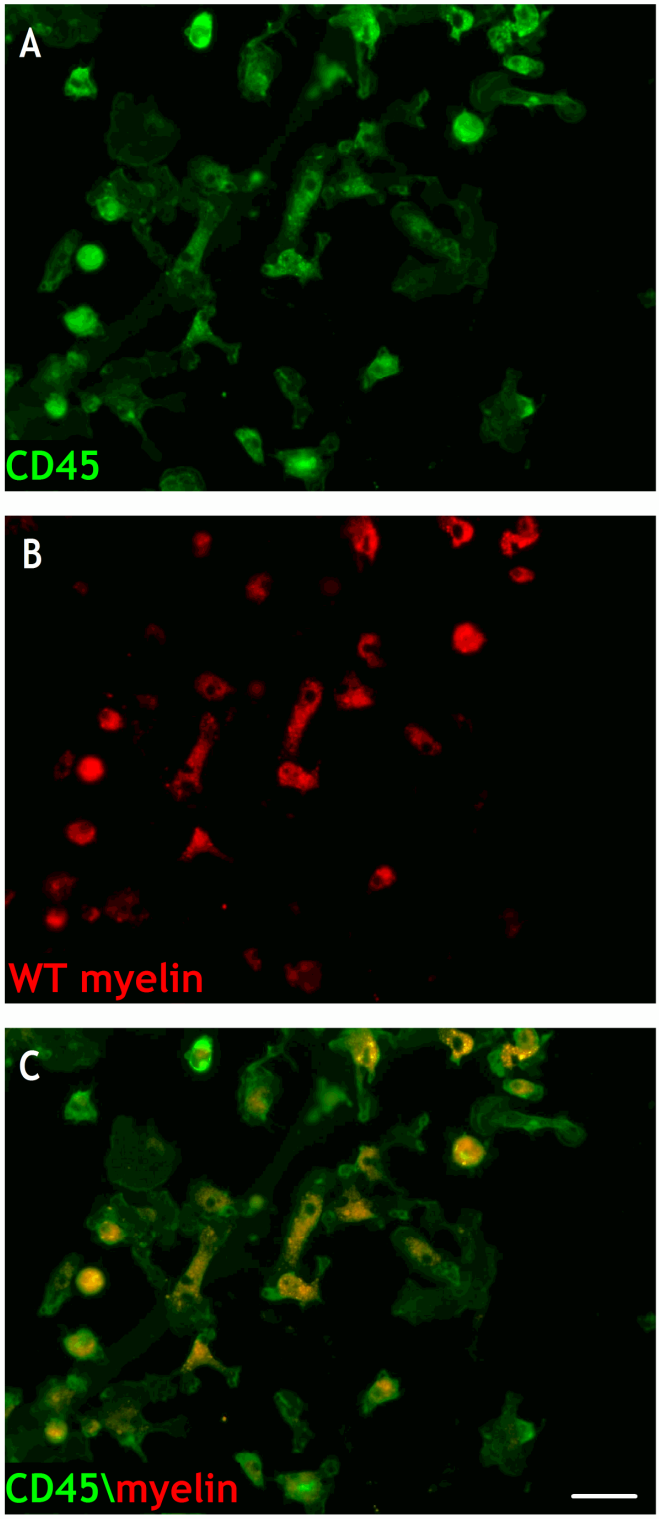

Figure 4: CD45 positive cells phagocytose Rhodamine-labelled myelin *in vitro*. CD45 staining of myelin treated cultures at 27 DIV. (A) FITC labelled CD45 positive cells after incubation with myelin for 7 days. (B) Rhodamine labelled wild type myelin in the same culture. (C) Merge of images (A) and (B) shows co-localisation of the CD45 positive staining and the rhodamine labelled myelin. Scale bar: 50 µm.

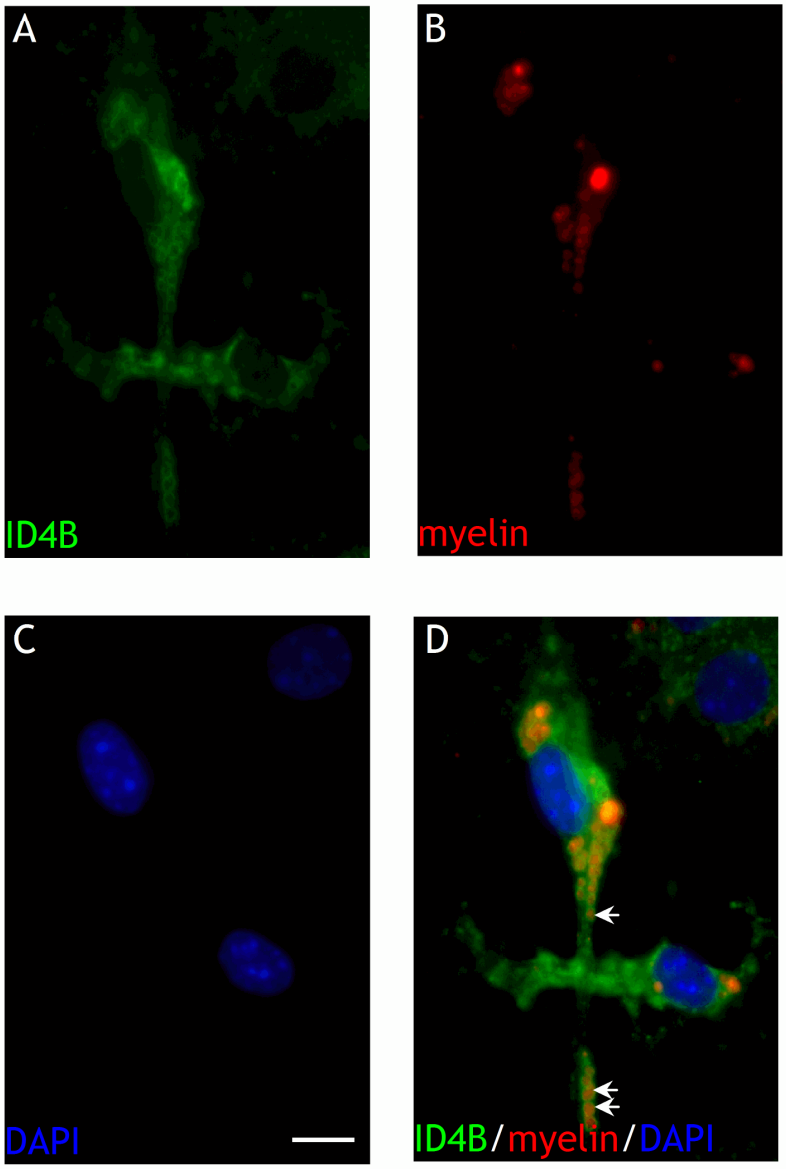

Figure 5: Rhodamine-labelled myelin debris is observed in lysosomes within microglia/macrophages *in vitro*. ID4B staining of cultures treated with rhodamine-labelled myelin at 27 DIV. (A) FITC labelled ID4B positive late endosomes/lysosomes within microglia/macrophages 7 days after treatment with rhodamine-labelled myelin (B). Merge of images (A), (B) and DAPI (C) shows rhodamine-labelled myelin debris within ID4B positive lysosomes (arrows). Scale bar 10 μm

3.3.4 Motile microglia/macrophages take-up myelin in vitro, but do not rapidly degrade it

To visualise myelin uptake and breakdown by the microglia/macrophages *in vitro*, cultures were imaged using time-lapse microscopy in the presence of a low concentration of rhodamine-labelled myelin (see attached CD for video). Time-lapse imaging demonstrated that this cell population was highly motile *in vitro* as illustrated by following a single cell over time (Figure 6 B-G). Within 35 minutes of the addition of myelin to the culture, cells could be observed taking it up. Over the 15 hour imaging period, these cells progressively internalised the myelin debris (Figure 6 B-H). As microglia/macrophages surveyed their environment, they sent out cell processes, apparently to 'pick up' the myelin debris (Figure 6 A). The cell processes then retracted and appeared to pull the debris towards the cell body (Figure 6 B). While the uptake and internalisation of the myelin debris could be observed during the 15 hour imaging period, myelin degradation was not evident.

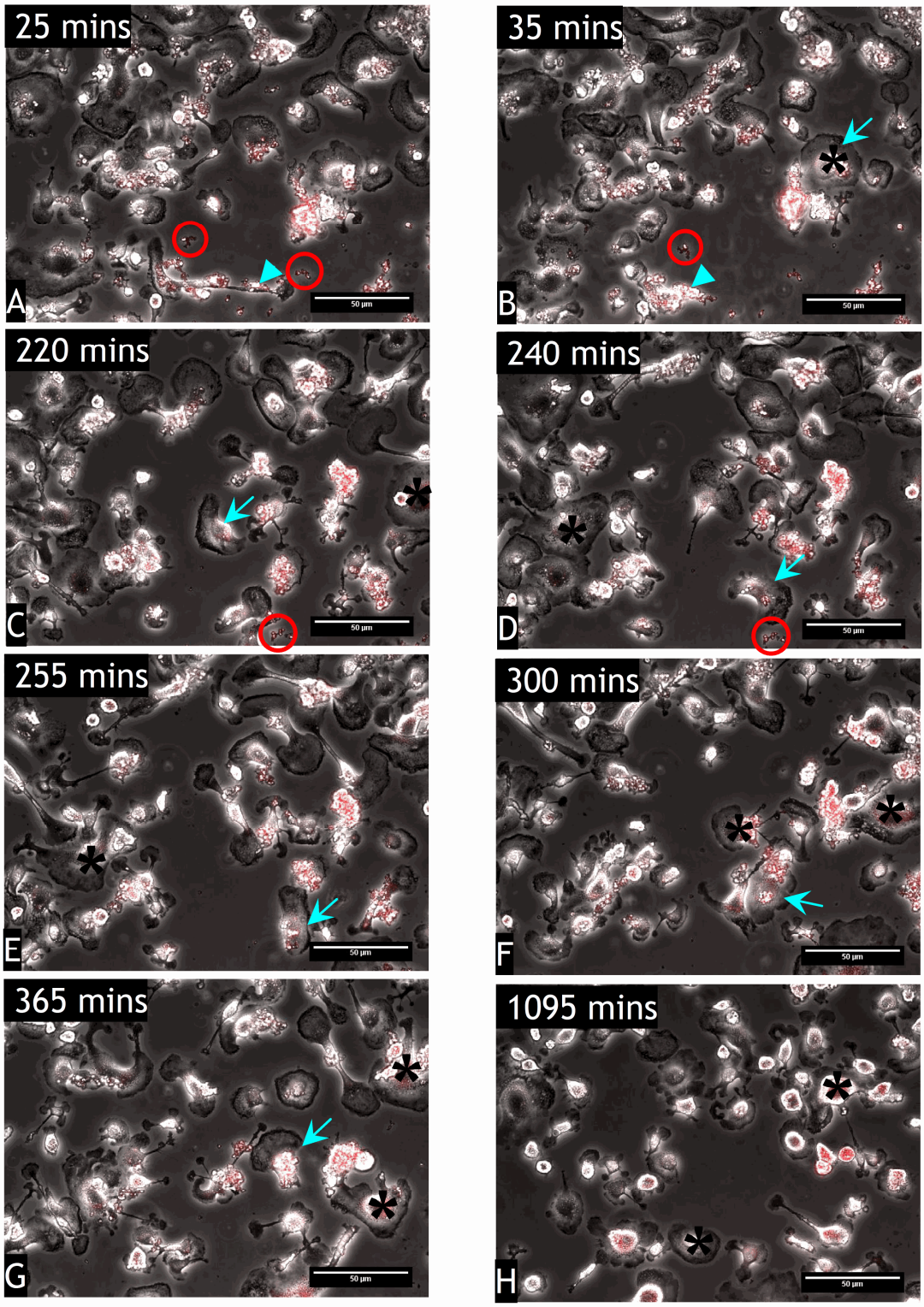

Figure 6: Time lapse imaging of rhodamine-labelled myelin debris treated culture showing myelin uptake and microglia/macrophage motility. Time lapse image stills taken over 1095 minutes showing phagocytosis of labelled myelin fraction (red). Rhodamine-labelled myelin debris (0.05 mg/ml) was added to myelinating cultures at 20 DIV. Images show that some labelled myelin debris is still present at 240 minutes after its addition at time 0 (A-D)(circled). Myelin-containing cells can be observed within 35 minutes of the addition of myelin to the cultures (*) and appear to have completely cleared the myelin debris by 1095 minutes (B-H). The microglia/macrophages are highly motile as they clear up the myelin debris. Using time-lapse, the path of a single cell can be mapped over time (B-G, arrows). Microglia/macrophages can be seen sending out cellular processes as they take up myelin debris (A, arrow heads) and then retract these processes as they pull the myelin debris towards the cell body (B). Scale bar 50 µm.

3.3.5 Quantification of myelin uptake

In order to assess how the phagocytosis of myelin by microglia/macrophages influences their phenotype, the concentration of myelin that represented saturating levels, was first determined. The proportion of CD45 positive cells containing exogenous myelin in cultures treated with increasing amounts of myelin for 24 hours was 25.29 ± 2.14%, 43.95 ± 8.24%, 66.66 ± 10.51% and 65.62 ± 13.22% (mean ± s.e.m; n =2 or 3 per myelin concentration) at 0.025, 0.05, 0.075 and 0.1 mg protein ml^{-1}, respectively. These data suggest that at 0.075 and 0.1 mg protein ml^{-1}, myelin is present at saturating amounts and subsequent studies were undertaken using these concentrations.

The proportion of CD45 positive cells that phagocytosed wild type or *Plp1*-transgenic myelin did not change significantly ($p > 0.05$) with increasing incubation times (Figure 7 A). This, despite the fact that even after incubation for 7 days, myelin debris, which was visible under phase contrast, was still available for phagocytosis.

To determine if myelin debris accumulated or was degraded with increasing incubation times, saturating concentrations of myelin were added to the cultures for 1, 3 or 7 days. The mean area of rhodamine-labelled myelin per CD45 positive cell was calculated, as an approximate measure of steady state levels. The results showed that there was no significant difference ($p > 0,05$) in the mean area of myelin per CD45 positive cell, with increasing myelin concentration or incubation time, in cultures treated with either wild type of *Plp1*-transgenic myelin (Figure 7 B).

Although there were slight differences in the average percentage of CD45 that had incorporated myelin and in the mean area of myelin per CD45 positive cell, between the wild type and the *Plp1*-transgenic myelin treated cultures, this was caused by a low number of CD45/rhodamine positive cells in one of the *Plp1*-transgenic myelin-treated cultures.

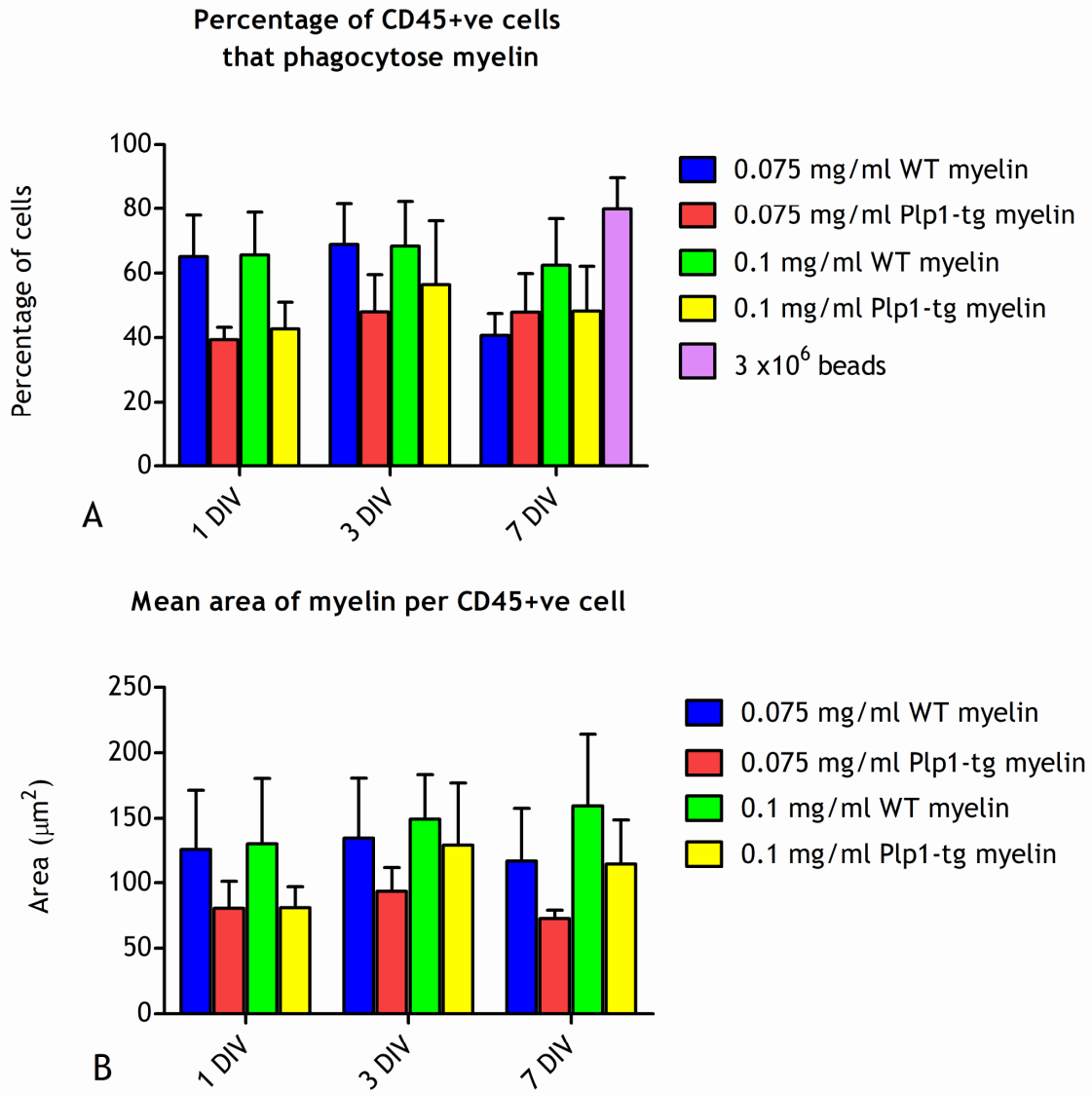

Graph 7: In the presence of saturating amounts of myelin debris the percentage of CD45 positive cells and mean area of myelin per CD45 positive cell in myelin treated cultures is unaltered. (A) After incubation with saturating amounts of myelin debris over three different time points, the percentage of cells that had phagocytosed myelin was calculated. There was no significant change in the percentage of CD45 positive cells that contained phagocytosed myelin with increasing myelin concentration or with increasing time. (B) The mean area of myelin per CD45 positive cell did not change with increasing incubation times, for myelin of either genotype. However, the results only represent the steady state levels of the myelin and do not take account for myelin incorporation or degradation. Bars represent means +s.e.m.. (n = 3 independent experiments per condition).

3.3.6 The phagocytosis of myelin debris does not alter CD45 positive cell morphology or density in vitro

To determine if the phagocytosis of myelin debris led to morphological changes in microglia/macrophages, cultures incubated with saturating concentrations of either wild type or *Plp1*-transgenic myelin on DIV 21 (± 1 day), 25 (± 1 day) or 27 (± 1 day), were assessed on day 28 (± 1 day). Qualitatively, there was no obvious change in CD45 positive cell morphology or density in the myelin or latex–bead treated cultures compared to PBS-treated controls, even after incubation with myelin for 7 days (Figure 8 A-D).

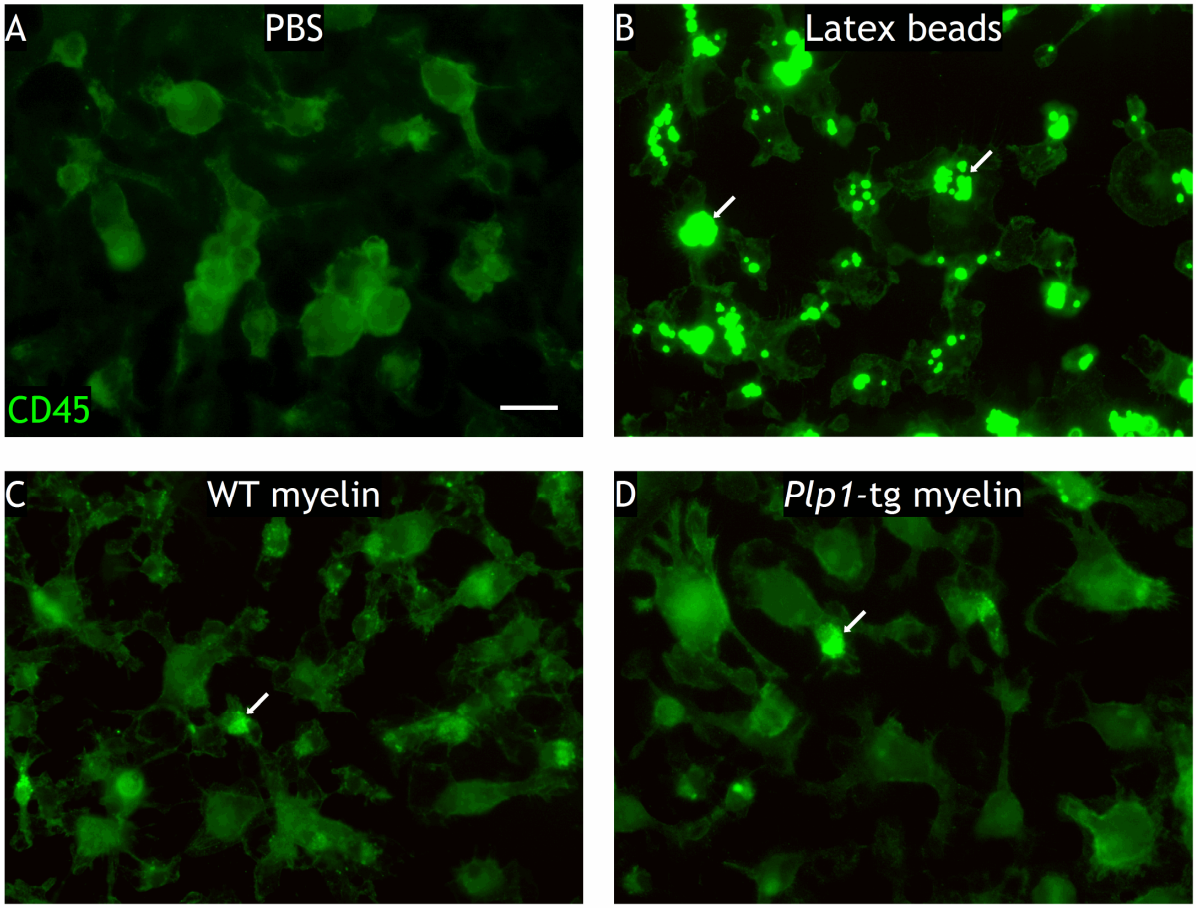

Figure 8: Microglial morphology appears similar in myelin or latex bead-treated cultures compared to PBS-treated control cultures. CD45 staining of cultures treated with PBS, latex beads or rhodamine-labelled wild type or *Plp1*-transgenic myelin for 7 days (A-D) CD45 +ve cell morphology and density appears unaltered in cultures treated with either wild type (WT) (C) or *Plp1*-tg (D) derived rhodamine-labelled myelin debris, compared to latex bead- (B) or PBS- (A) treated controls. Arrows indicate intense staining that is due to bleed-through into the green channel from the latex beads or the rhodamine-labelled myelin. Scale bar 20 μm.

To determine if myelin debris led to proliferation of CD45 positive cells, CD45 positive cell densities were compared between myelin- and bead-treated cultures or between myelin- or bead-treated cultures and PBS-treated controls. The density of CD45 positive cells was similar in cultures treated with saturating concentrations of myelin or with latex beads, after all incubation times. The density of CD45 positive cells in cultures incubated with myelin or latex beads for 7 days, was not significantly ($p > 0.05$) different from that in cultures treated only with PBS (Figure 9 A) suggesting that there was no increase in proliferation of CD45 positive cells in response to the presence or phagocytosis of myelin debris.

To determine if the phagocytosis of myelin debris resulted in a change in cell size, the average area per CD45 positive cell was determined. The mean area per CD45 positive cell was similar in myelin or latex-bead treated cultures after all incubation times (Figure 9B). The mean area per CD45 positive cells in cultures incubated with myelin or latex beads for 7 days was not significantly different ($p > 0.05$) from that in cultures treated only with PBS (Figure 9B). This was consistent for cultures treated with either the wild type or *Plp1*-transgenic derived myelin debris. These results suggested that the phagocytosis of a myelin-enriched fragment per se was not sufficient to cause a change in CD45 positive cell size, an indicator of activation.

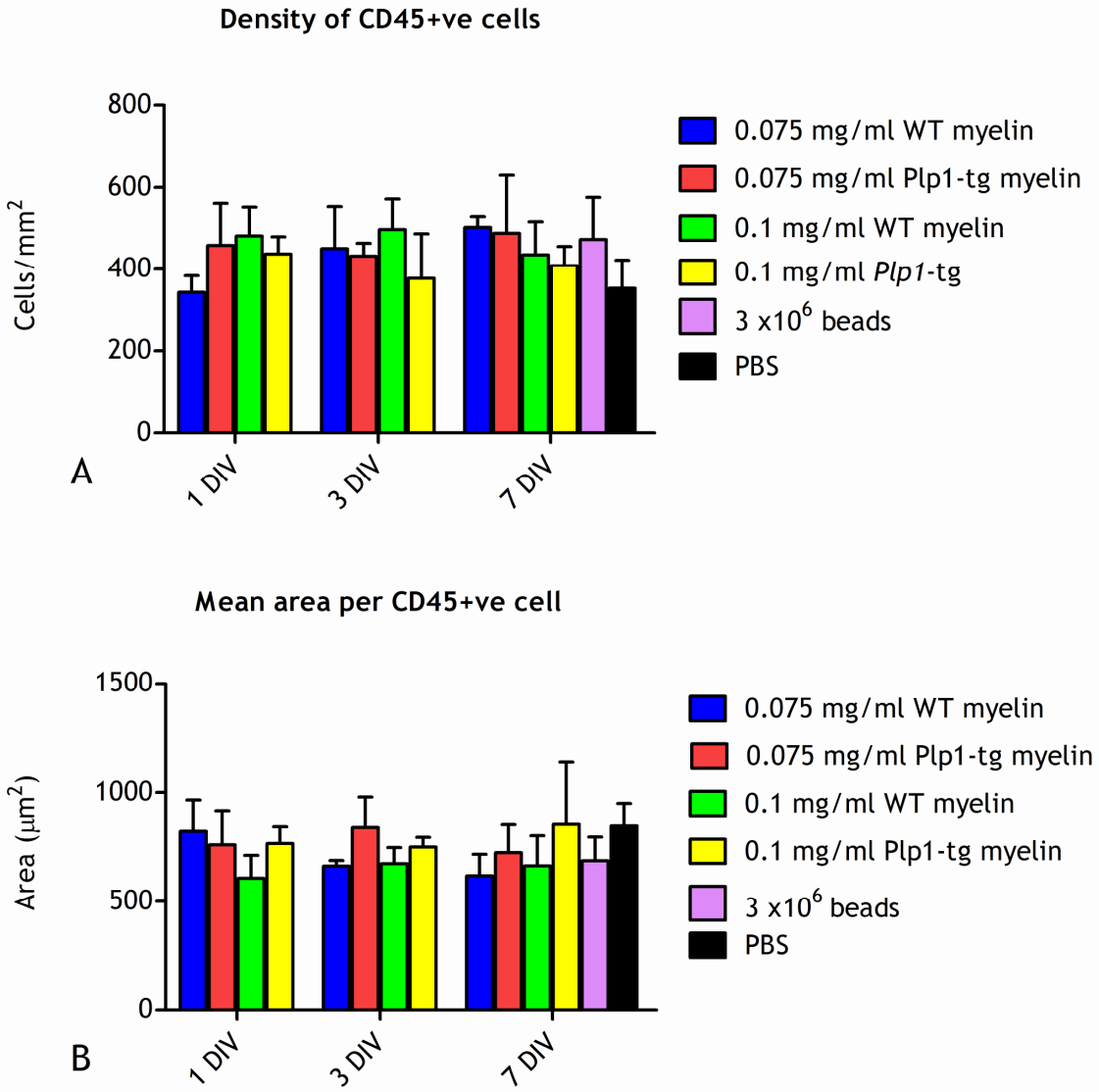

Figure 9: The phagocytosis of myelin has no effect on CD45+ve cell density or cell size. (A) The density of CD45 +ve cells was similar in cultures incubated with rhodamine-labelled myelin or with latex beads, for 1, 3 or 7 days. Statistical analysis showed that there was no significant change in the density of CD45 positive cells in the myelin or bead-treated cultures compared to the PBS treated controls, 7 days after treatment of the cultures. (B) Mean area per CD45 positive cell was similar in myelin and bead treated cultures after all incubation times. There was no significant difference in the mean area per cell in cultures treated with myelin or latex beads for 7 days, compared to PBS-treated control cultures. Bar represent means +s.e.m.. (n = 3 independent experiments per condition).

3.3.7 Microglia/macrophages in the myelinating cultures acquire an altered morphology after stimulation with endotoxin.

In light of the observations described above, it was important to determine if the microglia/macrophages in the myelinating culture system were already maximally activated as a result of the culture process, and therefore insensitive to stimulation. To test this, cultures were treated with LPS. In contrast to cultures treated with myelin debris or with PBS alone (Figure 10 A-B), there was an obvious change in the morphology of microglia/macrophages in LPS-treated cultures, whether the cells were previously treated with or without myelin (Figure 10 C-D). LPS-stimulated cells adopted a darker and more 'jagged' appearance compared to non-stimulated PBS-treated controls, when imaged under phase-contrast. Immunostaining with an antibody against CD45 confirmed the morphological changes were in the CD45+ve cell population (Figure 11).

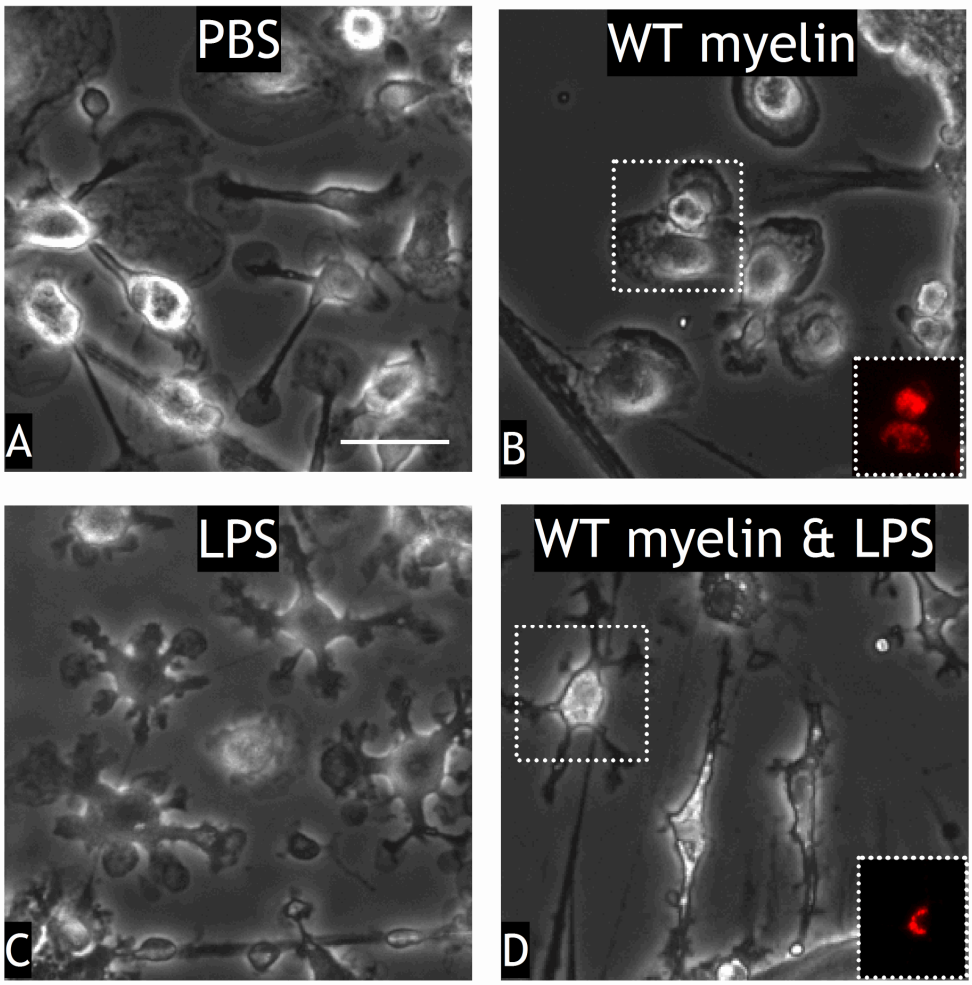

Figure 10: Lipopolysaccharide (LPS) induces morphological changes in cells resembling microglia/macrophages *in vitro*. Phase images of microglia/macrophages in myelinating cultures treated with either (A) PBS, (B) wild type (WT) myelin debris, (C) 100 ng/ml LPS or (D) myelin debris followed by 100 ng/ml LPS. There is no obvious change in microglia/macrophage morphology in cultures treated with myelin debris (B) compared to PBS treated controls (A). In both conditions the cells have an amoeboid appearance. However, after incubating with LPS there is an obvious morphological change in the microglia/macrophage from an amoeboid to a more 'jagged' appearance (C). This morphological change was observed in cultures treated with LPS in the presence or absence of myelin debris. Scale bar 50 μm.

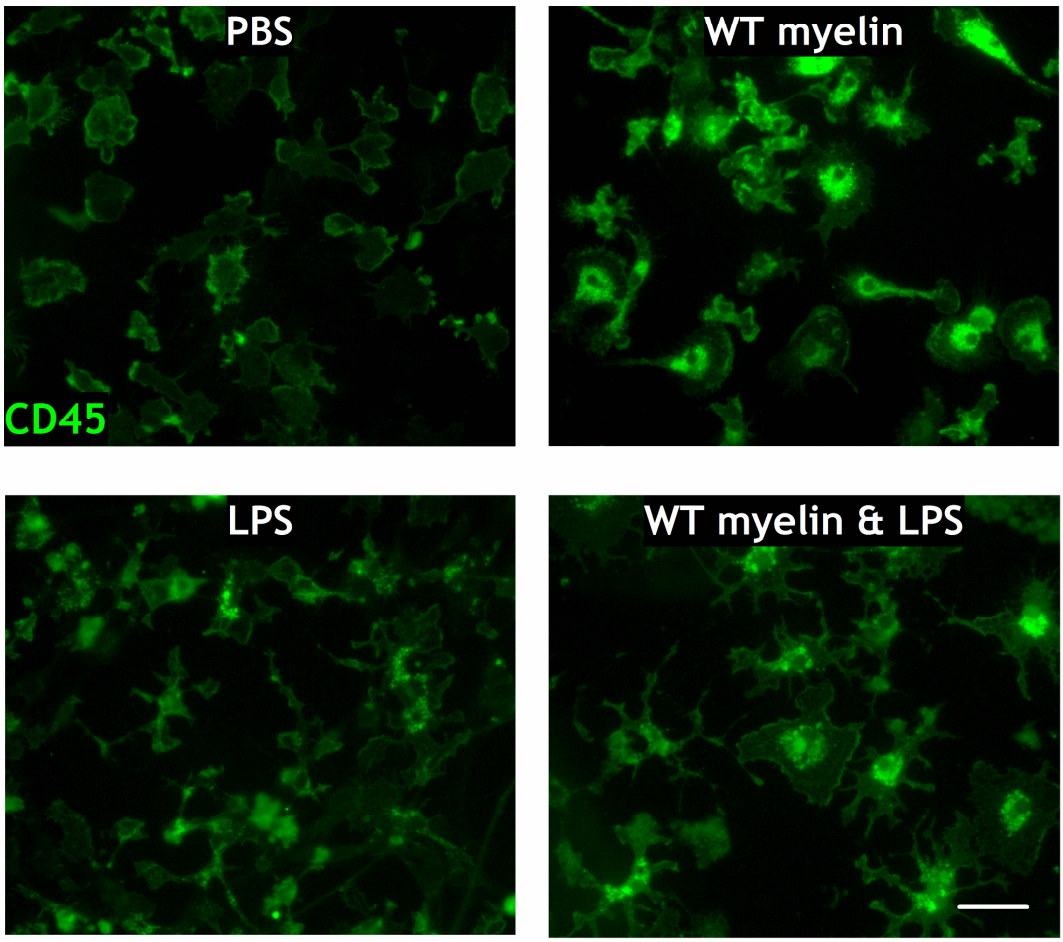

Figure 11: Lipopolysaccharide (LPS) induces morphological changes in CD45 positive cells *in vitro*. Images of CD45 stained cells in myelinating cultures. Cultures were treated with either (A) PBS, (B) WT myelin debris, (C) 100 ng/ml LPS or (D) myelin debris followed by 100 ng/ml LPS. There is no obvious change in CD45 positive cell morphology in cultures treated with myelin debris (B) compared to PBS treated controls (A),. However, after incubation with LPS there is an obvious morphological change in the microglia/macrophages (C). This morphological change was observed in cultures treated with LPS in the presence or absence of myelin debris. Scale bar 50 μm.

3.4 Discussion

The principal aim of this chapter was to optimise conditions for obtaining myelin-laden microglia/macrophages in the myelinating culture system. The system was then used to characterise a number of parameters (Perry et al., 2010;Walter and Neumann, 2009) to determine if the phagocytosis of an enriched myelin fraction was sufficient to cause morphological and proliferative changes in this population. The data presented in this chapter demonstrated that microglia/macrophages efficiently phagocytose exogenous myelin debris. However, there was no evidence that this led to changes in morphology or proliferation that are generally associated with 'activation' of these cells.

It was confirmed that the spinal cord parenchyma of the E13 mouse embryos contained microglia, as shown previously (Rigato et al., 2011). Therefore it can be concluded that at least a proportion of the CD45 positive cells in the myelinating cultures, were resident microglia. However, some contamination of the cultures by peripheral monocytes, present in blood vessels and in the sub-arachnoid space was likely.

Once it was established that the CD45 positive cells were capable of phagocytosing myelin debris, the concentration of myelin that represented saturating amounts was determined. As demonstrated previously (Hikawa and Takenaka, 1996) phagocytosis occurred in a 'dose-dependent' fashion, such that increasing myelin concentrations resulted in an increase in the proportion of myelin-containing CD45 positive cells. At concentrations equal to or above 0.075 mg/ml, the percentage of CD45 positive cells that incorporated myelin debris attained maximum levels.

The data suggest that only a proportion of CD45 positive cells phagocytosed myelin debris, even after incubation with saturating amounts of myelin for 7 DIV. This probably partly reflects the fact that after fixation and permeabilisation, the rhodamine signal faded, making some of the myelin

invisible. Indeed, observation of the cultures prior to fixation indicated that most cells with the morphology of microglial/macrophages contained at least some rhodamine labelled myelin. Since CD45 is a pan-leukocyte marker, it is also possible that the cultures were contaminated by T or B-lymphocytes. However, immunostaining with an antibody against CD3, which stains T-cell lymphocytes, showed very few (only 2 or 3 cells per 13 mm diameter cover slip) T-cells were present. B-lymphocytes were not specifically examined, but in the absence of significant numbers of T-lymphocytes, it seems unlikely that B-lymphocytes contributed.

In the presence of saturating amount of myelin debris there was no change with increasing time, in the area of myelin per CD45 positive cells. This could indicate that myelin debris is being taken up and broken down at a similar rate. Alternatively, if it is assumed that maximum uptake is attained within 1 DIV, the cells could begin to regulate the rate of myelin phagocytosis and degradation with simultaneous activation and down-regulation of the microglial/macrophage response (Gitik et al., 2011). (Gitik et al., 2011) and colleagues showed that, while activation of phagocytosis occurred following the binding of myelin to complement receptor-3 on the microglial cell surface, phagocytosis could also be down-regulated by the binding of myelin CD47 epitope to the immune inhibitory receptor signal regulatory protein-α (SIRPα), which also resides on the cell surface. Attempts were made to examine the dynamics of myelin uptake and degradation using time-lapse imaging. However myelin breakdown was not observed during the 15 hour image capture period, therefore it was not possible to draw a definitive conclusion.

To assess the putative effects of phagocytosis of myelin on microglia/macrophages population *in vitro*, cultures were treated with either wild type or *Plp1*-transgenic myelin. This was done to determine if the *Plp1*-transgenic myelin, which is biochemically abnormal (Karim et al., 2007) had a different effect compared to wild type myelin. In fact, no difference was observed in cell size, density or morphology whether the cells were treated with myelin of either type compared with PBS alone.

To exclude the possibility that the microglia/macrophages within the myelinating cultures were insensitive to stimulation, due to being maximally 'activated' as a result of the culture procedure alone, the cultures were treated with LPS (Domercq et al., 2007). A previous study, in which isolated neonatal rat microglia were treated with a low dose of LPS, showed dramatic changes to microglia cell morphology within 3 hours of incubation (Nakamura et al., 1999). In that study it was found that peak stimulation with LPS was at 6 hours when many cells had changed from an "amoeboid shape to a bipolar rod shape" (Nakamura et al., 1999). Treating the myelinating cultures used in the current study with LPS showed similar marked change in cell morphology, suggesting that the microglia/macrophages in the culture system remained sensitive to 'activating' stimuli.

The 'activation' of microglia as a result of the phagocytosis of CNS glial membranes *in vitro* is associated with phenotypic changes including increased proliferation, increased phagocytic activity and change in morphology (Beyer et al., 2000). In contrast, in the myelinating cultures used in the current study, no obvious change in CD45 positive cell morphology and no significant change in density or size of the CD45 positive cells, was observed, even after incubation in saturating amounts of myelin for up to 7 days. Also, in contrast to earlier findings (Beyer et al., 2000), there was no evidence that the phagocytosis of latex beads led to a change in the morphology of microglia/macrophages within the myelinating culture system.

The difference between the results obtained in Beyers' study and in the current study may arise for two reasons. First, (Beyer et al., 2000) treated cultures with isolated cellular membranes from either neuronal or glial origin while the cultures in the current study were incubated with an isolated enriched myelin fraction. Secondly, in contrast to the studies of (Beyer et al., 2000) and others (Williams et al., 1994;Boven et al., 2006), in which murine or human derived microglia/macrophages were cultured in isolation, the myelinating culture system is a mixed cell culture in which microglia/macrophages reside along with other neural populations

With this in mind, the single cell-type system (Beyer et al., 2000) is less similar to the *in vivo* situation, in which multiple cell types interact, than the system used in the current study. It is possible that isolated microglia/macrophages respond differently to stimuli compared to microglia in mixed cell culture. Certainly, there is cross-talk between cells of the immune system and neural cells (Kerschensteiner et al., 2009) that could potentially influence the responses of microglia/macrophages. There is increasing evidence that the dual role of the immune system, which can shift from a neurotoxic to a neuroprotective phenotype, is a result of overlapping cross-talk from factors secreted by both the immune (cytokines/chemokines) and nervous (neurotrophic factors) systems, neither of which is exclusive to either system (Kerschensteiner et al., 2003).

Previous studies investigating the effects microglia/macrophage 'activation' as a result of phagocytosis showed that the phagocytosis of human derived myelin could drive microglia/macrophages towards either a pro- (Williams et al., 1994) or anti-inflammatory (Boven et al., 2006) response. In these studies, microglia/macrophage 'activation' was measured by cytokine/chemokine secretion and not by a change in cell density or morphology. The cytokine/chemokine profile of the myelin-laden microglia in the current study will be described in Chapter 5.

From the *in vitro* characterisation of the CD45 positive microglia/macrophages, it can be concluded that the phagocytosis of a myelin-enriched tissue fraction does not cause morphological and proliferative changes that are generally associated with microglial/macrophage activation. Nonetheless, the process of isolating the spinal cord cells and maintaining them under cell culture conditions is itself, likely to change the phenotype of the cells and this could potentially mask subtle alterations.

4 The effects of myelin-laden microglia/macrophages on neuritic integrity in an *in vitro* model of myelination

4.1 Introduction

Axonal loss is the main determinant of permanent neurological disability in MS (Ferguson et al., 1997;Bjartmar et al., 2003;Trapp et al., 1998b) However, there remains uncertainty regarding the nature of the cellular factors that elicit axonal injury. In the *Plp1*-overexpressing mouse, a non-immune mediated model of demyelination, sites of acute axonal changes are most prevalent in regions of active demyelination where microglia/macrophages are phagocytosing myelin debris (Edgar et al., 2010) raising the possibility that myelin-laden microglia/macrophages are axono-toxic. However, the literature regarding myelin-laden macrophages is contradictory, with both pro-inflammatory (potentially axono-toxic) and anti-inflammatory (potentially axono-protective) properties having been demonstrated ((van der Laan et al., 1996;Williams et al., 1994;Boven et al., 2006;Mosley and Cuzner, 1996)). The results presented in Chapter 3 demonstrated that in an *in vitro* model of myelination, microglia/macrophages phagocytose an exogenous myelin-enriched tissue fraction. Here I used this mixed neural cell system to assess if myelin-laden microglia/macrophages exert either axono-toxic or axono-protective effects *in vitro*. The aims of this chapter were:

1. To develop a sensitive method for assessing and quantifying neuritic injury *in vitro*

2. To determine if myelin-laden microglia/macrophages injure or protect adjacent myelinated and non-myelinated CFP expressing neurites in an *in vitro* model of normal or inflamed CNS white matter.

4.2 Methods

4.2.1 Generation of myelinating cultures

Myelinating cultures were established from spinal cords of E13 *Thy1*-CFP mouse embryos and their wild type littermates, as described in Chapter 2.2.

4.2.2 Generation of myelin-laden microglia/macrophages

At 21 (± 1) DIV a sterile myelin-enriched tissue fraction, derived from either wild type or *Plp1*-tg mice (Chapter 2.4), was added directly to culture medium at a final concentration of 0.1 mg/ml. Cultures were incubated with myelin debris for 1 or 7 days, to determine if myelin-laden microglia-macrophages were detrimental to neighbouring neurites (Chapter 2.4.3), or for 3 days to generate myelin-laden 'foamy' microglia/macrophages to assess their putative axono-protective affects in the presence of LPS (Chapter 2.4.4).

4.2.3 Quantification of neuritic integrity

Cultures treated with (i) wild type or *Plp1*-tg myelin debris (Chapter 2.4.3) or (ii) myelin debris then LPS (Chapter 2.4.4) were immunostained with antibodies to GFP (which recognises CFP) and MBP. Neuritic integrity and neurite density was assessed and quantified in minimum of three independent experiments (Chapter 2.6.3). The integrity of CFP and non-CFP expressing neurites in an LPS-treated and PBS-treated culture was assessed following staining with an antibody (SMI31) against phosphorylated neurofilament (Chapter 2.5)

4.2.4 Hydrogen peroxide (H_2O_2) treatment of cultures

Myelinating cultures at 21 DIV (± 2 days) were treated with 100 mM of 30% hydrogen peroxide (H_2O_2) (Nikic et al., 2011) or PBS for 1 hour.

4.2.5 Statistical analysis

Neuritic changes after incubation with the myelin-enriched tissue fraction (wild type and *Plp1*-transgenic) or LPS, in the presence or absence of myelin-laden microglia/macrophages, were analysed using one way ANOVA. Comparisons between the myelin treated, LPS treated or both myelin and LPS treated cultures and the PBS treated controls were made using a Dunnett's multiple comparison test. Significance was set at $p < 0.05$.

4.3 Results

4.3.1 Cyan fluorescent protein as a sensitive marker of neuritic integrity

Yellow fluorescent protein (YFP), an analogue of GFP, is a very sensitive marker of axonal changes, *in vivo* (Bridge et al., 2007). To determine if CFP is a sensitive marker of neuritic integrity *in vitro*, cultures were immunostained with antibodies to CFP and to phosphorylated neurofilaments (SMI31). Both markers label neuronal processes, including axons.

Comparison of double labelled cultures showed that CFP was only expressed in a subset of neuronal processes, allowing individual neurites to be visualised over long distances (Figure 12 A). In contrast, SMI31 labelled many more neurites, making identification of individual fibres (especially over a distance) difficult (Figure 12B). CFP is not expressed in the embryo and therefore the proportion of embryos that were CFP positive could not be determined. However, based on Mendelian genetics, on average 50% of embryos should express the transgene, which is expressed in a subset of neurons (Feng et al., 2000).

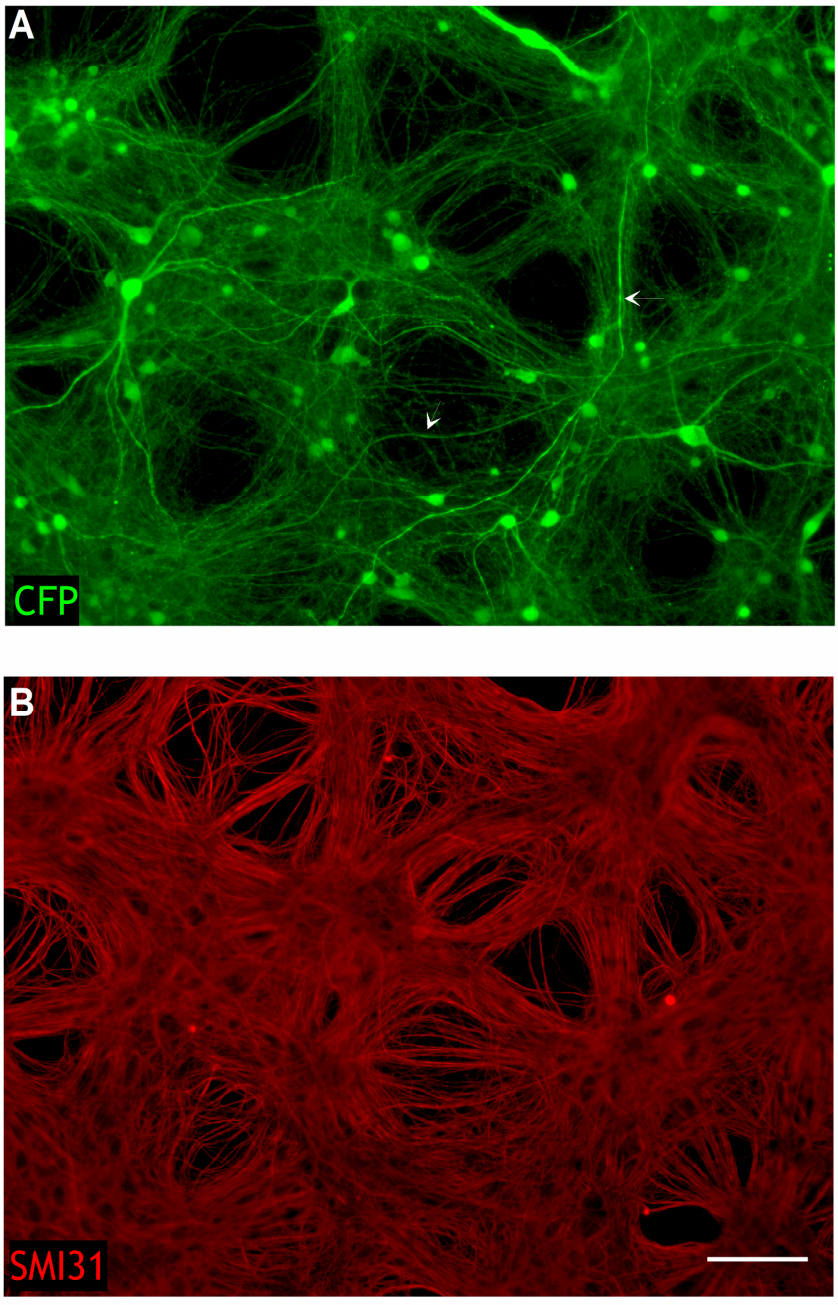

Figure 12: Individual CFP positive neurites can be visualised over long distances. Micrographs of a myelinating culture at 25 DIV stained with antibodies to (A) GFP (an analogue of CFP) and (B) SMI31 (a marker of phosphorylated neurofilament). CFP is expressed in a subset of neurons only, allowing individual neurites to be visualised over long distances (arrows). In contrast, neurofilament stained neurites are too densely packed to permit visualisation of individual fibres. Scale bar 50 μm

The expression of fluorescent proteins in neurons can subtly alter the neuron's response to injury (Comley et al., 2011). To confirm that CFP-rendered neurons are susceptible to injury *in vitro*, cultures were treated with H_2O_2, which has previously been shown to induce axonal injury *in vivo* (Nikic et al., 2011). In cultures treated with 100 m*M* H_2O_2 for 1 hour, neurites appeared (i) transected and (ii) developed numerous large focal swellings, or (iii) appeared fragmented, in some cases to the extent that individual neurites could not be discerned (Figure 13). This confirms that CFP expressing neurons are susceptible to injury and demonstrates that morphological changes in CFP positive neurites are a useful indicator of injury.

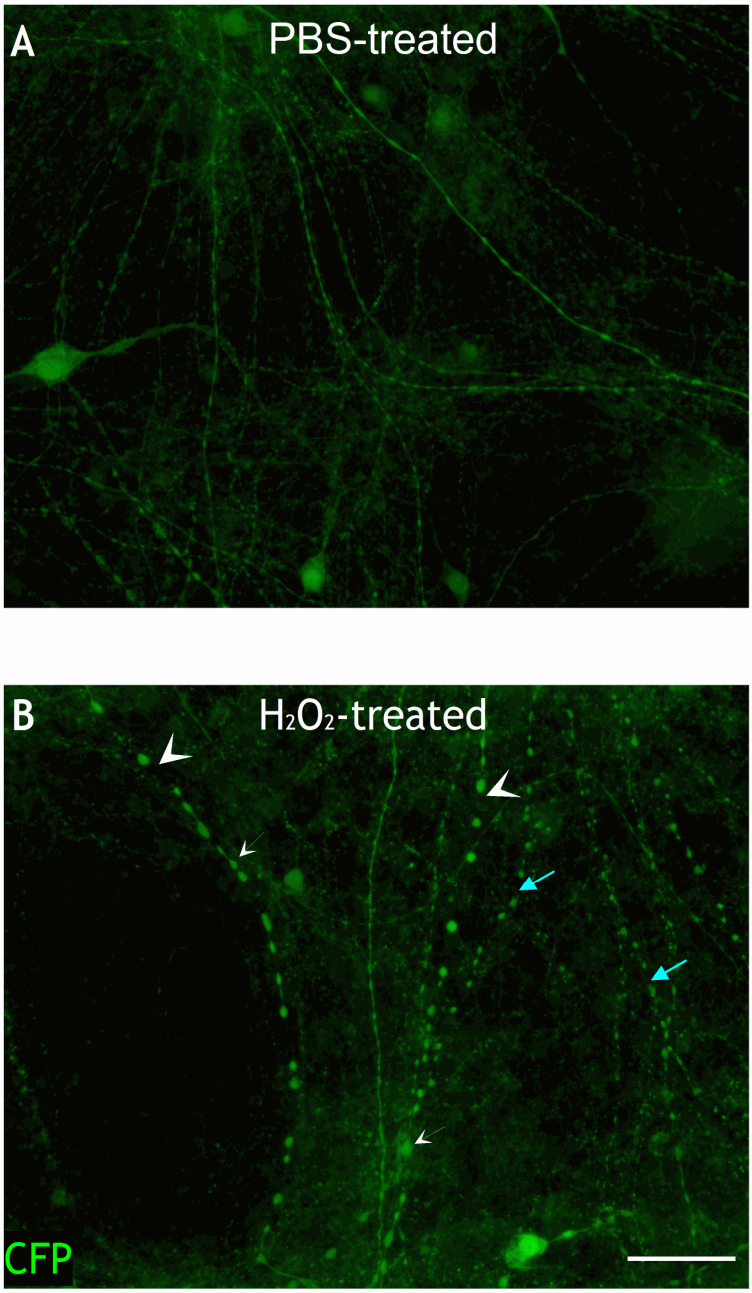

Figure 13: CFP-rendered neurites are susceptible to injury. At 22 DIV, cultures were treated with either (A) PBS or (B) 100 mM H_2O_2 for 1 hour then fixed and stained with an antibody to GFP (an analogue of CFP). Cultures treated with H_2O_2 developed signs of neuritic injury including (i) transection (arrowheads) and (ii) large focal swellings (small white arrows) or (iii) fragmentation (small blue arrows) when compared to PBS treated controls. Scale bar 50 μm.

Since putative microglial-mediated neuritic injury could potentially occur secondarily to oligodendroglial injury, it was important to determine if CFP positive neurites were myelination competent. Double labelling of DIV 27 cultures with antibodies to GFP and MBP showed that both non-myelinated and ensheathed/myelinated CFP positive neurites were present throughout the culture (Figure 14).

Together, these results confirm that CFP expression in neurites provides a valuable tool for assessing neuritic injury.

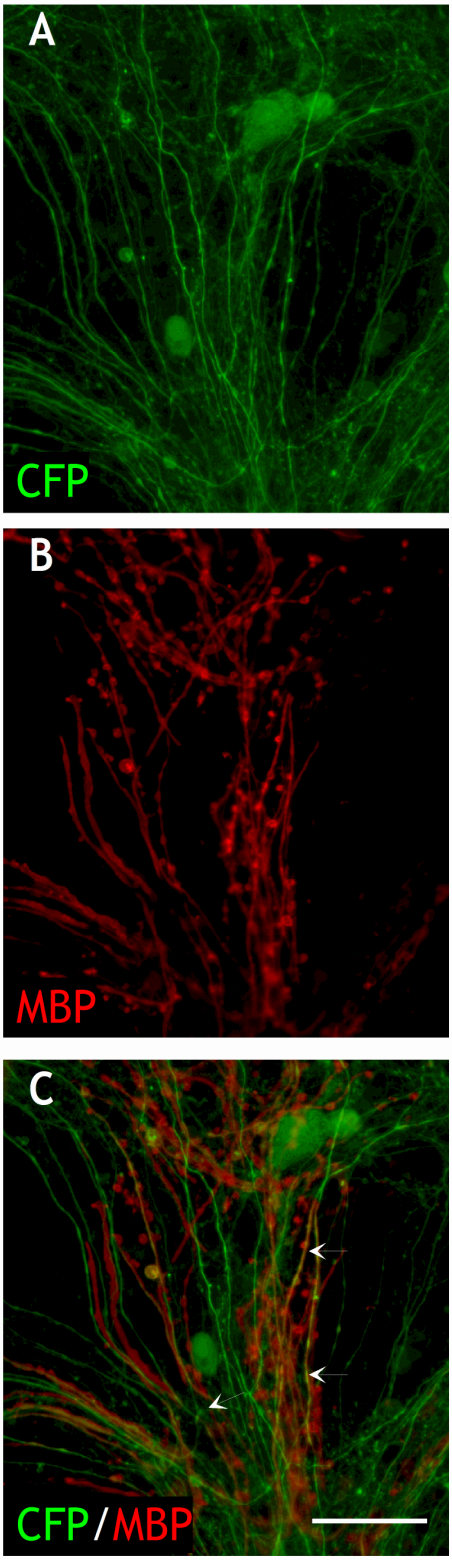

Figure 14: CFP positive neurites are myelination competent *in vitro*. Micrographs of cultures at 27 DIV stained with antibodies to (A) GFP (an analogue of CFP) or (B) myelin basic protein (MBP), showing both relatively mature (smooth) and immature (incomplete) sheaths. (C) Overlay of images (A) and (B) shows co-localisation of GFP and MBP, indicating myelin-like sheaths around axons (arrows) demonstrating that the CFP expressing neurites are myelination competent. Scale bar 50 μm.

4.3.2 Assessing neuritic integrity in cultures incubated with myelin debris

To determine if myelin-laden microglia/macrophages elicit injury to neurites, neuritic changes were quantified in cultures treated for 1 or 7 days with 0.1 mg/ml of either wild type or *Plp1* transgenic myelin. Neurites were examined and characterised as (i) normal, (ii) beaded (small focal swellings <20 μm2 along otherwise intact neurites), (iii) degenerate/transected (fragmented or severed) or (iv) focally swollen but intact (swellings greater than 20 μm2) (Figure 15) and further characterised as myelinated/ensheathed or non-myelinated. At DIV 28 (±1 DIV) many CFP positive neurites, even in control cultures, appeared beaded suggesting that this morphological feature was not a useful marker of injury. Therefore only swollen or degenerating/transected neurites were considered to be injured.

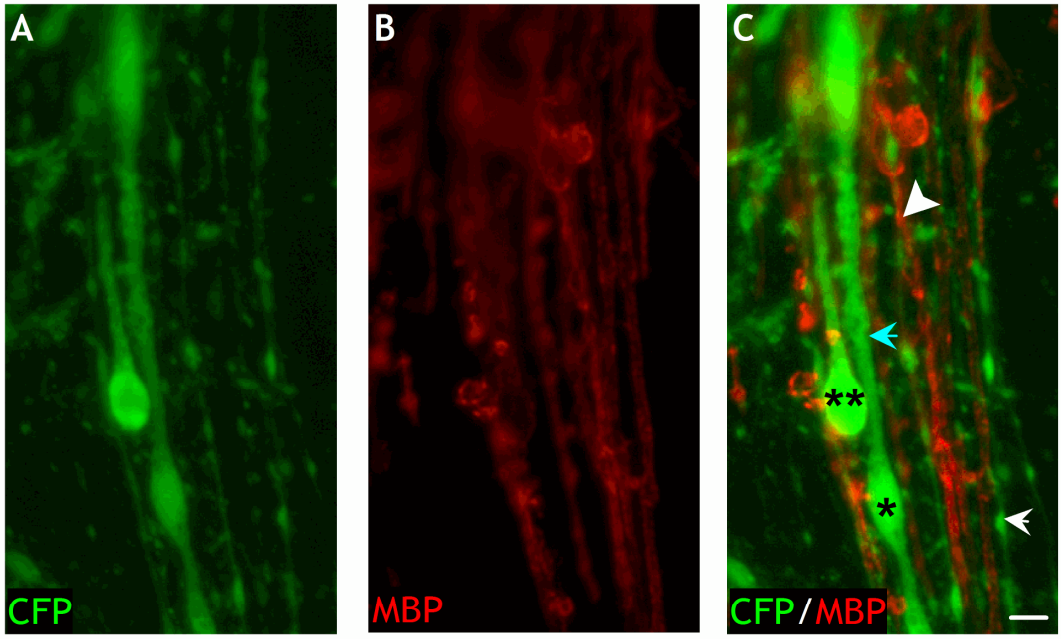

Figure 15: CFP-rendered neurites indicating various categories of neuritic changes. Micrographs of cultures at 27 DIV stained with antibodies to (A) GFP (an analogue of CFP) and (B) myelin basic protein (MBP), showing categories of neuritic changes synonymous with injury. Neurites were categorised as myelinated (arrowhead) or non-myelinated (blue arrow) (C). The neurites were then categorised by the degree of neuritic change, either beaded (swellings < 20 μm^2; arrow), containing swellings (>20 μm^2; *) or degenerating/transected (**). Bar 20 μm

At 28 (± 1) DIV in the presence of saturating amounts of myelin, in all treatment conditions and incubation times, a proportion (no more than 20 %) of neurites contained focal swellings >20 μm2, signs of transection or early indication of degeneration. However, there was no significant difference ($p > 0.05$) in the proportion of neurites containing changes in myelin or latex bead-treated cultures compared to PBS treated controls (Figure 16A and B). To test if neurite survival was altered in myelin-treated cultures, neuritic densities were quantified. Neuritic density also remained unaltered in myelin- or latex bead-treated cultures compared to PBS-treated controls (Figure 16C and D) ($p > 0.05$).

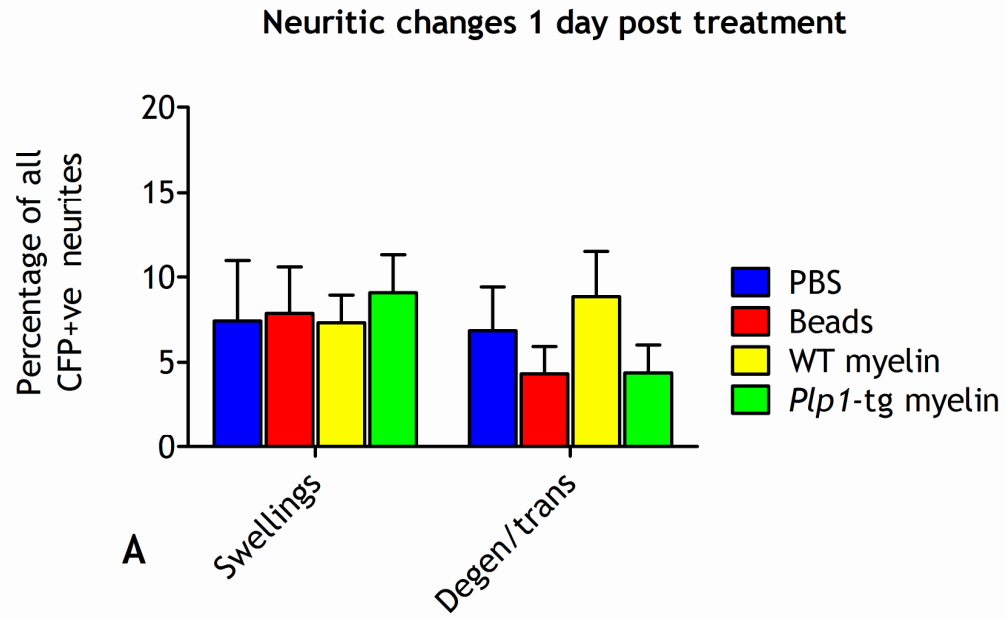
Neuritic changes 1 day post treatment
Percentage of all CFP+ve neurites
20
15
10
5
0
Swellings
Degen/trans
PBS
Beads
WT myelin
Plp1-tg myelin
A

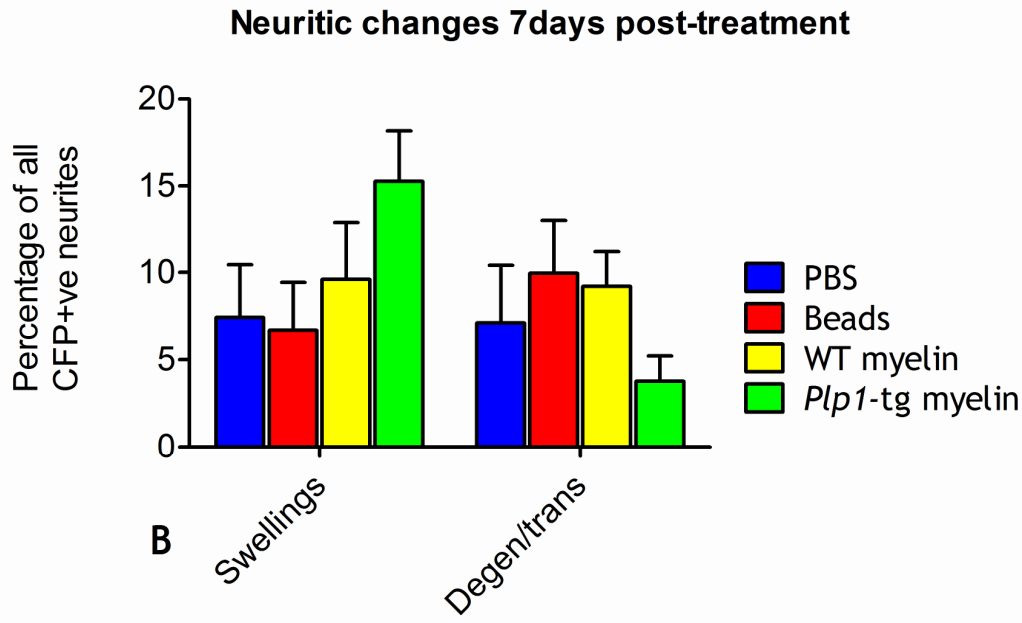
Neuritic changes 7days post-treatment
Percentage of all CFP+ve neurites
20
15
10
5
0
Swellings
Degen/trans
PBS
Beads
WT myelin
Plp1-tg myelin
B

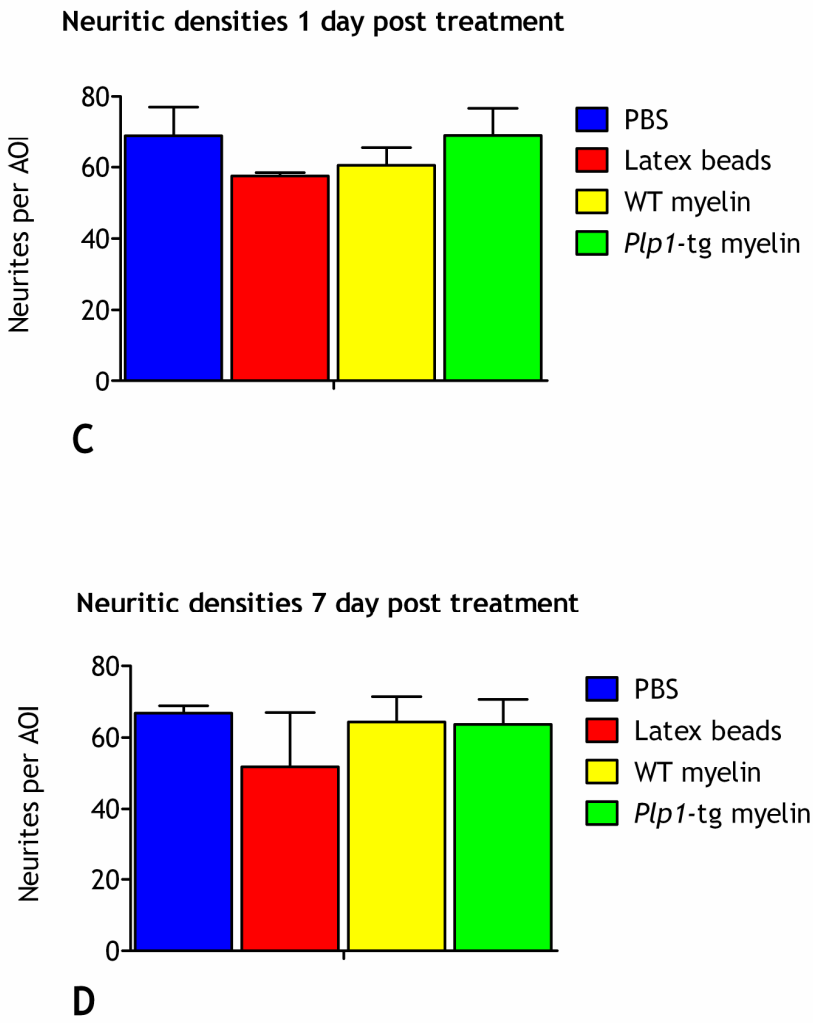

Figure 16: Quantification of neuritic changes and neuritic densities in myelin treated cultures compared to latex bead and PBS-treated controls. Cultures were treated with 0.1 mg/ml of wild type or *Plp1*-tg myelin at 20 DIV for either 1 or 7 days. **(A)** and **(B)** Graphs indicating mean percentages of all neurites (+ s.e.m). After incubation with either wild type or *Plp1*-tg myelin for 1 or 7 days the percentage of all (myelinated and non-myelinated) CFP positve neurites which showed signs synonymous with injury, were quantified. No statistically significant change was observed in the percentage of CFP positive neurites showing signs of swellings or degeneration in myelin or latex bead-treated cultures compared to PBS-treated controls at either time point. **(C)** and **(D)** Graphs indicating mean neuritic numbers per AOI (+ s.e.m). Neuritic densities were similar in all culture conditions, and after both1 and 7 days of treatment, demonstrating that there was no loss of neurites in myelin or latex bead-treated cultures compared to PBS-treated controls.

4.3.3 The effects of lipopolysaccharide stimulation of myelin-laden microglia/macrophages on neuritic integrity in vitro

Since no evidence was obtained to support the suggestion that myelin-laden microglia/macrophages were axono-toxic, the putative neuro-protective/anti-inflammatory effect of myelin-laden cells in an inflammatory environment, was assessed. Cultures were treated with PBS alone or with a saturating concentration of myelin debris for 3 DIV then stimulated for 48 hours with LPS. Previously, stimulation of microglia/macrophages with LPS resulted in morphological alterations associated with 'activation' of this population (Chapter 3.3.8). Neuritic changes were not more prevalent in cultures stimulated with LPS, either with or withour myelin-laden microglia than in non-LPS stimulated cultures ($p>0.05$) (Figure 17A). Neuritic density was also unchanged in LPS stimulated cultures compared to controls ($p>0.05$) (Figure 17B).

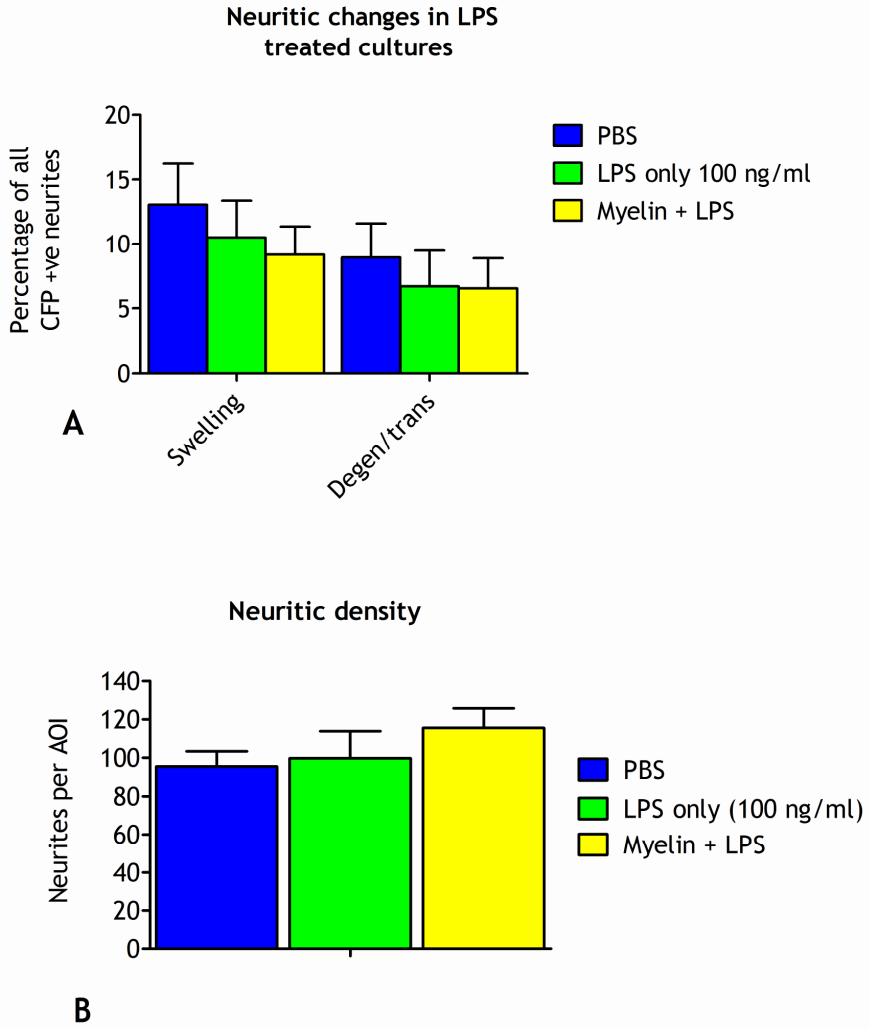

Figure 17: Neuritic changes and neuritic densities were similar in LPS treated cultures in the presence or absence of myelin-laden microglia/macrophages to PBS-treated controls. Cultures were treated with 0.1 mg/ml of wild type myelin at 20 DIV for 3 days until the microglia/macrophages developed a myelin-laden appearance and then treated with either LPS (100 ng/ml) or PBS for 48 hours. (A) Graph indicating mean percentage (+ s.e.m.) of all CFP positive neurites manifesting changes. No statistically significant difference was observed in the percentage of CFP positive neurites showing signs of swellings or degeneration/transection in LPS treated cultures, with or without myelin-laden microglia, compared to PBS-treated controls. (B). Graph showing mean neurite number (+ s.e.m.) per AOI. There was no statistically significant difference in neuritic density in LPS-treated cultures, with our without lipid-laden microglia, compared to PBS-treated controls.

To determine if myelinated neurites acquired neuritic changes secondarily to inflammatory-mediated injury to oligodendrocytes in the presence of LPS, number of myelinated neurites showing changes as a percentage of the total number of myelinated neurites was assessed in each experimental condition. The results demonstrated that there was no increase in the number of myelinated neurites manifesting signs of injury in the LPS-stimulated cultures (in the presence or absence of myelin-laden microglia/macrophages) compared to myelin only- or PBS only-treated controls (Figure 18) ($p > 0.05$).

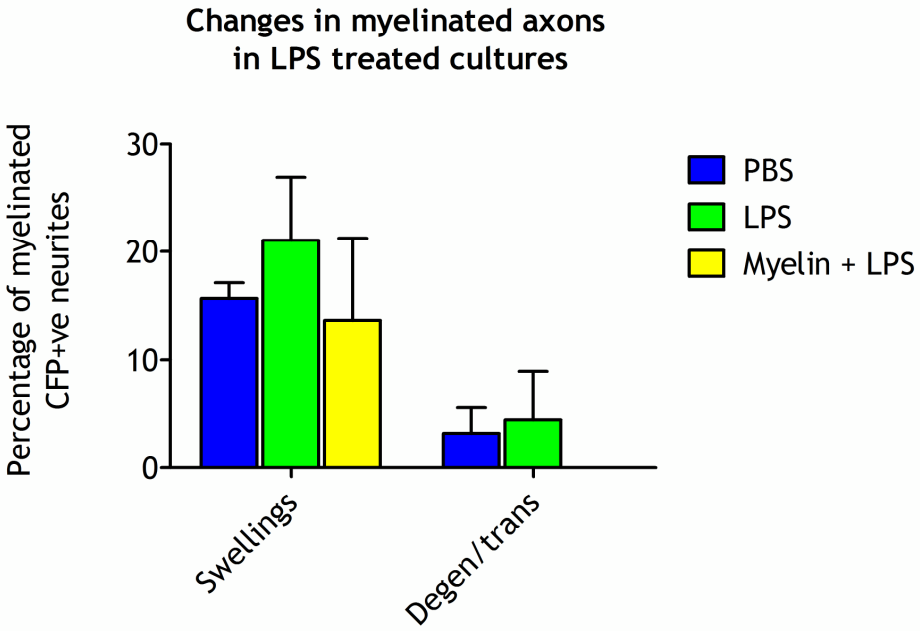

Figure 18: LPS stimulation of microglia/macrophages did not lead to injury of myelinated axons Cultures were treated with 0.1 mg/ml of wild type myelin or with PBS at 20 DIV for 3 days then treated with either LPS (100 ng/ml) or PBS for 48 hours. Graph indicating mean percentage (+ s.e.m.) of all myelinated CFP positive neurites manifesting changes. No statistically significant difference was observed in the percentage of myelinated CFP positive neurites showing signs of swellings or degeneration/transection in LPS treated cultures, with or without myelin-laden microglia, compared to PBS-treated controls.

4.3.4 Response of CFP and non-CFP expressing neurites to LPS-stimulation of microglia/macrophages.

To assess if non-CFP expressing neurites were more vulnerable to microglial-mediated induced injury after LPS stimulation, cultures were incubated with LPS for 48 hours and then immunostained with an antibody to GFP and with SMI31, which recognises phosphorylated neurofilament (Figure 19). Quantification of the area occupied by SMI31 staining demonstrated that there was no reduction in SMI31 staining in the LPS-treated cultures compared to PBS-treated controls (Figure 20). Similarly, the density of CFP positive neurites was not altered in the LPS-treated cultures (Figure 20), as demonstrated above (4.3.2). The results of this single experiment suggest that non-CFP expressing neurites are not more vulnerable to LPS induced injury compare to CFP positive neurites.

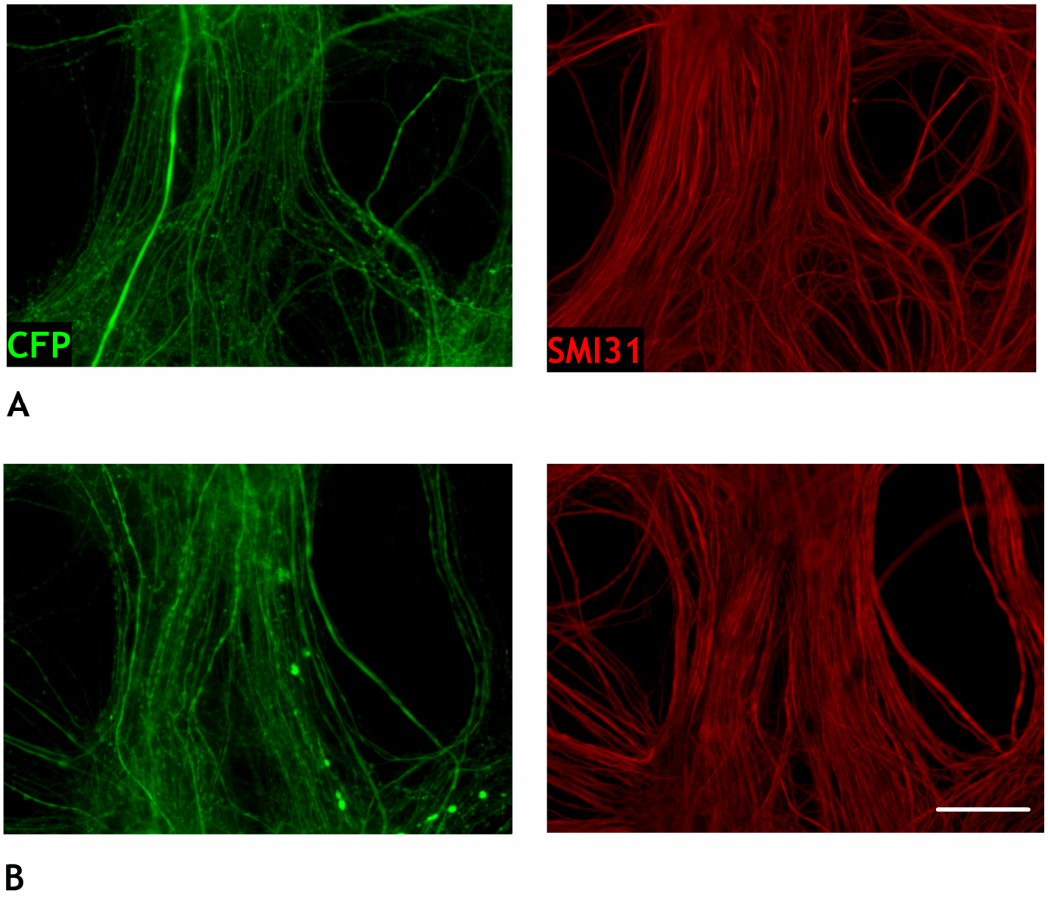

Figure 19: Non-CFP expressing neurites are not more vulnerable to LPS induced injury than CFP-rendered neurites. Micrographs of cultures at 25 DIV treated with either (A) PBS or (B) LPS for 48 hours and then stained with antiboties to SMI31 or GFP (an analogue to CFP). Both CFP and SMI31 staining show similar densities of neurites in the PBS and LPS treated cultures. This indicated that non-CFP expressing neurons are not more vulnerable to LPS induced injury compared to CFP expressing neurons *in vitro*. Scale bar 50 μm

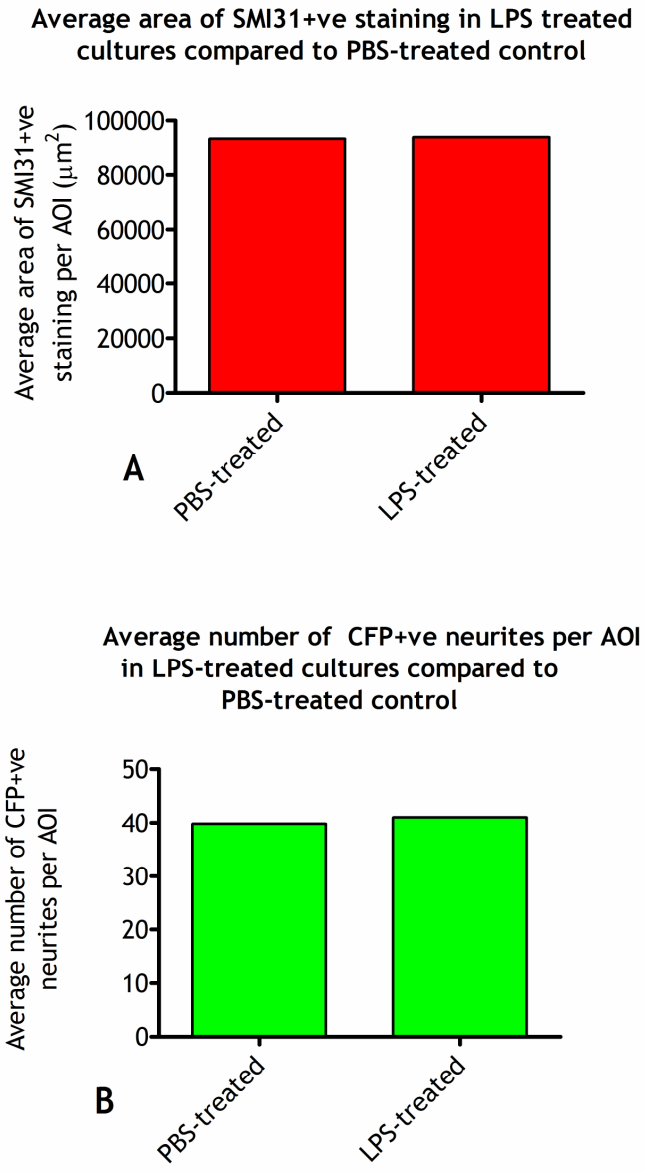

Figure 20: Non-CFP expressing neurons are not more vulnerable to LPS induced injury than CFP-expressing neurons. Cultures at 20 DIV were treated with either LPS or PBS for 48 hours and then stained with antibody to neurofilament or GFP (an analogue of CFP). Graphs showing (A) area occupied by neurofilament staining and (B) densities of CFP-rendered neurites.

4.4 Discussion

Identification of the cellular and molecular effectors of neuritic injury is a key factor in developing potential treatments for neurodegenerative diseases. One of the advantages of the *in vitro* system used in this thesis is that it comprises all neural cell types, that is, neurons, oligodendroglia and astroglia, as well as microglia. Therefore, the complex cellular interactions that occur *in vivo* are partially reproduced. Furthermore, in comparison to *in vivo* situations, the system can be manipulated readily, in order to address simple questions. Here, this system was used to determine if myelin-laden microglia/macrophages were either axono-toxic in a normal environment or axono-protective in an inflammatory environment.

Several studies have shown that microglia/macrophages secrete pro-inflammatory factors in response to the phagocytosis of myelin (Williams et al., 1994;Mosley and Cuzner, 1996;van der Laan et al., 1996) including TNF-a, IL-1, IL-6 and soluble nitric oxide. Since factors such as TNFα or nitric oxide can injure neurites *in vitro* (Stagi et al., 2005;Stagi et al., 2006;De Vos et al., 2000) and *in vivo* (Smith et al., 2001) by disrupting axonal transport status, and agents that inhibit microglial action, for example Glatiramer acetate (GA) or minocycline, can protect against axonal injury (Gilgun-Sherki et al., 2003;Howell et al., 2010), it seemed reasonable to speculate that neuritic injury might represent a consequence of myelin phagocytosis. However, in the work described in this chapter, no evidence was obtained to support the suggestion that the phagocytosis of a myelin-rich tissue fraction drives microglia/macrophages to become axono-toxic. Due to the failure of LPS stimulated microglia/macrophages to induce injury, the putative protective effects could not be determined.

The absence of increased neuritic injury in myelin-treated cultures is, in retrospect, perhaps not surprising. Microglia are part of the innate immune system whose primary role it is to protect from pathogens and remove debris

such as apoptotic cells and myelin debris (Napoli and Neumann, 2009). While there is evidence in the literature to support the suggestion that 'activated' microglia/macrophages elicit injury to neighbouring neural cells (Howell et al., 2010;Lehnardt et al., 2003;Pang et al., 2010), it was recently demonstrated that microglia in the developing CNS that phagocytose apoptotic supernumerary neurons (McArthur et al., 2010), or respond to experimentally induced Wallerian degeneration (Palin et al., 2008) acquire an anti-inflammatory or 'alternatively activated' phenotype, respectively.

Nonetheless the absence of increased neuritic injury in myelin treated cultures cannot be considered to provide conclusive evidence that myelin-laden microglia/macrophages do not injure neurites. For example, it is possible that this population secrete potentially injurious factors but that these become diluted out in the relatively large volume of medium in which the cells are grown. Furthermore, it is possible that direct contact between microglia and neurites does not take place in culture, limiting the potential of the cells to induce injury. These possibilities are addressed further in Chapter 5.

To determine if myelin-laden microglia/macrophages protected neurites in an inflammatory environment, cultures containing myelin-laden cells were stimulated with LPS. LPS-stimulation act through expression of Toll-like receptor 4 (TLR 4) expressed on the cell surface of microglia and leads to 'activation' and the production of inflammatory factors including TNF-α, IL-1β, IL-12p40 and IL-6 (Nakamura et al., 1999;Boven et al., 2006;Glim et al., 2010). It has previously been shown that LPS stimulation of mixed neural cultures leads to extensive, microglial mediated neuronal death *in vitro* (Lehnardt et al., 2003). Surprisingly, LPS did not drive these intrinsic cells to induce neuritic injury, leaving the axono-protective effects of the myelin-laden microglia/macrophages yet to be determined.

Due to this unexpected result, it was important to demonstrate that CFP expressing neurites were not resistant to inflammation-mediated injury compared to non-CFP positive neurites. A study by (Comley et al., 2011)

examining the biological relevance of fluorescent proteins *in vivo* suggested that *Thy1* driven fluorescent protein expression triggered multiple cell stress responses that subtly altered neuronal morphology and influenced the rate of neurodegeneration in experimental axonopathy. Thus CFP positive neurites could potentially be resistant to injury because cellular stress responses are already triggered. However, immunocytochemical analysis of LPS treated cultures showed that overall, neurites (including CFP positive and CFP negative) did not demonstrate more signs of injury in LPS treated cultures compared to PBS treated cultures. Furthermore incubation of the cultures with 100 mM hydrogen peroxide treatment of the cultures demonstrated that CFP expressing neurites were vulnerable to reactive oxygen species-induced injury, which manifested as fragmentation, focal swelling and/or transection.

Previous studies have shown that LPS stimulated microglia are detrimental to oligodendrocytes (Domercq et al., 2007) and their precursors (Pang et al., 2010) *in vitro*, suggesting that myelinated axons may be vulnerable to secondary damage as a consequence of primary injury to the oligodendrocyte. However, myelinated neurites did not demonstrate increased susceptibility to injury in LPS treated cultures compared to PBS treated control cultures. Furthermore, the proportion of myelinated neurites that appeared injured was similar to the proportion of all neurites manifesting changes.

The failure of LPS-stimulated microglia/macrophages to induce injury in the present study may be due to the fact that this population represents a small proportion of the total cell population in the myelinating cultures. In order to maintain the biosynthetically active cultures in optimal condition, they have to be cultured in a relatively large volume of medium. This could dilute out potentially injurious factors and result in reduced LPS-induced cytotoxicity. It has been demonstrated previously that extracellular KCl enhances LPS-induced cytotoxicity (Chang et al., 2000), resulting in the loss of neurons, oligodendrocytes and astrocytes in mixed neural cell cultures (Lehnardt et al., 2003). It would be of interest to determine if KCl in addition to a similar or increased dose of LPS would be sufficient to cause LPS-induced neuritic injury,

thereby allowing the anti-inflammatory effects of the myelin-laden microglia/macrophages to be determined.

(Perry, 2010) recently showed that in aged or diseased brain, microglia adapt a primed phenotype that makes them more susceptible to systematic infection and drives a more aggressive disease pathology. It seems possible the microglia in myelinating cultures generated from wild type mice are not primed to drive a pathologically relevant response as a result of LPS stimulation.

Conversely, CNS inflammation involves cross-talk between cells of both the innate and adaptive immune systems (Kerschensteiner et al., 2003). Although myelin-laden or LPS-stimulated resident microglia may not be axono-toxic themselves, they have been shown to secrete pro-inflammatory cytokines or chemoattractants, when cultured in isolation (Williams et al., 1994;Mosley and Cuzner, 1996;van der Laan et al., 1996). *In vivo*, this would eventually encourage recruitment of T-cells from the periphery. Secondary T-cell responses have a pathogenically relevant impact on CNS axons (Ip et al., 2006) in a mouse model of a primary genetic defect in the oligodendrocyte. Clearly, the myelinating cell culture system used in this study contains no cytotoxic T-cells. As the results of this chapter would suggest, the phagocytosis of myelin debris is not sufficient to 'activate' microglia/macrophages towards an axono-toxic phenotype. Since neither an axono-toxic or axonal-protective phenotype could be identified for this population the reason for this will be assessed further in Chapter 5 in which the soluble cytokine/chemokine profile of myelin and LPS-treated cultures is assessed.

5 The dynamic interaction between myelin-laden microglia/macrophages and neurites and secretion of soluble factors *in vitro*

5.1 Introduction

The overall aim of this study was to determine if the phagocytosis of myelin debris by microglia/macrophages would drive these cells towards either an axono-toxic or axono-protective phenotype. The data presented in Chapter 4 demonstrates that cultures containing myelin-laden microglia are not characterised by an increase in neuritic changes synonymous with injury.

Potentially, microglia/macrophages could harm axons through contact mediated effects as suggested by the proximity and elevated numbers of microglia at sites of axonal injury in MS and in demyelinating models (Nikic et al., 2011;Edgar et al., 2010;Pohl et al., 2011). Alternatively, injury could be elicited by secretion of pro-inflammatory cytokines and nitric oxide (van der Laan et al., 1996;Mosley and Cuzner, 1996;Williams et al., 1994;Jeon et al., 2008;Sun et al., 2010). Nitric oxide and TNF-α have been shown to cause injury to oligodendrocytes (Domercq et al., 2007), in particular to oligodentrocyte precursor cells (Pang et al., 2010). These factors have also been shown to impinge on axonal mitochondria (Haider et al., 2011) and obstruct axonal transport *in vitro* (Stagi et al., 2005;Stagi et al., 2006;De Vos et al., 2000).

In relation to the putative axono-protective phenotype of microglia, these could not be determined in the work undertaken in the previous chapter because stimulation of microglia/macrophages by phagocytosis of myelin debris, did not result in neuritic injury (Chapter 4). Others have shown that myelin-laden microglia/macrophages secrete anti-inflammatory cytokines (Boven et al., 2006;Liu et al., 2006) including IL-6 and IL-10 that ameliorate the effects of LPS-induced stimulation of macrophages.

In light of the unanticipated results reported in Chapter 4, the overall aim of this chapter was to determine if the lack of injury could pertain to (i) absence of contact between microglia/macrophages and neurites or (ii) failure of microglia/macrophages in the myelinating culture system to secrete harmful cytokines/chemokines.

The aims of this chapter were:

1. To examine the physical interaction of phagocytic migroglia/macrophages and adjacent neurites

2. Characterise the cytokine/chemokine profile of the myelin-treated cultures

3. Determine if LPS stimulation initiated a pro-inflammatory response in this *in vitro* system and if this was ameliorated in the presence of myelin-laden microglia/macrophages.

5.2 Materials and methods

5.2.1 Time-lapse imaging of myelinating cultures

Time lapse imaging of cultures was undertaken over a period of 15 hours. Image capture started immediately after the addition of myelin to the culture (for further detail, see Chapter 2.7). Images were taken on bright field (phase contrast), 'cherry' (rhodamine labelled myelin) and CFP/YFP (neurites) channels, from randomly selected areas using a 20x objective, with 5 minute intervals between frames. For each area imaged, a composite movie was generated from the bright field and cherry channels.

5.2.2 Proteome array analysis of culture medium collected from treated cultures

Medium from the cultures analysed in Chapter 4 was collected and stored at -80^{o}C, then analysed using a proteome array panel (mouse cytokine array panel A kit from R&D systems, Abingdon) containing over 40 different anti-cytokine, anti-chemokine antibodies (see Appendix 2 for list of chemokines/cytokines tested) dotted in duplicate onto a nitrocellulose membrane (for further detail see Chapter 2.8).

5.2.3 Quantification of cytokine/chemokine steady state levels

Steady state levels of soluble cytokine/chemokines in conditioned culture medium were quantified from analysis of the signal volume of each array spot generated from scanned X-ray films, using array analysis software (TotalLab TL100 Array v2008; Newcastle upon Tyne). For each membrane (one membrane per experimental condition), the average signal volume of each of the cytokine/chemokine pairs was normalised to the average spot intensity of the 6 positive control spots on each membrane.

5.2.4 Statistical analysis

Statistical analysis was carried out using GraphPad Prism 5 software. Comparrisons between relative spot volumes of myelin or bead-treated cultures and PBS-treated controls were made using one way ANOVA followed by Dunnett's multiple comparison post-test. Significance was set at $p < 0.05$.

5.3 Results

5.3.1 Physical interaction between myelin-laden microglia/macrophages and neurites

Microglia/macrophages could potentially injure axons through physical contact or by the release of soluble factors. To determine whether there is physical contact between phagocytic myelin-laden microglia/macrophages and neighbouring neurites, cultures were incubated with rhodamine-labelled myelin debris and imaged using time-lapse microscopy.

Time-lapse microscopy (see attached CD) demonstrated that phagocytic microglia/macrophages were highly motile and made physical contact with neighbouring neurites (Figure 21). In some cases the microglia/macrophages appeared to ‘pluck’ the neuritic bundles, physically relocating them (as illustrated in the stills in Figures 21 C-G), as they phagocytosed the surrounding myelin debris (Figure 21 D-L).

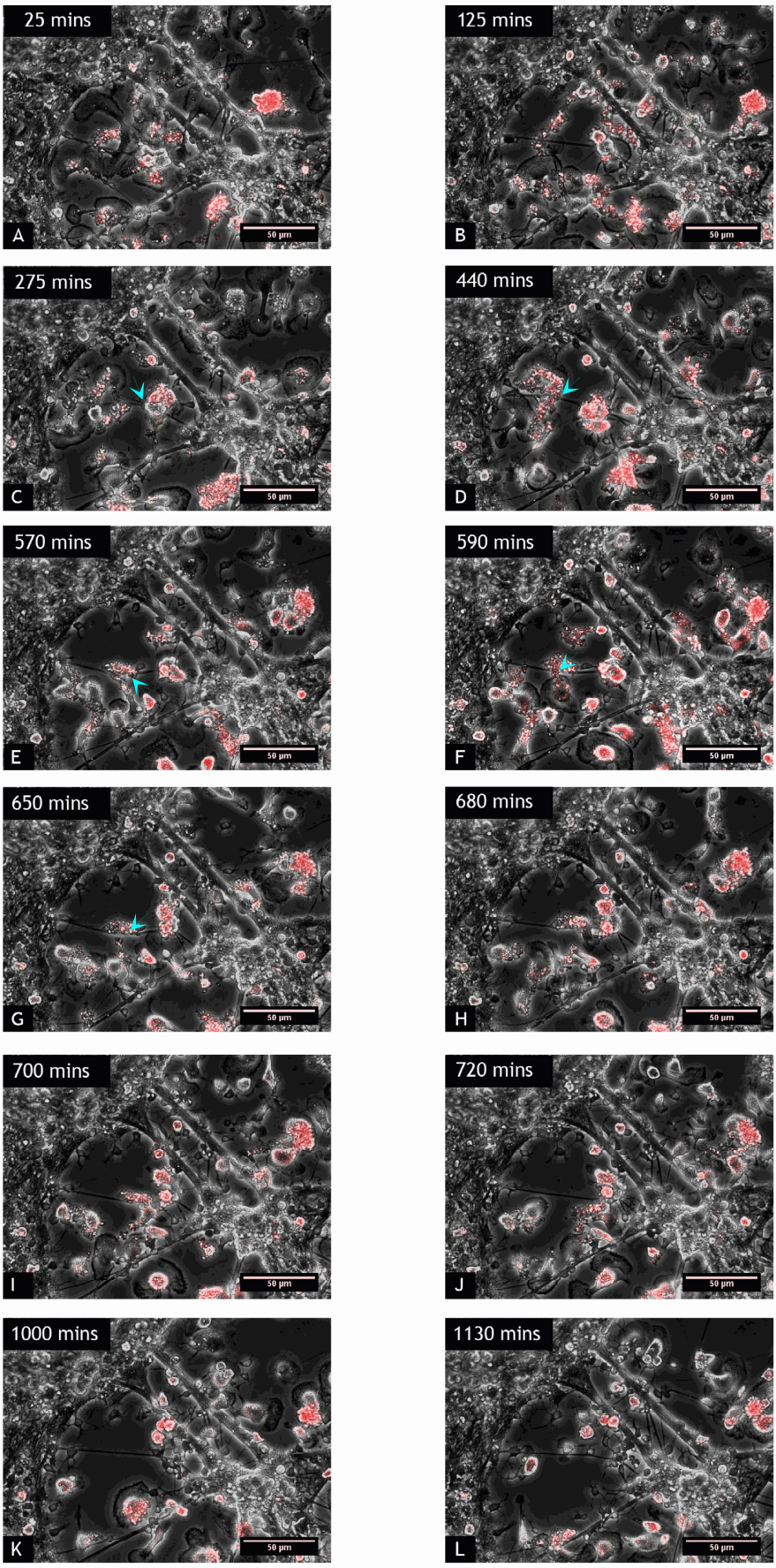

Figure 21: Time lapse imaging of rhodamine-labelled myelin fraction treated culture showing physical contact between microglia/macrophages and neighbouring neurites. Time lapse stills over 1130 minutes showing phagocytosis of labelled myelin fraction (red). Images show labelled myelin debris at time of addition (A-C) and then being phagocytosed by endogenous microglia/macrophages (D-L). Images (C-G) show the physical interaction between microglia/macrophages and neighbouring neurites. Neurites are physically 'plucked' (arrows) by microglia/macrophages as they survey for surrounding myelin debris. Scale bar 50 µm.

5.3.2 Proteome array analysis of culture medium from myelin treated cultures 1 and 7 days post treatment

To examine the array of soluble factors secreted by the phagocytic microglia/macrophages in response to myelin debris, proteome array analysis was carried out on medium collected from the myelin treated cultures.

Visual examination of the cytokine/chemokine profile of the myelin treated cultures suggested that the steady state levels of soluble cytokines/chemokines was similar in cultures treated with wild type or *Plp1* transgenic myelin, or with latex beads, compared to PBS-treated controls at 1 day post-treatment (Figure 22 A-D). In cultures treated for 7days, the results tended to be more variable with a number of cyokines/chemokines appearing up- or down-regulated in the myelin-treated cultures compared to controls (a typical result is illustrated in Figure 22 E-H).

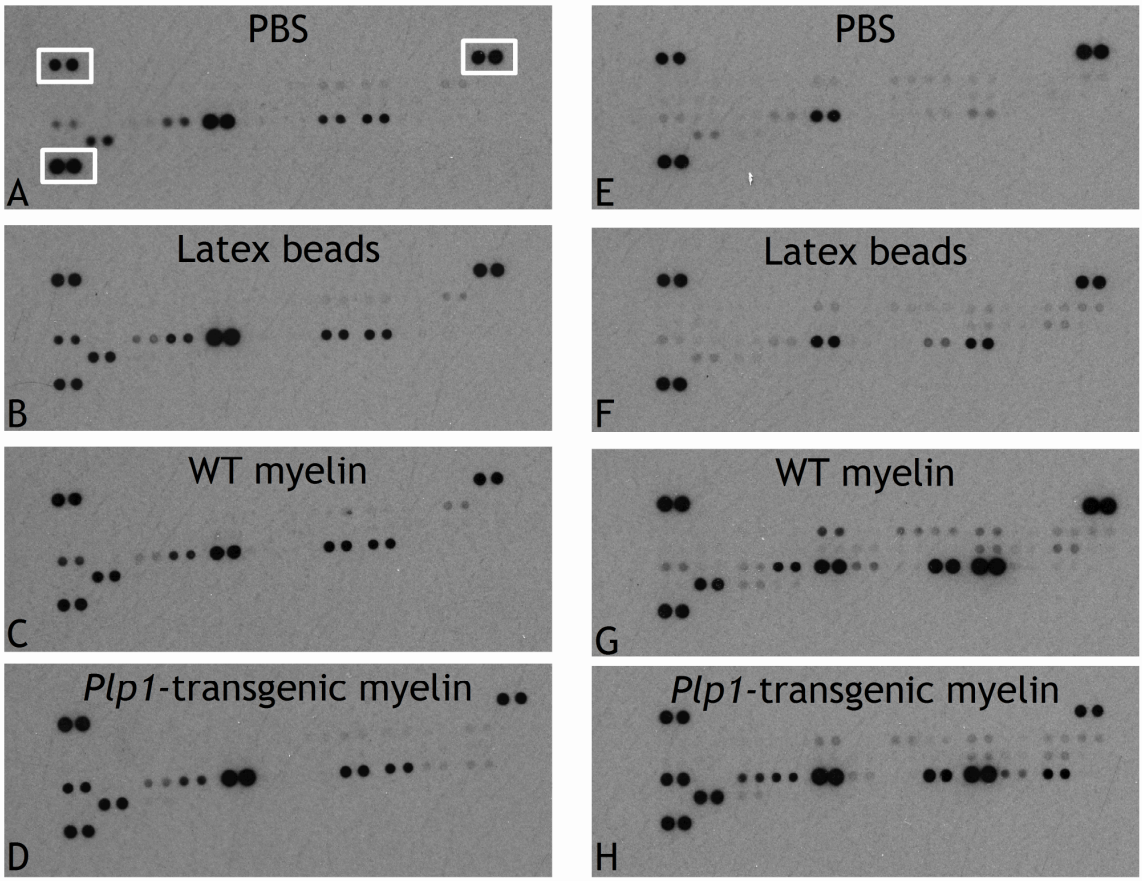

Figure 22: Proteome array analysis of media collected from myelin treated cultures. Typical profiles from cultures 1 (A-D) or 7 (E-H) days post incubation with either PBS, latex beads or 0.1 mg/ml wild type of *Plp1* transgenic myelin debris. Culture medium was tested with antibodies to 40 different cytokines/chemokines, spotted in duplicate on a nitrocellulose membrane. Normalising each pair of chemokines/cytokines to the 6 positive controls (white boxes) within each membrane, there was no visible difference in profiles obtained from myelin-treated cultures compared to latex bead or PBS-treated cultures 1 day post treatment. In cultures treated for 7 days there was a tendency for more variation, however this was not consistent when examined across 3 independent experiments.

Semi-quantitative analysis of two independent cultures incubated with myelin for 1 DIV, demonstrated a tendency for a transient reduction in interleukin 1 receptor antagonist (IL-1ra) in the myelin-treated cultures compared to PBS and latex bead-treated cultures (Figure 23A). Aside from this, no other of the 40 cytokines/chemokines tested, including pro- and anti-inflammatory facts previously shown to be up- or down-regulated in response to the phagocytosis of myelin, demonstrated any consistent alteration (Figure 23 B-C).

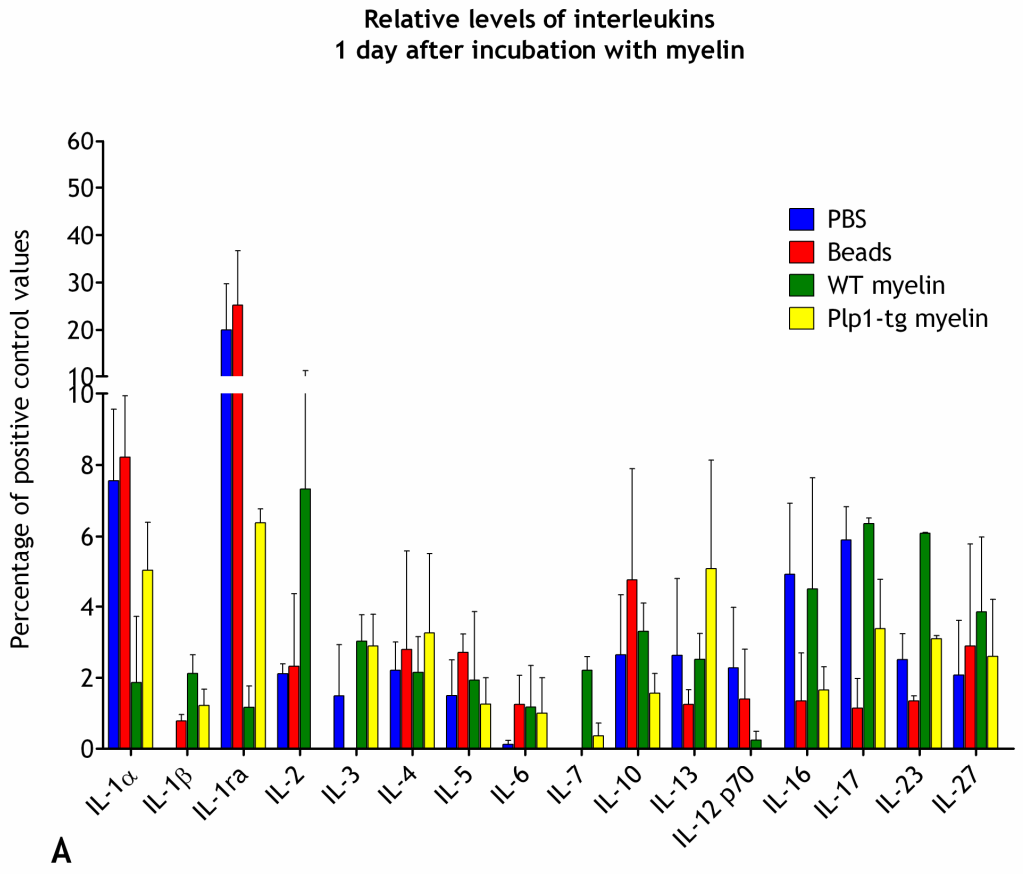
Relative levels of interleukins
1 day after incubation with myelin
Percentage of positive control values
PBS
Beads
WT myelin
Plp1-tg myelin
IL-1α
IL-1β
IL-1ra
IL-2
IL-3
IL-4
IL-5
IL-6
IL-7
IL-10
IL-13
IL-12 p70
IL-16
IL-17
IL-23
IL-27
A

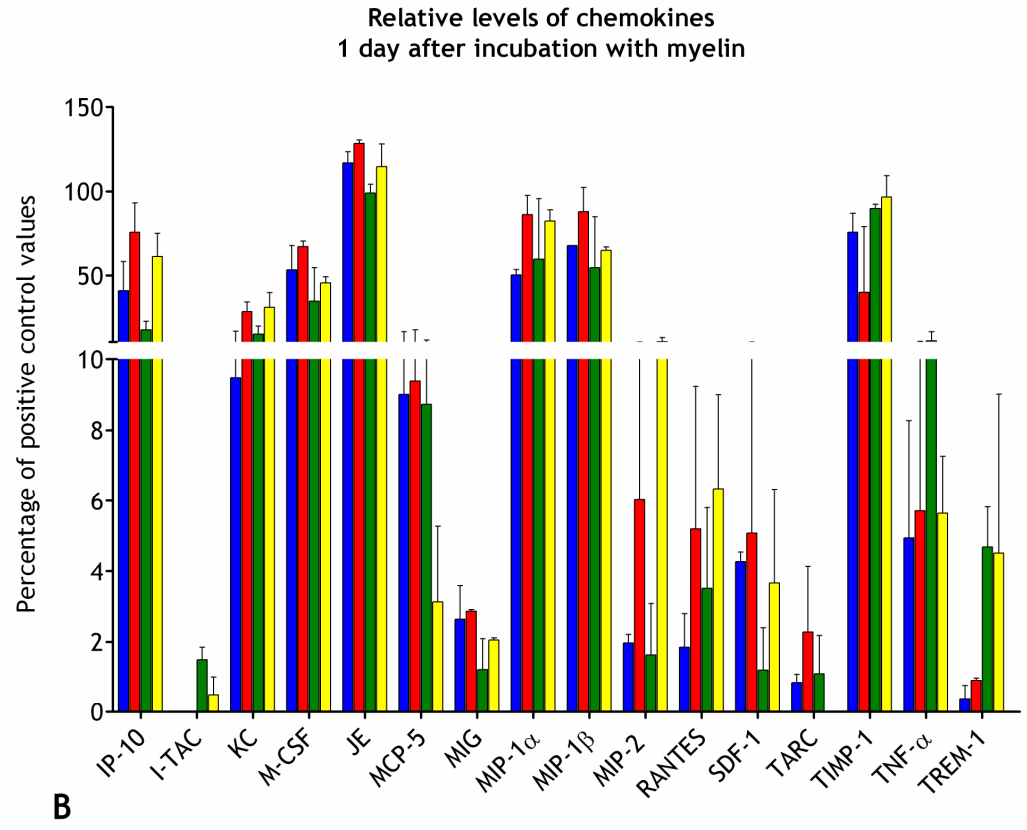
Relative levels of chemokines
1 day after incubation with myelin
Percentage of positive control values
IP-10
I-TAC
KC
M-CSF
JE
MCP-5
MIG
MIP-1α
MIP-1β
MIP-2
RANTES
SDF-1
TARC
TIMP-1
TNF-α
TREM-1
B

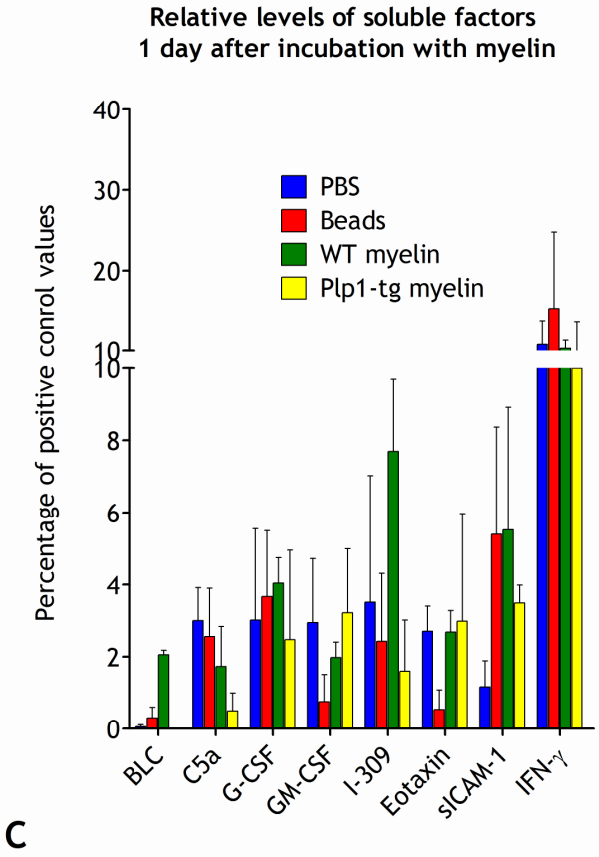

Figure 23: Cytokine/chemokine profiles from cultures incubated with myelin debris for 1 day. Medium from cultures treated with either wild type or *Plp1*-transgenic myelin, latex beads or PBS for 1 day, was analysed using a proteome array containing antibodies to 40 different cytokines/chemokines. (A, B and C) Graphs showing results of semi-quantitative analysis of relative levels (mean + s.e.m.) showed a consistent reduction in IL-1ra (see graph A) in cultures treated with myelin debris compared to latex bead- or PBS-treated controls. However, there was no other consistent alteration in the levels of any of the soluble factors tested (n=2).

Semi-quantitative analysis of three independent cultures incubated with myelin for 7 DIV demonstrated a tendency for chemokines KC, macrophage colony stimulating factor (M-CSF), macrophage inflammatory protein 1α (MIP-1α) and MIP-1β to be slightly, but not significantly, up regulated in the myelin treated cultures compared to latex bead-treated and PBS- treated controls (Figure 24 B). This was also true for IP-10 (alternative nomenclature CXCL10) and RANTES, in the *Plp1*-transgenic myelin-treated cultures compared to all other conditions (Figure 24 B). Steady state levels of sICAM1 was significantly ($p < 0.001$) elevated in wild type and in *Plp1* transgenic myelin-treated cultures compared to latex bead or PBS-treated controls (Figure 24 C).

Most cytokines including the interleukin family members, IL-1, IL-2, IL-6 and IL-12, were less than 10 % of the control spot values in the profiles from either the myelin- or latex bead-treated cultures or the PBS-treated controls after either 1 or 7 day incubations (Figure 23 A and 24A).

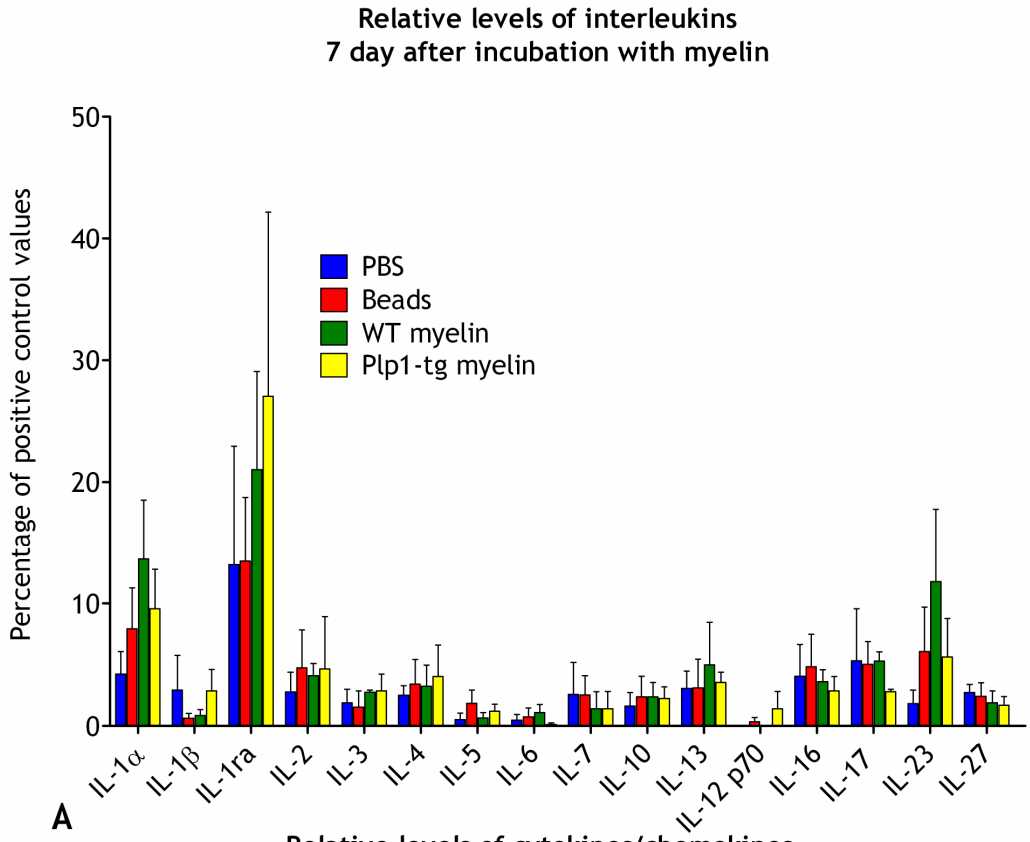
Relative levels of interleukins
7 day after incubation with myelin
Percentage of positive control values
50
40
30
20
10
0
PBS
Beads
WT myelin
Plp1-tg myelin
IL-1α
IL-1β
IL-1ra
IL-2
IL-3
IL-4
IL-5
IL-6
IL-7
IL-10
IL-13
IL-12 p70
IL-16
IL-17
IL-23
IL-27
A

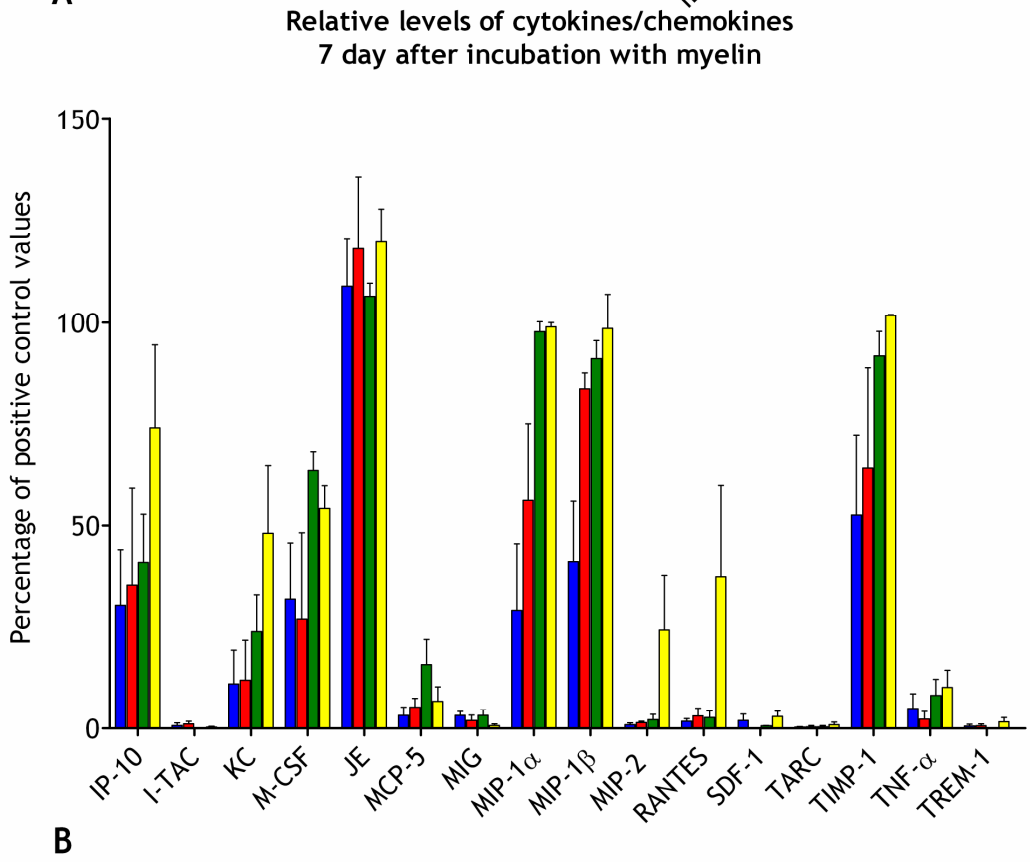
Relative levels of cytokines/chemokines
7 day after incubation with myelin
Percentage of positive control values
150
100
50
0
IP-10
I-TAC
KC
M-CSF
JE
MCP-5
MIG
MIP-1α
MIP-1β
MIP-2
RANTES
SDF-1
TARC
TIMP-1
TNF-α
TREM-1
B

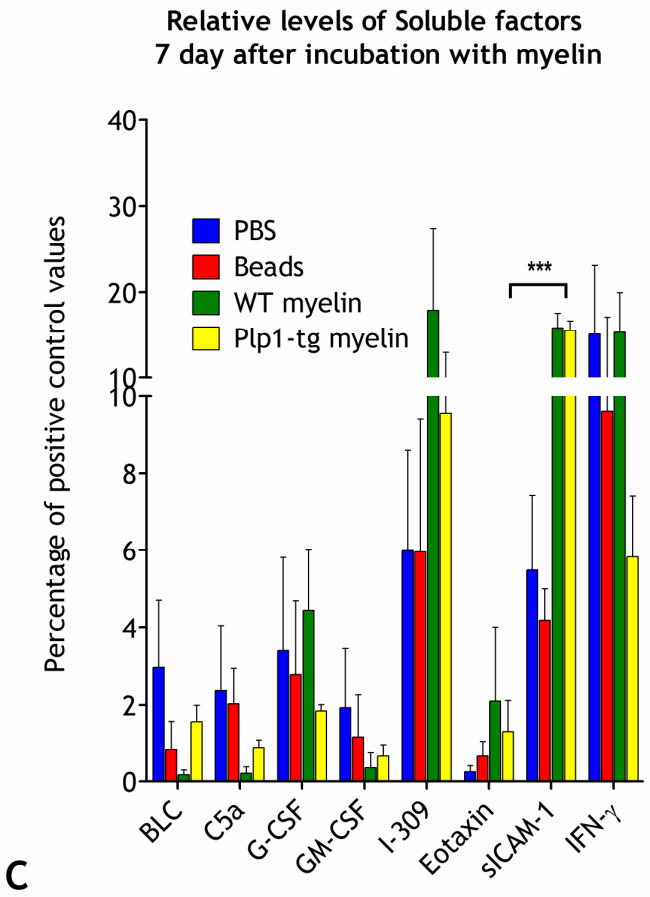

Figure 24: Cytokines/chemokines profiles from cultures incubated with myelin debris for 7 days. Medium from cultures treated with either wild type or *Plp1*-transgenic myelin, latex beads or PBS for 1 day was analysed using a proteome array containing antibodies to 40 different cytokines/chemokines. (A, B and C) Graphs showing results of semi-quantitative analysis of relative levels (mean + s.e.m.) showed no significant alteration of cytokines in myelin treated cultures compared to latex bead or PBS-treated controls. A tendency for up-regulation of certain chemokines including significant up-regulation of sICAM-1 (see graph B) was observed in the myelin-treated cultures compared to controls. Stars indicate p values: ***$p < 0.001$. There was no other consistent alteration in the levels of any of the soluble factors analysed (n=3).

5.3.3 Proteome array analysis of culture medium collected from myelin-laden microglia/macrophages in response to lipopolysaccaride treatment

No increase in neuritic changes synonymous with injury were observed in response to treatment with LPS (see section 4.3.3 Chapter 4). To determine the cytokine/chemokines profile of LPS stimulated cultures culture medium was collected from LPS treated cultures in the presence or absence of myelin-laden microglia.

Proteome array analysis of two independent experiments, showed there was an up-regulation of inflammatory cytokines in the LPS-treated cultures for example IL-1α, IL-1β, IL-6, and TNF-α, compared to PBS-treated controls (Figure 25). From the profiles obtained, this inflammatory response did not appear altered by the presence of myelin-laden microglia/macrophages (Figure 25 C). This was confirmed by semi-quantitative analyses of cytokine/chemokine levels, which showed that there was no marked change in steady-state levels of cytokines/chemokines in myelin-treated cultures compared to PBS-treated controls, after LPS stimulation (Figure 26 A-C).

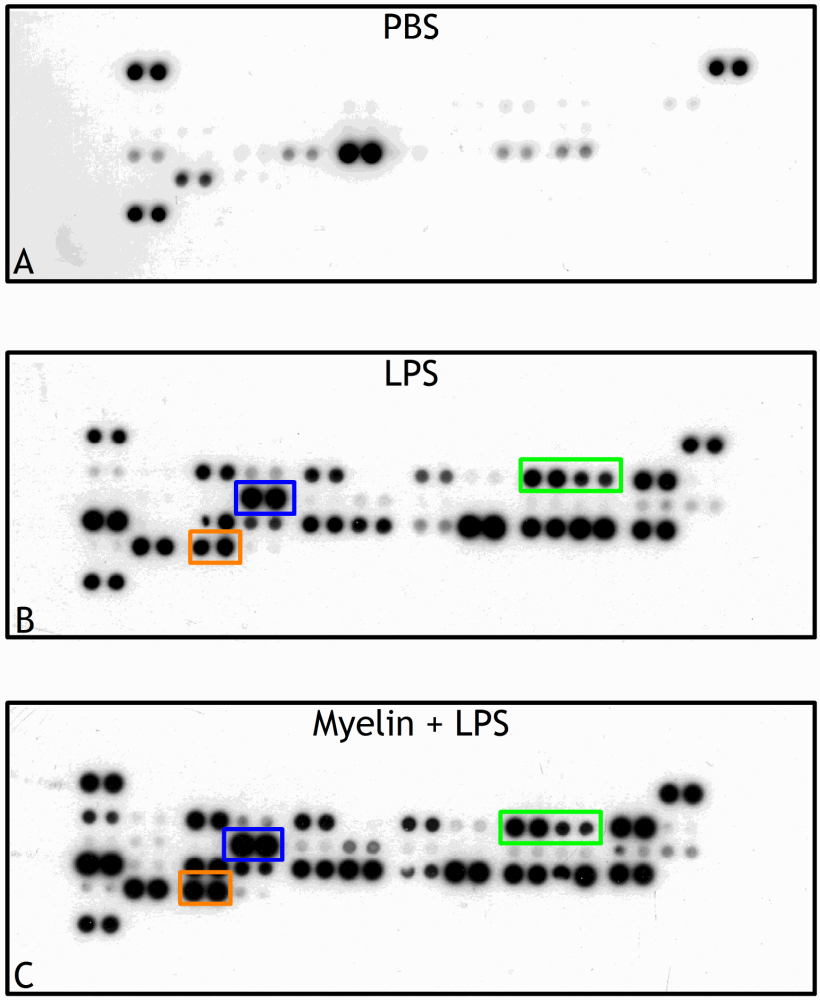

Figure 25: Proteome array analysis of media collected from LPS treated cultures in the presence or absence of myelin-laden microglia/macrophages. Medium was collected from cultures at 26 DIV (± 1 DIV) treated with either (A) PBS, (B) LPS for 48 hours or (C) LPS after treatment with 0.1 mg/ml myelin debris for 3 DIV until the microglia/macrophages became myelin-laden. After treatment with LPS there was obvious up-regulation of key inflammatory cytokines including TNF-α (orange box), IL-1α, IL-1β (green box) and IL-6 (blue box), which did not appear ameliorated by the presence of myelin-laden microglia/macrophages.

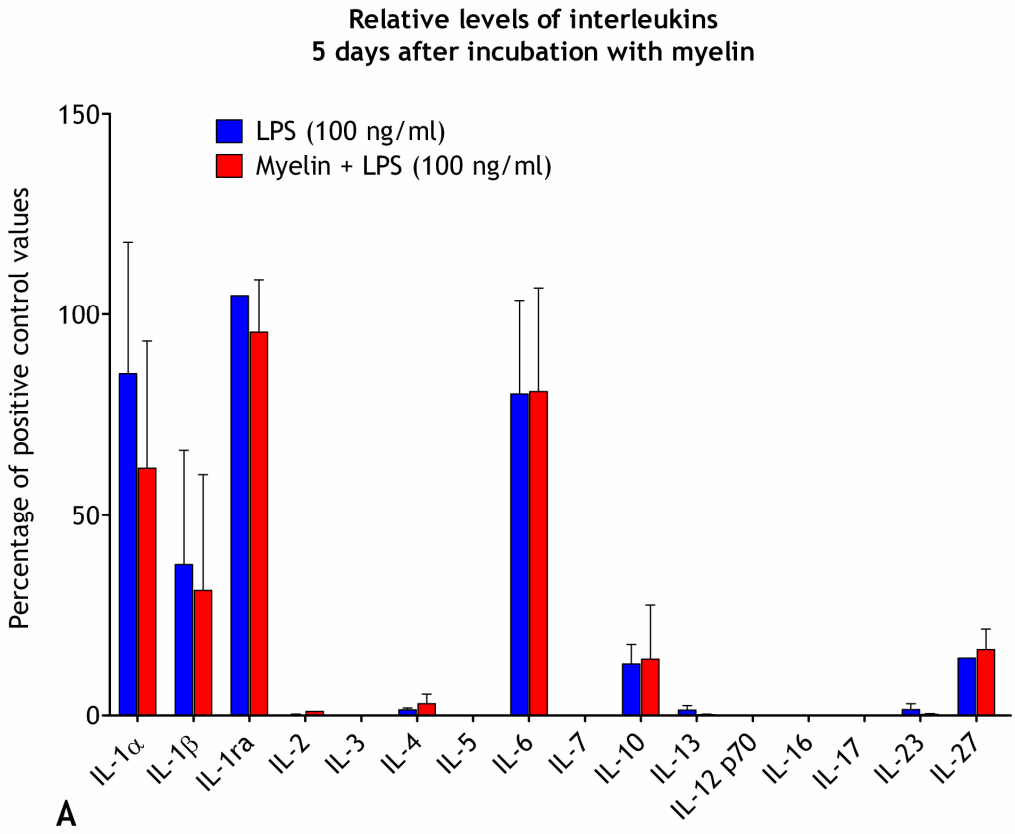
Relative levels of interleukins
5 days after incubation with myelin
LPS (100 ng/ml)
Myelin + LPS (100 ng/ml)
Percentage of positive control values
150
100
50
0
IL-1α
IL-1β
IL-1ra
IL-2
IL-3
IL-4
IL-5
IL-6
IL-7
IL-10
IL-13
IL-12 p70
IL-16
IL-17
IL-23
IL-27
A

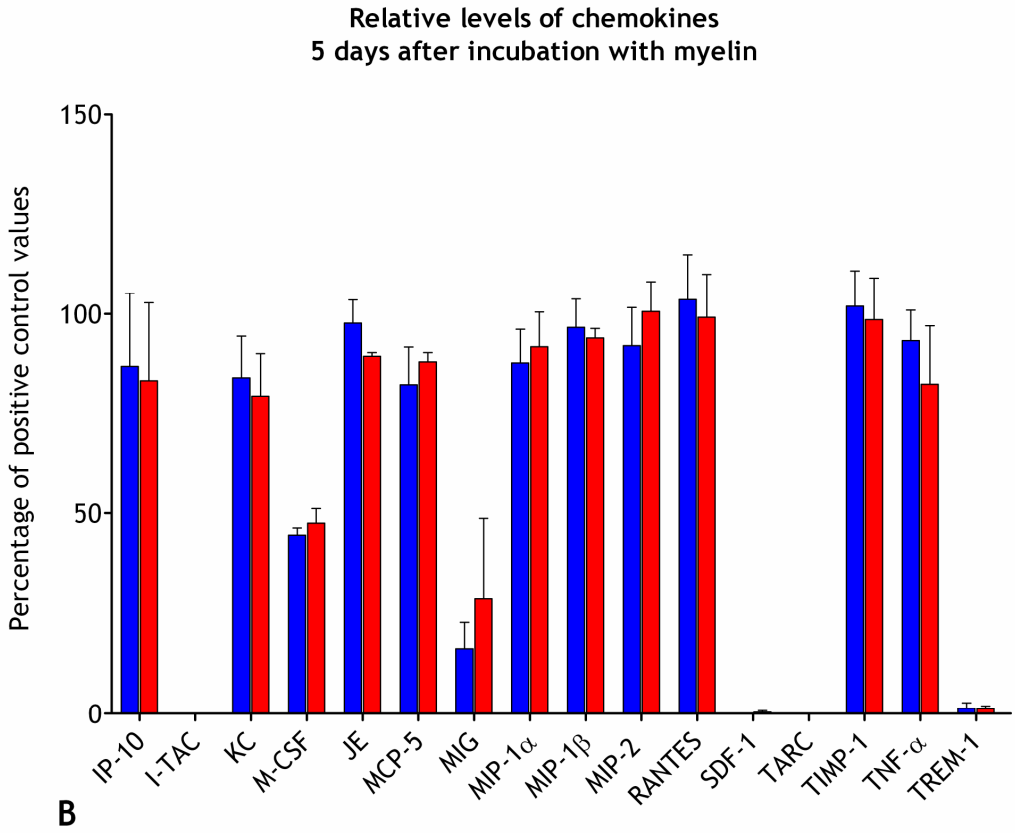
Relative levels of chemokines
5 days after incubation with myelin
Percentage of positive control values
150
100
50
0
IP-10
I-TAC
KC
M-CSF
JE
MCP-5
MIG
MIP-1α
MIP-1β
MIP-2
RANTES
SDF-1
TARC
TIMP-1
TNF-α
TREM-1
B

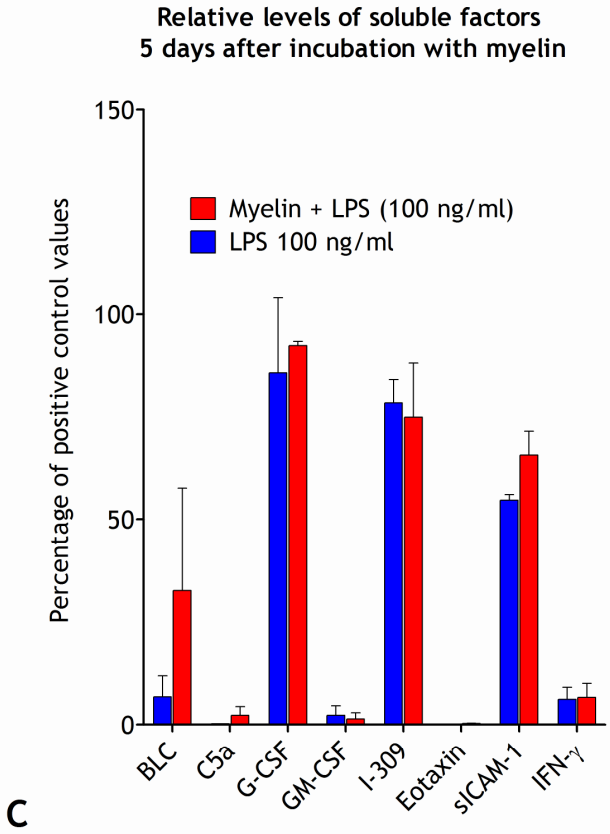

Figure 26: Cytokine/chemokine profiles from cultures stimulated with LPS in the presence or absence of myelin-laden microglia/macrophages. Medium from cultures pre-treated for 3 days with either PBS or myelin debris and then stimulated with LPS for 48 hours was analysed using a proteome array containing antibodies to 40 different cytokines/chemokines. (A, B and C) Graphs showing results of semi-quantitative analysis of relative levels (mean + s.e.m.) showed no amelioration of LPS induced cytokine/chemokine release in the presence of myelin-laden microglia/macrophages. (n=2).

5.4 Discussion

As previously discussed, identifying the cellular effectors that are responsible for neuritic injury is key to understanding the process of axonal loss in inflammatory diseases. Using an *in vitro* myelinating culture system to examine the putative role of the phagocytic microglia in neuritic injury, it was demonstrated that, at least within the myelinating culture system used in this study, the phagocytosis of myelin debris was not sufficient to drive these cells towards an axon-toxic phenotype. In this chapter, the physical interaction between microglia/macrophages and neurites, and the soluble cytokine/chemokine profiles of the cultures were examined.

The failure of the microglia/macrophages to elicit neuritic injury, as demonstrated in Chapter 4, supports the conclusion that myelin-laden microglia/ macrophages are not axono-toxic. *In vivo*, axons are tightly intertwined with the processes of macro- and microglial cell and the failure of the microglia/macrophages to elicit neuritic injury *in vitro* could potentially be due to a lack of physical contact between microglia/macrophages and neurites. However, time-lapse microscopy of the cultures showed that the highly motile phagocytic cells make physical contact with neurites. Within 5 minutes of adding an exogenous myelin tissue fraction to the cultures, the intrinsic microglial/macrophage population began to phagocytose the debris and in doing so, physically contacted adjacent neurites, pulling them action in various directions from their initial trajectory. Therefore it can be concluded that the absence of neuritic injury is not due to the absence of contact between microglia/macrophages and neurites.

Neuritic injury *in vivo* could be induced by soluble factors secreted by 'activated' microglia. It has previously been documented that microglia/macrophages secrete harmful inflammatory factors including TNF-α, IL-1α, IL-1β or IL-6 in response to the phagocytosis of myelin debris (van der Laan et al., 1996;Mosley and Cuzner, 1996;Williams et al., 1994). In particular,

TNF-α and soluble nitric oxide have been shown to injure axons *in vitro* (Stagi et al., 2005;Stagi et al., 2006;De Vos et al., 2000) and *in vivo* (Smith et al., 2001) by interrupting axonal transport of synaptic vesicle precursors, in particular, synaptophysin (Stagi et al., 2005;Stagi et al., 2006) and causing early stage anterograde degeneration in conducting axons (Smith et al., 2001). However, in the current study no up-regulation of key inflammatory cytokines such as TNF-α, IL-1α, IL-1β or IL-6, in response to the addition of myelin was observed. Due to the time constraints of the project, the levels of soluble nitric oxide secreted by the myelin-laden microglia/macrophages in this culture system remains to be assessed. However, one could speculate that because there was no increase in neuritc changes (see Chapter 4) in the myelin-treated cultures compared to controls, the levels of nitric oxide would remain comparable between the myelin-treated cultures and controls.

The differences between the findings of the current study and the aforementioned studies could be a result of the different systems used. For example (van der Laan et al., 1996;Mosley and Cuzner, 1996) added opsonised rat myelin to macrophage-enriched rat cultures and (Williams et al., 1994) treated microglial-enriched human cell cultures with myelin from human CNS. In contrast, the current study was undertaken using a mixed murine neural cell culture, to which non-opsonised myelin was added. However, opsonisation was previously shown not to influence the cytokine profile (van der Laan et al., 1996), therefore, as discussed below, the differences could be due to the nature of the cells used and the multiple-cell type interactions that occur in the system used in the present study.

In agreement with an earlier study (van et al., 2010), steady state levels of certain chemokines, such as MIP-1α, MIP-1β, MIP-2 and RANTES, had a tendency to be elevated in myelin-treated cultures compared to controls, after 7 days of incubation, although the differences were not significant. It is difficult to draw any definitive conclusions from these results as the slight elevation in the levels of MIP-1α, MIP-1β, MIP-2 and RANTES was not consistent across all experiments.

In the current study there was significant up-regulation of the soluble inter-cellular adhesion molecule 1 (sICAM-1) in the myelin-treated cultures compared to controls. sICAM-1 facilitates transmigration of leukocytes into tissues. Together, the results of the cytokine/chemokine array analyses suggest that the phagocytosis of myelin debris by microglia/macrophages in the myelinating culture system does not drive a pro-inflammatory phenotype but could confer a phenotype that facilitates recruitment of peripheral monocytes and T-lymphocytes.

In vitro, monocyte recruitment is not possible, but *in vivo*, recruited monocytes could drive pathogenesis by stimulating microglia/macrophages to adapt a pro-inflammatory phenotype (Hanisch and Kettenmann, 2007) or act themselves directly in a contact mediated fashion or through secretion of soluble factors to injure axons (Medana et al., 2001). The pathogenically relevant influence of T-lymphocytes in genetically determined demyelinating disease models has been demonstrated using RAG null mice, in which the lack of mature lymphocytes led to a reduction in the numbers of CD11b positive cells and a significant amelioration of pathological changes, including axonal injury ((Ip et al., 2006).

Several groups have demonstrated that LPS-mediated stimulation of microglia/macrophages *in vitro* results in the production of inflammatory cytokines and nitric oxide (Nakamura et al., 1999;Boven et al., 2006;Glim et al., 2010). In Chapter 3, an obvious morphological change in microglia/macrophages in response to LPS stimulation, was demonstrated. A visual comparison of proteome arrays of medium from LPS-treated cultures compared to PBS-treated controls demonstrated a clear up-regulation of key inflammatory cytokines including IL-1α, IL-1β, IL-6 and TNF-α, indicating that cells in the culture system were susceptible to stimulation by LPS. However, this difference requires final quantification.

In contrast to a previous study that showed that the phagocytosis of myelin debris drives microglia/macropahges to adapt an anti-inflammatory phenotype that can ameliorate the effects of LPS-induced stimulation (Boven et al., 2006),

the results of the current study found no evidence for an anti-inflammatory phenotype. This is demonstrated by the lack of reduction in the secretion of pro-inflammatory cytokines in cultures stimulated with LPS, in the presence of myelin-laden microglia/macrophages. In contrast to the enriched macrophage system employed by (Boven et al., 2006), in the mixed cell culture system used here, astrocytes, which also express TLR4 *in vitro*, will also become activated in response to LPS (Bowman et al., 2003). Indeed the absence of IL-12 upregulation, reflects the cytokine profile of activated mouse astrocytes which do not secrete IL-12 after stimulation. In contrast, microglia secrete both IL-12 p35 and p75 after stimulation with IFN-γ/LPS in isolated cell cultures (Aloisi et al., 1997). Therefore, the activated astrocytes could possibly contribute to the inflammatory response (Bowman et al., 2003) masking any down-regulation in secretion by microglia/macrophages after phagocytosis of myelin debris. Further, the secretion of IL-10 by astrocytes could down-regulate the secretion the inflammatory cytokines IL-12 p35 and p75 by microglia in a regulatory manner as has been previously shown in IFN-gamma/LPS stimulated mouse astrocyte/microglia co-cultures (Aloisi et al., 1997).

The lack of shift in microglia/macrophage cytokine/chemokine profiles in response to myelin phagocytosis may reflect the fact that the cells are in a more physiologically relevant environment in comparison to cells cultured in isolation, in which neuro-immune cross-talk is inevitably absent and is in keeping with the observation of Glim et al (2010).

However, the possibility that changes in cytokine/chemokine profiles are masked in the system used in this study cannot be excluded. Although densities of microglia/macrophages in the myelinating culture system (~400,000 cells/mm2) are similar to that in a 10 μm thick tissue section of murine white matter, the relative volume of medium in which the cultures are grown is much greater than the volume occupied by extracellular fluid in the CNS. This will inevitably result in a dilution of secreted cytokine/chemokines.

Therefore, it is impossible to exclude the possibility that in a lower volume of medium, a significant shift in these secreted chemokines/cytokines compared to controls could potentially arise. Culturing the cells in a smaller volume of medium would concentrate the levels of secreted chemokines/cytokines, potentially unmasking changes that were undetectible in the current study. However, the cultures which are biosynthetically active (producing myelin membrane), grow optimally in the volume of medium used in the present study. Preliminary experiments using a more sensitive array system and smaller volume of medium also failed to show an increase in the levels of secreted chemokines/cytokines in myelin or LPS treated cultures, therefore suggesting potential changes were not being masked.

In conclusion, the phagocytosis of myelin debris by this intrinsic microglia/macrophage population, in the culture system used here, did not drive these cells towards an axono-toxic phenotype. Neither did it lead to up-regulation of inflammatory cytokines. The data provide no support for the suggestion that myelin-laden microglia/macrophages are axono-toxic. The results of this chapter and Chapters 3 and 4 are considered together and discussed in Chapter 6.

6 Final Discussion and Future Studies

The main purpose of this study was to determine if the phagocytosis of myelin debris per se was sufficient to drive microglia towards an axono-toxic phenotype, or alternatively towards an axono-protective phenotype which would protect adjacent axons in a pro-inflammatory environment. The results of this study show that neither saturating levels of myelin debris (including biochemically abnormal *Plp1*-tg myelin) and/or its phagocytosis were sufficient to drive the phagocytic cells to elicit neuritic injury. Axonal protection could not be determined.

The work was carried out using a myelinating culture system. Characterisation of the intrinsic microglia/macrophages within the culture system showed that they were able to phagocytose exogenous myelin debris. However, this was not associated with a quantifiable change in cellular morphology, cell size or cell density. Although the expression of cell surface receptors on microglia in the culture system remains to be examined, the lack of overt signs of activation or increase in neuritc changes prompted an examination of steady-state levels of soluble factor within myelin treated cultures to determine if pro- or anti-inflammatory cytokines were present. The results showed no shift towards either a pro- or an anti-inflammatory phonotype at the time points tested, either 1 or 7 days post incubation with myelin debris. However, a transient change in cytokines/chemokines levels within shorter or intermediate time intervals cannot be excluded (discussed below).

6.1 The myelinating culture system as a tool for investigating the influence of myelin phagocytosis and axonal integrity

The myelinating culture system used in these studies had several specific advantages over other experimental systems. First, in comparison to isolated microglia/macrophages (Williams et al., 1994;Boven et al., 2006;Mosley and Cuzner, 1996;van der Laan et al., 1996), the system contains most (though not all) of the cells that are present in the CNS *in vivo*. This permits many of the cell-cell interactions that occur *in vivo* to take place.

For example, activated astrocytes have been shown to influence microglia in mixed cortical neuron/glia rat cultures through elevated expression of RANTES. This resulted in activation of the adjacent microglial population as evidenced by morphological changes, and increased numbers of MHC I- MHC II and IL-6 positive microglia cells *in vitro* (Ovanesov et al., 2008). The activation of microglia may also impact downstream on other cell populations including oligodendrocytes (Pang et al., 2010) and adjacent neurites (Howell et al., 2010). Although, the results of the current study showed that LPS-stimulated microglia did not prove deleterious to oligodendrocytes (based on the presence of myelinated axons) or to axons in the myelinating culture system, a previous study by (Pang et al., 2010) has shown that LPS-activated microglia, in OPC-microglia co-cultures, impedes the oligodendrocytes lineage progression of OPCs, resulting in a reduction in MBP production. Furthermore, it has been demonstrated *in vivo* using EAE models of chronic MS, that sites of paranodal axoglial disruption and of acute axonal injury correlated with local microglial inflammation, that was independent of demyelination or lymphocyte infiltration (Howell et al., 2010).

Secondly, in contrast to *in vivo* systems such as that used by (Howell et al., 2010) and colleagues, the myelinating culture system can be used to address the very specific effect of the presence of myelin debris, *per se*. In order to address the same question *in vivo*, myelin debris would have to be injected directly into the CNS, inevitably breaching the blood brain barrier, or through the induction

of demyelination by chemical or genetic means (Skripuletz et al., 2010;Linington et al., 1988;Bradl and Linington, 1996;Nikodemova et al., 2010;Pohl et al., 2011), which would inevitably induce collateral damage, and confound the interpretation of the results.

Thirdly, the myelinating culture system is a 'closed-system' that does not contain recruited monocytes/macrophages, therefore results can be interpreted in relation to the endogenous microglial population.

However, one disadvantage of the system used in the current study, is that LPS stimulates other cell types, including astrocytes, through TLR4 (Bowman et al., 2003) as discussed in Chapter 5. This stimulation of the astrocytes may cause a secretion of chemokines/cytokines that could potentially mask any influence of the microglia/macrophages after phagocytosis of myelin debris.

6.2 The effects of myelin-laden microglia/macrophages on neurites *in vitro*

The results of this study failed to demonstrate neuritic injury in response the addition of either myelin or LPS to the cultures. However these results must be interpreted with some caution. First, although there was no increase in neuritic changes at the time points tested, the presence of transient neuritic changes within just a few hours of treatment or at intermediate time points (i.e after 2, 3, or 4 days) which resolve (Kerschensteiner et al., 2005) cannot be excluded. Secondly, as discussed in Chapter 5, soluble factors that could potentially harm axons may be present in insufficient quantities to induce neuritic injury, due to a dilutional effect. However, preliminary data obtained using a more sensitive Luminex system (Merck Millipore, Dundee) revealed similar results to the proteome profiles. Excluding these caveats, the data fail to support the initial hypothesis that myelin-laden microglia are axono-toxic.

In demyelinating situations *in vivo*, signalling between injured oligodendrocyte and microglia/macrophages may be responsible for altering the status of the cells, thus rendering them harmful to axons. For example, cross-talk between oligodendrocytes harbouring a genetic mutation such as in the *Plp1*-transgenic mouse (Anderson, 1997) or those injured after exposure to infections, toxins or in instances of autoimmune disease such as those which occur in MS, may influence the phenotype of the microglia causing them to become axono-toxic or to recruit peripheral monocytes that drive forward the pathogenesis of disease.

In the context of genetically determined or immune mediated demyelination, recruited cells (macrophages or T-cells) may be responsible for axonal injury. Indeed, T-cells can injure axons *in vitro* (Medana et al., 2001) and recruited CD8 +ve T-lymphocytes has been shown to have a pathogenically relevant action in myelin injury and also in axonal injury in a mouse model of PMD (Ip et al., 2006). The secretion of chemokines by microglia that phagocytose myelin debris could recruit T cells under some circumstances. In the current study the presence of chemokines; MIP-1α, MIP-1β, RANTES and sICAM-1 revealed a tendency to be up-regulated in the myelin-treated cultures compared to latex bead or PBS –treated controls. These particular chemokines are known chemoattractants involved in monocyte chemotaxis (Uguccioni et al., 1995)

6.3 Future experiments

In the current study it was shown that the phagocytosis of myelin debris was not sufficient to cause morphological changes synonymous with activation. However, changes in morphology do not always correlate with a shift in cellular phenotype (Schenk et al., 1999). Even in the absence of a change in cellular morphology, microglia could still shift phenotype by the up-regulation/presentation of surface antigen receptors (Block et al., 2007)) and FcR, specifically FCγRIII or FCγRIV which are expressed on 'activated' microglia (Lunnon et al., 2011) as well as, CD86 which is expressed on by APCs (Bauer et al., 1994).

In order to assess if moncocyte/macrophages recruited to sites of active demyelination are responsible for axonal injury in the context of myelin debris, the experimental protocol would have to be undertaken *in vivo*, for example by injecting myelin directly into the corpus callosum. Nevertheless, injection into the CNS involves breaching both the blood-brain barrier and CNS tissue which, in itself, would lead to local inflammation and a degree of leukocyte infiltration. This would have to be taken into consideration when designing control experiments and in interpretation of results.

Even previous studies using other non-invasive models such as the cuprizone toxic demyelinating model, have shown a degree of local inflammation at sites of mass demyelination post treatment (Lindner et al., 2009;Matsushima and Morell, 2001). With this in mind, it appears that is difficult to find an ideal system to ask such a specific question such as the one addressed in this study.

As there was no change in the pro- or anti-inflammatory profile in the myelin treated cultures compared to controls, future studies could focus on assessing the effects of adding either (i) enriched 'activated' myelin-laden microglia/macrophges or (ii) their conditioned medium, directly to the myelinating cultures to determine if this could result in neuritc injury or be protective in a pro-inflammatory environment. This would overcome the dilutional effects that may have contributed to the results obtained in the current study. However, this scenario is far from mimicking what would occur *in vivo* and the relevance requires consideration.

A somewhat more realistic scenario, and one which is more relevant to MS, would involve stimulating the cultures with IFN-γ, which is a predominant pro-inflammatory cytokine associated with MS. IFN-γ is secreted in response to Th1 cell differentiation resulting in the activation of the downstream innate immune cells (Satoh and Kuroda, 2001;Panitch et al., 1987). Earlier studies investigating the potential of IFN-γ as a treatment for MS have shown that treatment with low dose IFN-γ exacerbates symptoms in patients with relapsing-remitting forms of MS (Satoh and Kuroda, 2001;Panitch et al., 1987).

6.4 Conclusion

From the results of this *in vitro* study investigating the role of microglia/macrophage on neuritic damage, in the context of demyelination, I can conclude, that within this myelinating culture system, the presence of saturating myelin debris and/or its phagocytosis is not sufficient to drive the intrinsic microglia/macrophage population towards an axono-toxic phenotype. Due to the unexpected results of the LPS treated cultures, the axono- protective effects of the myelin-laden microglia/macrophages are yet to be determined. The findings of this investigation suggest that phagocytic microglia in a relatively physiological environment (versus in isolation) possess a quiescent phenotype in the context of myelin debris. With the functions of microglia/macrophages having already been outlined, the results of this study are perhaps not so surprising. Since the primary role of the innate immune system is to protect the CNS, it would seem a terrible evolutionary design if the cells that are meant to protect us actually proved to be detrimental in their role.

7 Appendix 1

7.1 Buffers

7.1.1 Tris acetate EDTA buffer x10 (TAE buffer)

48.4g Tris base (Fisher Scientific)

11.4 ml Glacial acetic acid (Fisher Scientific)

20 ml 0.5 M EDTA (Sigma-Aldrich)

made up to 1L with distilled water

7.1.2 Phosphate buffer saline (PBS)

8 g Sodium Chloride (Sigma-Alderich)

1.44 g Disodium phosphate (Sigma-Alderich)

0.24 g potassium dihydrogen (Fisher Scientific)

0.2 g potassium chloride (Fisher Scientific)

Dissolved in 800 ml of distilled water, adjusted to pH 7.4 with 1 M HCl (Fisher Scientific) and then made up to 1 L with distilled water

7.1.3 Towbin transfer buffers

7.1.3.1 Anode 1

36 g Tris (Fisher Scientific)

74 ml Methanol (Fisher Scientific)

Make up to 1 l in distilled water

7.1.3.2 Anode 2

3 g Tris (Fisher Scientific)

75 ml Methanol (Fisher Scientific)

Make up to 1 l with distilled water

7.1.3.3 Cathode

3 g Glycine (Sigma-Alderich)

3 g Tris (Fisher Scientific)

74 ml Methanol (Fisher Scientific)

made up to 1 L using distilled water

7.1.4 Ponceau S

0.1% Ponceau S powder (Sigma-Alderich)

1% glacial acid (Fisher Scientific)

made up to 1 L in distilled water)

7.1.5 Tris buffer saline Tween (10 x)

12 g Tris base (Fisher Scientific)

87 g sodium chloride (Sigma-Alderich)

10 ml Tween (Sigma-Alderich)

Make up to 800 ml with distilled water and adjust to pH 7.4 with 1 M HCl top up to 1 L with more distilled water.

7.1.6 5 X SDS/DTT denaturing buffer

Bromophenol blue (0.25%)

DTT (dithiothreitol; 0.5 M)

Glycerol (50%)

SDS (sodium dodecyl sulfate; 10%)

Tris base (0.25 M, pH 6.8) (Fisher Scientific)

7.2 Myelinating cell culture

7.2.1 Soyabean trypsin inhibitor and DNAase solution

Soyabean trypsin inhibator (0.52 mg/ml, Sigma-Alderich)

Bovine serum albumin factor V (3 mg/ml, Sigma-Alderich)

DNAase (0.04 mg/ml, Sigma-Alderich) added immediately prior to addition to cell suspension

made up in 1X Lebovitz medium 15 (L-15) (Gibco, Invitroge, Paisley)

7.2.2 Plating medium

50% 1X DMEM (Gibco, Invitrogen, Paisley)

25% heat inactivated horse serum (Invitrogen, Paisley)

23% 1X HBSS with Mg^{2+} and Ca^{2+} (Gibco, Invitrogen, Paisley)

2% glutamine (Sigma-Alderich)

7.2.3 Differentiation medium

Final concentrations of differentiation medium ingredients are as follows:

1X DMEM (Gibco, Invitrogen, Paisley) with penicillin (100U/ml)/streptomycin (100µg/ml) (Gibco, Invitrogen, Paisley)

Glucose (4.500mg/L, Sigma-Alderich)

Hydrocortisone (50 nmols/ml, Sigma-Alderich)

N1 hormone mix (0.5%)(see 7.2.4)

Insulin (0.01mg/ml, Sigma-Alderich)

Biotin (10ng/ml, (Sigma-Alderich)

7.2.4 N1 hormone mix

Final concentrations of N1 hormone mix ingredients are as follows:

Apo-transferrin (1 mg/ml, Sigma-Aldrich)

Putrescine (20 mM, Sigma-Aldrich)

Progesterone (4 µM, Sigma-Aldrich)

Sodium selenate (6 µM, Sigma-Aldrich)

7.3 Tissue fixation

7.3.1 Periodate-lysine-paraformaldehyde fixative (P-L-P)

Immediately prior to use the buffered lysine solution (below) was added to 10% paraformaldehyde and the solution was then made up to 1 L using 0.1 M phosphate buffer. Finally, 2.14 g of sodium periodate was dissolved in the solution directly before use.

7.3.2 Buffered lysine solution

13.7 g lysine monohydrate (Sigma-Aldrich) dissolved in 375 ml of distilled water

1.8 g sodium hydrogen phosphate (Fisher Scientific) dissolved in 100 ml distilled water

Solutions were then mixed together and pHd to pH 7.4

7.3.4 10% paraformaldehyde

20 g paraformaldehyde (Fisher Scientific) dissolved in 200 ml of distilled water and heated to 65 ºC using a few drops of 1 M NaOH were added to clear. The solution was then allowed to clear and was filtered through qualitative filter paper (Starlab).

8 Appendix 2

8.1 Proteome array cytokine/chemokine list

1. BLC
2. C5a
3. G-CSF
4. GM-CSF
5. I-309
6. Eotaxin
7. sICAM-1
8. IFN-γ
9. IL1-α
10. IL-1β
11. IL-1ra
12. IL-2
13. IL-3
14. IL-4
15. IL-5
16. IL-6
17. IL-7
18. IL-10
19. IL-13
20. IL-12 p70
21. IL-16
22. IL-17
23. IL-23
24. IL-27
25. IP-10
26. I-TAC
27. KC
28. M-CSF
29. JE
30. MCP-5
31. MIG
32. MIP-1α
33. MIP-1β
34. MIP-2
35. RANTES
36. SDF-1
37. TARC
38. TIMP-1
39. TNF-α
40. TREM-1

9 Reference list

Alcázar A, Regidor I, Masjuan J, Salinas M, Alvarez-Cermeño JC (2000) Axonal damage induced by cerebrospinal fluid from patients with relapsing-remitting multiple sclerosis. J Neuroimmunol 104:58-67.

Aloisi F (2001) Immune function of microglia. Glia 36:165-179.

Aloisi F, Penna G, Cerase J, Menendez IB, Adorini L (1997) IL-12 production by central nervous system microglia is inhibited by astrocytes. J Immunol 159:1604-1612.

Anderson TJ (1997) Effects of increased dosage of the *Plp* gene: a study in transgenic mice. University of Glasgow.

Arnett HA, Hellendall RP, Matsushima GK, Suzuki K, Laubach VE, Sherman P, Ting JP (2002) The protective role of nitric oxide in a neurotoxicant-induced demyelinating model. J Immunol 168:427-433.

Arnett HA, Mason J, Marino M, Suzuki K, Matsushima GK, Ting JPY (2001) TNFα promotes proliferation of oligodendrocyte progenitors and remyelination. Nat Neurosci 4:1116-1122.

Arnett HA, Wang Y, Matsushima GK, Suzuki K, Ting JP (2003) Functional genomic analysis of remyelination reveals importance of inflammation in oligodendrocyte regeneration. J Neurosci 23:9824-9832.

Bauer J, Sminia T, Wouterlood FG, Dijkstra CD (1994) Phagocytic activity of macrophages and microglial cells during the course of acute and chronic relapsing experimental autoimmune encephalomyelitis. J Neurosci Res 38:365-375.

Beyer M, Gimsa U, Eyüpoglu IY, Hailer NP, Nitsch R (2000) Phagocytosis of neuronal or glial debris by microglial cells: Upregulation of MHC class II expression and multinuclear giant cell formation in vitro. Glia 31:262-266.

Bjartmar C, Wujek JR, Trapp BD (2003) Axonal loss in the pathology of MS: consequences for understanding the progressive phase of the disease. J Neurol Sci 206:165-171.

Bjartmar C, Yin X, Trapp BD (1999) Axonal pathology in myelin disorders. J Neurocytol 28:383-395.

Block ML, Zecca L, Hong JS (2007) Microglia-mediated neurotoxicity: uncovering the molecular mechanisms. Nat Rev Neurosci 8:57-69.

Boven LA, Van Meurs M, Van Zwam M, Wierenga-Wolf A, Hintzen RQ, Boot RG, Aerts JM, Amor S, Nieuwenhuis EE, Laman JD (2006) Myelin-laden macrophages are anti-inflammatory, consistent with foam cells in multiple sclerosis. Brain 129:517-526.

Bowman CC, Rasley A, Tranguch SL, Marriott I (2003) Cultured astrocytes express toll-like receptors for bacterial products. Glia 43:281-291.

Bradl M, Linington C (1996) Animal models of demyelination. Brain Pathol 6:303-311.

Bridge KE, Berg N, Adalbert R, Babetto E, Dias T, Spillantini MG, Ribchester RR, Coleman MP (2007) Late onset distal axonal swelling in YFP-H transgenic mice. Neurobiol Aging.

Brown A (2003) Axonal transport of membranous and nonmembranous cargoes: a unified perspective. J Cell Biol 160:817-821.

Chang RC, Hudson PM, Wilson BC, Liu B, Abel H, Hong JS (2000) High concentrations of extracellular potassium enhance bacterial endotoxin lipopolysaccharide-induced neurotoxicity in glia-neuron mixed cultures. Neuroscience 97:757-764.

Cleveland DW, Monteiro MJ, Wong PC, Gill SR, Gearhart JD, Hoffman PN (1991) Involvement of neurofilaments in the radial growth of axons. J Cell Sci 100 Suppl. 15:85-95.

Comley LH, Wishart TM, Baxter B, Murray LM, Nimmo A, Thomson D, Parson SH, Gillingwater TH (2011) Induction of cell stress in neurons from transgenic mice expressing yellow fluorescent protein: implications for neurodegeneration research. PLoS ONE 6:e17639.

De Stefano N, Matthews PM, Fu LQ, Narayanan S, Stanley J, Francis GS, Antel JP, Arnold DL (1998) Axonal damage correlates with disability in patients with relapsing-remitting multiple sclerosis - Results of a longitudinal magnetic resonance spectroscopy study. Brain 121:1469-1477.

De Vos K, Severin F, Van Herreweghe F, Vancompernolle K, Goossens V, Hyman A, Grooten J (2000) Tumor necrosis factor induces hyperphosphorylation of kinesin light chain and inhibits kinesin-mediated transport of mitochondria. J Cell Biol 149:1207-1214.

Domercq M, Sanchez-Gomez MV, Sherwin C, Etxebarria E, Fern R, Matute C (2007) System xc- and glutamate transporter inhibition mediates microglial toxicity to oligodendrocytes. J Immunol 178:6549-6556.

Edgar JM, Anderson TJ, Dickinson PJ, Barrie JA, McCulloch MC, Nave K-A, Griffiths IR (2002) Survival of, and competition between, oligodendrocytes expressing different alleles of the *Plp* gene. J Cell Biol 158:719-729.

Edgar JM, Griffiths IR (2009) Whiter Matter Structure: A Microscopist's View. In: Diffusion MRI (Johansen-Berg H, Behrens TEJ, eds), pp 75-103. London: Elsevier.

Edgar JM, McCulloch MC, Montague P, Brown AM, Thilemann S, Pratola L, Gruenenfelder FI, Griffiths IR, Nave KA (2010) Demyelination and axonal preservation in a transgenic mouse model of Pelizaeus-Merzbacher disease. EMBO Mol Med 2:42-50.

Edgar JM, McCulloch MC, Thileman S, Barrie JA, Nave K-A, Griffiths IR (2007) Axonal transport stasis correlates with inflammation in a demyelinating mouse model. pp 362.

Edgar JM, McLaughlin M, McCulloch MC, Barrie JA, Nave K-A, Griffiths IR (2001) Proteolipid protein deficient myelin induces axonal swellings in shiverer mice. pp 103:11.

Edgar JM, Nave KA (2009) The role of CNS glia in preserving axon function. Curr Opin Neurobiol 19:498-504.

Feng GP, Mellor RH, Bernstein M, Keller-Peck C, Nguyen QT, Wallace M, Nerbonne JM, Lichtman JW, Sanes JR (2000) Imaging neuronal subsets in transgenic mice expressing multiple spectral variants of GFP. Neuron 28:41-51.

Ferguson B, Matyszak MK, Esiri MM, Perry VH (1997) Axonal damage in acute multiple sclerosis lesions. Brain 120:393-399.

Friede RL, Samorajski T (1970) Axon caliber related to neurofilaments and microtubules in sciatic nerve fibers of rats and mice. Anat Rec 167:379-388.

Garbern J, Yool DA, Moore GJ, Wilds I, Faulk M, Klugmann M, Nave K-A, Sistermans EA, van der Knaap MS, Bird TD, Shy ME, Kamholz J, Griffiths IR (2002a) Patients lacking the major CNS myelin protein, proteolipid protein 1, develop length-dependent axonal degeneration in the absence of demyelination and inflammation. Brain 125:551-561.

Garbern JY, Yool DA, Moore GJ, Wilds IB, Faulk MW, Klugmann M, Nave KA, Sistermans EA, van der Knaap MS, Bird TD, Shy ME, Kamholz JA, Griffiths IR (2002b) Patients lacking the major CNS myelin protein, proteolipid protein 1, develop length-dependent axonal degeneration in the absence of demyelination and inflammation. Brain 125:551-561.

Gilgun-Sherki Y, Panet H, Holdengreber V, Mosberg-Galili R, Offen D (2003) Axonal damage is reduced following glatiramer acetate treatment in C57/bl mice with chronic-induced experimental autoimmune encephalomyelitis. Neurosci Res 47:201-207.

Ginhoux F, Greter M, Leboeuf M, Nandi S, See P, Gokhan S, Mehler MF, Conway SJ, Ng LG, Stanley ER, Samokhvalov IM, Merad M (2010) Fate mapping analysis reveals that adult microglia derive from primitive macrophages. Science 330:841-845.

Gitik M, Liraz-Zaltsman S, Oldenborg PA, Reichert F, Rotshenker S (2011) Myelin down-regulates myelin phagocytosis by microglia and macrophages through interactions between CD47 on myelin and SIRPalpha (signal regulatory protein-alpha) on phagocytes. J Neuroinflammation 8:24.

Glim JE, Vereyken EJ, Heijnen DA, Vallejo JJ, Dijkstra CD (2010) The release of cytokines by macrophages is not affected by myelin ingestion. Glia 58:1928-1936.

Graf vK, Schramm U (1984) Diameter of axons and thickness of myelin sheaths of the pyramidal tract fibres in the adult human medullary pyramid. Anat Anz 157:97-111.

Griffiths IR, Klugmann M, Anderson TJ, Yool D, Thomson CE, Schwab MH, Schneider A, Zimmermann F, McCulloch MC, Nadon NL, Nave K-A (1998) Axonal swellings and degeneration in mice lacking the major proteolipid of myelin. Science 280:1610-1613.

Haider L, Fischer MT, Frischer JM, Bauer J, Hoftberger R, Botond G, Esterbauer H, Binder CJ, Witztum JL, Lassmann H (2011) Oxidative damage in multiple sclerosis lesions. Brain 134:1914-1924.

Hanisch UK, Kettenmann H (2007) Microglia: active sensor and versatile effector cells in the normal and pathologic brain. Nat Neurosci 10:1387-1394.

Hendriks JJ, Teunissen CE, De Vries HE, Dijkstra CD (2005) Macrophages and neurodegeneration. Brain Res Brain Res Rev 48:185-195.

Hikawa N, Takenaka T (1996) Myelin-stimulated macrophages release neurotrophic factors for adult dorsal root ganglion neurons in culture. Cell Mol Neurobiol 16:517-528.

Hoffman PN, Griffin JW, Price DL (1984) Control of axonal caliber by neurofilament transport. J Cell Biol 99:705-714.

Howe CL, Ure D, Adelson JD, LaFrance-Corey R, Johnson A, Rodriguez M (2007) CD8+ T cells directed against a viral peptide contribute to loss of motor function by disrupting axonal transport in a viral model of fulminant demyelination. J Neuroimmunol 188:13-21.

Howell OW, Rundle JL, Garg A, Komada M, Brophy PJ, Reynolds R (2010) Activated Microglia Mediate Axoglial Disruption That Contributes to Axonal Injury in Multiple Sclerosis. J Neuropathol Exp Neurol.

Ip CW, Kohl B, Kleinschnitz C, Reuss B, Nave KA, Kroner A, Martini R (2008) Origin of CD11b+ macrophage-like cells in the CNS of PLP-overexpressing mice: low influx of haematogenous macrophages and unchanged blood-brain-barrier in the optic nerve. Mol Cell Neurosci 38:489-494.

Ip CW, Kroner A, Bendszus M, Leder C, Kobsar I, Fischer S, Wiendl H, Nave KA, Martini R (2006) Immune cells contribute to myelin degeneration and axonopathic changes in mice overexpressing proteolipid protein in oligodendrocytes. J Neurosci 26:8206-8216.

Janeway C.A., Travers P, Walport M, Shlomchik MJ (2005) Immunology. In: immunology Garland Science.

Jeon SB, Yoon HJ, Park SH, Kim IH, Park EJ (2008) Sulfatide, a major lipid component of myelin sheath, activates inflammatory responses as an endogenous stimulator in brain-resident immune cells. J Immunol 181:8077-8087.

Karim SA, Barrie JA, McCulloch MC, Montague P, Edgar JM, Kirkham D, Anderson TJ, Nave K-A, Griffiths IR, McLaughlin M (2007) PLP overexpression perturbs myelin protein composition and myelination in a mouse model of Pelizaeus-Merzbacher disease. Glia 55:341-351.

Kerschensteiner M, Meinl E, Hohlfeld R (2009) Neuro-immune crosstalk in CNS diseases. Neuroscience 158:1122-1132.

Kerschensteiner M, Schwab ME, Lichtman JW, Misgeld T (2005) *In vivo* imaging of axonal degeneration and regeneration in the injured spinal cord. Nature Med 11:572-577.

Kerschensteiner M, Stadelmann C, Dechant G, Wekerle H, Hohlfeld R (2003) Neurotrophic cross-talk between the nervous and immune systems: implications for neurological diseases. Ann Neurol 53:292-304.

Klugmann M, Schwab MH, Jung M, Pühlhofer A, Schneider A, Zimmermann F, Griffiths IR, Nave K-A (1997a) Mutations of the X-linked proteolipid protein gene: molecular mechanisms of dysmyelination. In: Cell Biology and Pathology of Myelin:Evolving Biological Concepts and Therapeautic Approaches (Devon RM,

Doucette JR, Juurlink BHJ, Schreyer DJ, Verge VMK, eds), New York: Plenum Press.

Klugmann M, Schwab MH, Pühlhofer A, Schneider A, Zimmermann F, Griffiths IR, Nave K-A (1997b) Assembly of CNS myelin in the absence of proteolipid protein. Neuron 18:59-70.

Kotter MR, Zhao C, van RN, Franklin RJ (2005) Macrophage-depletion induced impairment of experimental CNS remyelination is associated with a reduced oligodendrocyte progenitor cell response and altered growth factor expression. Neurobiol Dis 18:166-175.

Lawson LJ, Perry VH, Dri P, Gordon S (1990) Heterogeneity in the distribution and morphology of microglia in the normal adult mouse brain. Neuroscience 39:151-170.

Lehnardt S, Massillon L, Follett P, Jensen FE, Ratan R, Rosenberg PA, Volpe JJ, Vartanian T (2003) Activation of innate immunity in the CNS triggers neurodegeneration through a Toll-like receptor 4-dependent pathway. Proc Natl Acad Sci U S A 100:8514-8519.

Lindner M, Fokuhl J, Linsmeier F, Trebst C, Stangel M (2009) Chronic toxic demyelination in the central nervous system leads to axonal damage despite remyelination. Neurosci Lett 453:120-125.

Linington C, Bradl M, Lassmann H, Brunner C, Vass K (1988) Augmentation of demyelination in rat acute allergic encephalomyelitis by circulating mouse monoclonal antibodies directed against a myelin/oligodendrocyte glycoprotein. Am J Path 130:443-454.

Liu Y, Hao W, Letiembre M, Walter S, Kulanga M, Neumann H, Fassbender K (2006) Suppression of microglial inflammatory activity by myelin phagocytosis: role of p47-PHOX-mediated generation of reactive oxygen species. J Neurosci 26:12904-12913.

Lunnon K, Teeling JL, Tutt AL, Cragg MS, Glennie MJ, Perry VH (2011) Systemic inflammation modulates Fc receptor expression on microglia during chronic neurodegeneration. J Immunol 186:7215-7224.

Magnus T, Chan A, Grauer O, Toyka KV, Gold R (2001) Microglial phagocytosis of apoptotic inflammatory T cells leads to down-regulation of microglial immune activation. J Immunol 167:5004-5010.

Matsushima GK, Morell P (2001) The neurotoxicant, cuprizone, as a model to study demyelination and remyelination in the central nervous system. Brain Pathol 11:107-116.

McArthur S, Cristante E, Paterno M, Christian H, Roncaroli F, Gillies GE, Solito E (2010) Annexin A1: a central player in the anti-inflammatory and neuroprotective role of microglia. J Immunol 185:6317-6328.

Medana I, Martinic MA, Wekerle H, Neumann H (2001) Transection of major histocompatibility complex class I-induced neurites by cytotoxic T lymphocytes. Am J Pathol 159:809-815.

Morris RL, Hollenbeck PJ (1993) The regulation of bidirectional mitochondrial transport is coordinated with axonal outgrowth. J Cell Sci 104:917-927.

Mosley K, Cuzner ML (1996) Receptor-mediated phagocytosis of myelin by macrophages and microglia: effect of opsonization and receptor blocking agents. Neurochem Res 21:481-487.

Nakamura Y, Si QS, Kataoka K (1999) Lipopolysaccharide-induced microglial activation in culture: temporal profiles of morphological change and release of cytokines and nitric oxide. Neurosci Res 35:95-100.

Napoli I, Neumann H (2009) Microglial clearance function in health and disease. Neuroscience 158:1030-1038.

Nash B, Thomson CE, Linington C, Arthur AT, McClure JD, McBride MW, Barnett SC (2011) Functional duality of astrocytes in myelination. J Neurosci 31:13028-13038.

Nave KA (2010) Myelination and the trophic support of long axons. Nat Rev Neurosci 11:275-283.

Neumann H, Kotter MR, Franklin RJ (2009) Debris clearance by microglia: an essential link between degeneration and regeneration. Brain 132:288-295.

Neumann J, Sauerzweig S, Ronicke R, Gunzer F, Dinkel K, Ullrich O, Gunzer M, Reymann KG (2008) Microglia cells protect neurons by direct engulfment of invading neutrophil granulocytes: a new mechanism of CNS immune privilege. J Neurosci 28:5965-5975.

Nikic I, Merkler D, Sorbara C, Brinkoetter M, Kreutzfeldt M, Bareyre FM, Bruck W, Bishop D, Misgeld T, Kerschensteiner M (2011) A reversible form of axon damage in experimental autoimmune encephalomyelitis and multiple sclerosis. Nat Med 17:495-499.

Nikodemova M, Lee J, Fabry Z, Duncan ID (2010) Minocycline attenuates experimental autoimmune encephalomyelitis in rats by reducing T cell infiltration into the spinal cord. J Neuroimmunol 219:33-37.

Nimmerjahn A, Kirchhoff F, Helmchen F (2005) Resting microglial cells are highly dynamic surveillants of brain parenchyma in vivo. Science 308:1314-1318.

Norton WT, Poduslo SE (1973) Myelination in the rat brain: method of myelin isolation. J Neurochem 21:749-757.

Ovanesov MV, Ayhan Y, Wolbert C, Moldovan K, Sauder C, Pletnikov MV (2008) Astrocytes play a key role in activation of microglia by persistent Borna disease virus infection. J Neuroinflammation 5:50.

Palin K, Cunningham C, Forse P, Perry VH, Platt N (2008) Systemic inflammation switches the inflammatory cytokine profile in CNS Wallerian degeneration. Neurobiol Dis 30:19-29.

Pang Y, Campbell L, Zheng B, Fan L, Cai Z, Rhodes P (2010) Lipopolysaccharide-activated microglia induce death of oligodendrocyte progenitor cells and impede their development. Neuroscience 166:464-475.

Panitch HS, Hirsch RL, Schindler J, Johnson KP (1987) Treatment of multiple sclerosis with gamma interferon: exacerbations associated with activation of the immune system. Neur 37:1097-1102.

Peri F, Nusslein-Volhard C (2008) Live imaging of neuronal degradation by microglia reveals a role for v0-ATPase a1 in phagosomal fusion in vivo. Cell 133:916-927.

Perry VH (1994) Functions of microglia. In: Macrophages and the nervous system (Perry VH, ed), pp 44-52. Austin: R.G. Landes.

Perry VH (2010) Contribution of systemic inflammation to chronic neurodegeneration. Acta Neuropathol 120:277-286.

Perry VH, Nicoll JA, Holmes C (2010) Microglia in neurodegenerative disease. Nat Rev Neurol 6:193-201.

Pohl HB, Porcheri C, Mueggler T, Bachmann LC, Martino G, Riethmacher D, Franklin RJ, Rudin M, Suter U (2011) Genetically induced adult oligodendrocyte cell death is associated with poor myelin clearance, reduced remyelination, and axonal damage. J Neurosci 31:1069-1080.

Polazzi E, Monti B (2010) Microglia and neuroprotection: from in vitro studies to therapeutic applications. Prog Neurobiol.

Popovich PG, Longbrake EE (2008) Can the immune system be harnessed to repair the CNS? Nat Rev Neurosci 9:481-493.

Prinz M, Priller J, Sisodia SS, Ransohoff RM (2011) Heterogeneity of CNS myeloid cells and their roles in neurodegeneration. Nat Neurosci 14:1227-1235.

Ransohoff RM, Perry VH (2009) Microglial physiology: unique stimuli, specialized responses. Annu Rev Immunol 27:119-145.

Rasmussen S, Wang Y, Kivisakk P, Bronson RT, Meyer M, Imitola J, Khoury SJ (2007) Persistent activation of microglia is associated with neuronal dysfunction of callosal projecting pathways and multiple sclerosis-like lesions in relapsing--remitting experimental autoimmune encephalomyelitis. Brain 130:2816-2829.

Readhead C, Schneider A, Griffiths IR, Nave K-A (1994) Premature arrest of myelin formation in transgenic mice with increased proteolipid protein gene dosage. Neuron 12:583-595.

Renault-Mihara F, Okada S, Shibata S, Nakamura M, Toyama Y, Okano H (2008) Spinal cord injury: emerging beneficial role of reactive astrocytes' migration. Int J Biochem Cell Biol 40:1649-1653.

Rigato C, Buckinx R, Le Corronc H, Rigo JM, Legendre P (2011) Pattern of invasion of the embryonic mouse spinal cord by microglial cells at the time of the onset of functional neuronal networks. Glia 59:675-695.

Rock RB, Gekker G, Hu S, Sheng WS, Cheeran M, Lokensgard JR, Peterson PK (2004) Role of microglia in central nervous system infections. Clin Microbiol Rev 17:942-64, table.

Satoh J, Kuroda Y (2001) Differing effects of IFN beta vs IFN gamma in MS: gene expression in cultured astrocytes. Neur 57:681-685.

Schenk D, et al. (1999) Immunization with amyloid-beta attenuates Alzheimer-disease-like pathology in the PDAPP mouse. Nature 400:173-177.

Schwartz M, Butovsky O, Bruck W, Hanisch UK (2006) Microglial phenotype: is the commitment reversible? Trends Neurosci 29:68-74.

Shy ME, Hobson G, Jain M, Boespflug-Tanguy O, Garbern J, Sperle K, Li W, Gow A, Rodriguez D, Bertini E, Mancias P, Krajewski K, Lewis R, Kamholz J (2003) Schwann cell expression of PLP1 but not DM20 is necessary to prevent neuropathy. Ann Neurol 53:354-365.

Skripuletz T, Bussmann JH, Gudi V, Koutsoudaki PN, Pul R, Moharregh-Khiabani D, Lindner M, Stangel M (2010) Cerebellar cortical demyelination in the murine cuprizone model. Brain Pathol 20:301-312.

Smith KJ, Kapoor R, Hall SM, Davies M (2001) Electrically active axons degenerate when exposed to nitric oxide. Ann Neurol 49:470-476.

Sobottka B, Harrer MD, Ziegler U, Fischer K, Wiendl H, Hunig T, Becher B, Goebels N (2009) Collateral bystander damage by myelin-directed CD8+ T cells causes axonal loss. Am J Pathol 175:1160-1166.

Stagi M, Dittrich PS, Frank N, Iliev AI, Schwille P, Neumann H (2005) Breakdown of axonal synaptic vesicle precursor transport by microglial nitric oxide. J Neurosci 25:352-362.

Stagi M, Gorlovoy P, Larionov S, Takahashi K, Neumann H (2006) Unloading kinesin transported cargoes from the tubulin track via the inflammatory c-Jun N-terminal kinase pathway. FASEB J 20:2573-2575.

Sun X, Wang X, Chen T, Li T, Cao K, Lu A, Chen Y, Sun D, Luo J, Fan J, Young W, Ren Y (2010) Myelin activates FAK/Akt/NF-kappaB pathways and provokes CR3-dependent inflammatory response in murine system. PLoS One 5:e9380.

Thomson CE, McCulloch M, Sorenson A, Barnett SC, Seed BV, Griffiths IR, McLaughlin M (2008) Myelinated, synapsing cultures of murine spinal cord--validation as an in vitro model of the central nervous system. Eur J Neurosci 28:1518-1535.

Trapp BD, Peterson J, Ransohoff RM, Rudick R, Mork S, Bo L (1998a) Axonal transection in the lesions of multiple sclerosis. N Engl J Med 338:278-285.

Trapp BD, Peterson J, Ransohoff RM, Rudick R, Mörk S, Bö L (1998b) Axonal transection in the lesions of multiple sclerosis. N Engl J Med 338:278-285.

Uguccioni M, D'Apuzzo M, Loetscher M, Dewald B, Baggiolini M (1995) Actions of the chemotactic cytokines MCP-1, MCP-2, MCP-3, RANTES, MIP-1 alpha and MIP-1 beta on human monocytes. Eur J Immunol 25:64-68.

van der Laan LJ, Ruuls SR, Weber KS, Lodder IJ, Dopp EA, Dijkstra CD (1996) Macrophage phagocytosis of myelin in vitro determined by flow cytometry: phagocytosis is mediated by CR3 and induces production of tumor necrosis factor-alpha and nitric oxide. J Neuroimmunol 70:145-152.

van ZM, Wierenga-Wolf AF, Melief MJ, Schrijver B, Laman JD, Boven LA (2010) Myelin ingestion by macrophages promotes their motility and capacity to recruit myeloid cells. J Neuroimmunol 225:112-117.

Wake H, Moorhouse AJ, Jinno S, Kohsaka S, Nabekura J (2009) Resting microglia directly monitor the functional state of synapses in vivo and determine the fate of ischemic terminals. J Neurosci 29:3974-3980.

Walter L, Neumann H (2009) Role of microglia in neuronal degeneration and regeneration. Semin Immunopathol 31:513-525.

Williams K, Ulvestad E, Waage A, Antel JP, McLaurin J (1994) Activation of adult human derived microglia by myelin phagocytosis in vitro. J Neurosci Res 38:433-443.

Yool DA, Edgar JM, Montague P, Malcolm S (2000) The *proteolipid* protein gene and myelin disorders in man and animal models. Hum Mol Genet 9:987-992.

Zhang SC, Goetz BD, Carré JL, Duncan ID (2001) Reactive microglia in dysmyelination and demyelination. Glia 34:101-109.

Zhang SC, Goetz BD, Duncan ID (2003) Suppression of activated microglia promotes survival and function of transplanted oligodendroglial progenitors. Glia 41:191-198.